PROCESS INTENSIFICATION FOR THE IRON-CATALYSED SLURRY-PHASE FISCHER-TROPSCH REACTOR SYSTEM

André Peter Steynberg

Thesis Presented for the Degree of

MASTER OF SCIENCE

in the Department of Chemical Engineering

Faculty of Engineering & the Built Environment

UNIVERSITY OF CAPE TOWN

2014

Abstract

A set of operating conditions was identified with the potential to enable improved slurry-phase reactor productivity for hydrocarbon production using Fischer-Tropsch synthesis. Compared to the most relevant prior art publication, this requires operation at higher gas velocity, higher catalyst concentration and at higher temperature and/or pressure. The closest prior art proposal was published by Van der Laan *et al*. (1999) and a target was set to improve the reactor productivity by at least 50 %, relative to this reference, while also ensuring stable catalyst performance.

Prediction of gas holdup in the reactor is essential to determine the reactor productivity and previous correlations used to predict gas holdup are potentially unreliable for extrapolation to the new proposed conditions. A new approach is adapted, from previous theoretical approaches, to provide a more fundamental and reliable basis for gas holdup prediction. Referred to as the 'adapted two-phase theory' it predicts the gas holdup at any slurry solids concentration using data from a representative solids-free liquid. This approach is shown to provide accurate predictions for paraffinic liquids using data covering a wide range of solids concentrations.

Two laboratory reactor experiments were performed, at 260 and 270 ˚C, to characterise the selected catalyst performance at conditions relevant to the newly proposed operating regime. An achievable reactor performance was calculated corresponding to the catalyst performance from the experiment at 270 ˚C and using the new approach to predict gas holdup. Compared to the proposal by Van der Laan *et al*. (1999), a reactor with a given diameter is able to produce almost double the amount of product (94 % more with a lower slurry bed height). This is achievable by using higher catalyst concentrations and, most importantly, using a higher operating temperature. The undesirable methane selectivity, at or below 4 %, is still acceptable when operating at 270 ˚C. In spite of the higher reactor productivity with increasing temperature, the optimum operating temperature, in the range from 250 to 270 ˚C, may depend on the selectivity to the desired hydrocarbon products. The scope for further potential reactor productivity improvement is described.

More work is needed to accurately quantify the selected iron catalyst selectivity performance, in the proposed temperature range, but the hydrocarbon selectivity was found to be insensitive to other operating conditions (i.e. pressure and gas composition). It is now possible to better quantify the reactor productivity in the trade-offs which are made with the selectivity performance and the overall plant design configuration which requires recycle of carbon dioxide to the methane reformers to adjust feed gas H_2/CO ratio for natural gas applications. The carbon dioxide selectivity for the selected catalyst at the conditions tested was found to be too high for gas-to-liquid (GTL) applications using a natural gas feed.

Synopsis

When this work was initiated in 2007, it was identified that there was a gap in the knowledge base for the potentially promising alkali-promoted precipitated iron catalyst for hydrocarbon synthesis in a slurry-phase reactor at higher operating temperatures and pressures. The catalyst system investigated, i.e. an alkali promoted precipitated iron catalyst, was prepared so as to provide a catalyst with a performance which is directly comparable to the catalyst performance reported by Fletcher (2009). At this time, improved understanding of the capacity constraints for slurry-phase reactor systems in general had been developed, which indicated potential for higher reactor productivity. In particular, the possibility to use higher, than previously envisaged, gas velocity and catalyst concentration was identified.

The preferred higher gas velocity in the slurry was found to be outside of the range of the data used to develop reported correlations to predict the gas holdup in the reactor. Unpublished data from Koop (2003), reported in a confidential report to Sasol, was produced using paraffin liquids in a non-reactive mock-up and included data at higher gas velocities. This data was used to validate a new fundamental approach to the gas holdup prediction.

The literature indicated that the system is kinetically controlled so it was necessary to obtain kinetic data at the new proposed operating conditions. Experiments were performed at the Sasol laboratories in Sasolburg to obtain the required kinetic data at relevant new operating conditions. The kinetic data was then used with the new gas holdup correlation to calculate the reactor productivity for a range of gas velocities and catalyst concentrations. A unique feature of the selected catalyst system is that the catalyst composition adapts to the synthesis environment so that kinetic data developed in one particular synthesis environment is not necessarily directly relevant to another synthesis environment.

It is found that it is possible to significantly improve on the previously proposed reactor productivity for the iron-catalysed slurry-phase reactor system for hydrocarbon synthesis.

The most comparable previously proposed approach was modelled by Van der Laan *et al*. (1999) who recommended an optimum reactor feed H_2/CO ratio of 1.5. This feed composition can be compatible with a process used to convert natural gas to liquid hydrocarbon products in a gas-to-liquids (GTL) process. Benham *et al*. (2003) describe how such a reactor can be used in a GTL process. Higher catalyst concentrations, gas velocities, temperatures and pressures have now been explored.

Benham *et al*. (2003) reported good product yields with feed gas H_2/CO ratios ranging from 1.3 to 2.0 (at about 15 bar and 250 ˚C). They also showed that similar product yields can be obtained with shifting and non-shifting catalysts in a GTL process. Rather than the single stage reactor approach described in this patent, it is considered more likely that such a reactor application would be applied in a two stage configuration, as proposed by Van der Laan *et al*. (1999). It has further been found that the similar product yield result is not achievable if the carbon dioxide selectivity is too high for the shifting catalyst.

From the literature, it can be concluded that there is still scope to improve the catalyst stability and carbon dioxide selectivity relative to the activity of the catalyst tested for this thesis. Promotion with manganese (Yang *et al*., 2005[ab]; Li *et al*., 2006; Liu *et al*., 2007; Ding *et al*., 2009; Li *et al*., 2009) appears to be particularly promising.

Breman (2014) disclosed the advantages of applying a slurry-phase reactor for hydrocarbon synthesis with an inlet superficial gas velocity above 0.50 m/s which is also supported by this work.

The synthesis reactor hydrocarbon production per unit of metal surface (used to construct the reactor shell containing the slurry bed) was calculated using the new gas holdup correlation fitted to match the data from Koop (2003) (see Figure 1). This was done by varying the slurry bed height to keep the conversion constant when using a fully mixed continuous stirred tank reactor (CSTR) model with the rate equation proposed by Botes and Breman (2006).

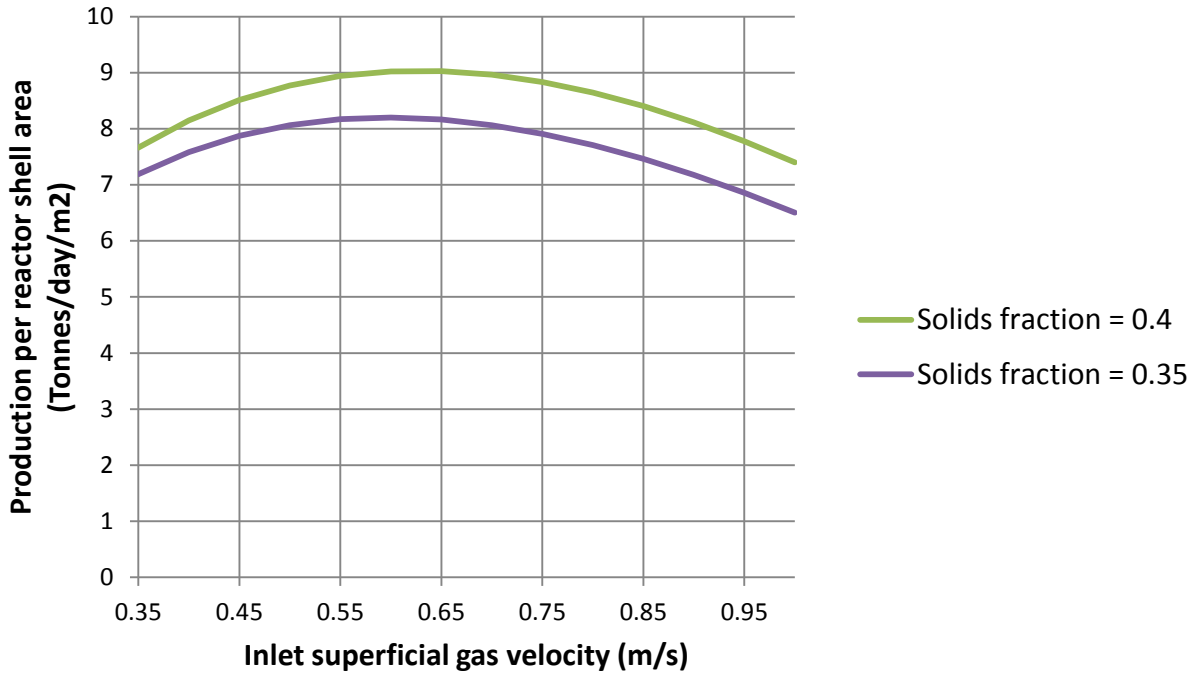

Figure 1: Reactor productivity versus gas velocity at 60 % H_2 + CO conversion

The modelling approach used in this work indicates optimum reactor productivity at an inlet gas velocity between about 0.55 and 0.75 m/s for the catalyst activity measured for a three day period ending at 450 hours of operation. Reactor productivity per unit of shell surface area is considered to be a better measure than production per unit reactor volume used in previous investigations, e.g. by Van der Laan *et al*. (1999).

With the average catalyst activity measured for the last three days up to 450 hours and a solids volume fraction of 0.35, the required bed height is 12.8 m at 0.6 m/s. This is less than the reactor bed height of 24 m selected by Van der Laan *et al*. (1999) when evaluating the same solids fraction. The catalyst concentration can be further increased, allowing operation at a higher optimum gas velocity up to 0.75 m/s.

The significance of the catalyst activity decline measured in the laboratory was investigated by illustrating that it is practical to maintain manageable reactor performance using a solids volume fraction ranging from 0.3 to 0.4 (which is within the range of applicability of a published gas holdup correlation). On-line partial catalyst replacement can be used after reaching the maximum allowable catalyst concentration.

The new fundamental approach developed to predict the gas holdup at any slurry solids concentration using data from a representative solids-free liquid is described as the 'adapted two-phase theory'. A slightly better fit to the data from Koop (2003) was found for this new approach than for the application of the correlations of Behkish *et al*. (2006) and Luo *et al*. (2009). The proposed approach is increasingly more conservative (higher gas holdup prediction) at higher solids concentrations. The new approach provides improved gas holdup predictions for paraffin liquids with a solids volume fraction at or above 0.3 and for gas velocities between 0.35 and 0.85 m/s.

The 'adapted two-phase theory' is based on the hypothesis that, above a certain gas velocity, the dense phase is saturated with small bubbles and that the small bubble fraction in the dense phase decreases as the slurry viscosity increases. The small bubble fraction is re-defined to be only the bubbles which remain in circulation in the slurry in the churn-turbulent regime.

An experiment, using a laboratory slurry micro-reactor (a so called continuous-stirred-tank reactor (CSTR)), at a selected higher temperature (270 ˚C) and similar pressure (30 bar) relative to the conditions selected by Van der Laan *et al*. (1999) (i.e. 250 ˚C and 30 bar) was used to determine the rate constant for the Fischer-Tropsch (FT) reaction. The CO conversion was initially 73.5 % with 50 % of the CO converted to hydrocarbon products and the synthesis gas (H_2 + CO) conversion was about 60 %. Higher operating temperature has a very positive impact on the reactor productivity.

It is sensible to use a reactor design procedure which targets a conversion level which is selected to support stable catalyst activity. The selected conversion for the reported experiment at 270 ˚C, which was found to exhibit reasonably stable catalyst activity, fits well with a two stage reactor design approach at 90 % synthesis gas (H_2 + CO) conversion overall and about 60 % conversion in the first stage reactor (which is also proposed in the literature which was reviewed).

For a selected target conversion, the reactor productivity is directly proportional to the amount of catalyst loaded into the reactor and, to achieve the target conversion, the required reactor bed height decreases as the catalyst concentration is increased and the maximum concentration is restricted by practical considerations.

A new comparatively high pressure (40 bar), low H_2/CO ratio (1.0) experiment (this work) was performed at 260 ˚C with a high average space velocity of 25000 ml_n/g-cat.h. The CO conversion to FT products for this experiment is rather low at around 20 %. The measured CO_2 selectivity was 24 % which may be acceptable for GTL applications but is still higher than desired and would require a long run to verify acceptable carbon dioxide selectivity.

Average partial pressures for new experimental data at 260 ˚C were:

Component	Average (bar)	Maximum (bar)	Minimum (bar)
Hydrogen	14.5	15.1	14.3
CO	15.8	16.0	15.3
Water	2.7	2.8	2.6
CO_2	1.25	1.1	1.35

Methane formation is not very temperature sensitive – the methane selectivity of 4.0 % measured at 270 ˚C (at 30 bar with H_2/CO ratio of 1.56) is constant with catalyst age. At 260 ˚C, a methane selectivity of 2.6 % was measured (at start-of-run conditions only).

The experiment at 270 ˚C was performed with a lower space velocity (11700 $ml_{(n)}$/g-cat.h) which increased the conversion to a level similar to the conversion range investigated by Van der Laan *et al*. (1999). Average (for 5 days at the beginning of the run) partial pressures of kinetically relevant components for the new experimental data at 270 ˚C were:

Component	Average (bar)	Maximum (bar)	Minimum (bar)
Hydrogen	12.0	12.3	11.71
CO	4.05	4.3	3.65
Water	3.9	4.15	3.55
CO_2	3.75	3.6	3.9

The measured product selectivity indicates that operation at a lower temperature between 250 and 270 ˚C may be desirable from the perspective of producing a larger proportion of the desired products.

The measured usage ratio was about 1.05, hence the accumulation of hydrogen relative to CO in the reactor. The carbon dioxide selectivity was 33 % which is too high to be suitable for GTL applications. For a GTL process, the carbon dioxide selectivity needs to be taken into account in the overall plant design which will involve the recycle of carbon dioxide to the reformer in order to reverse shift it to CO, but excessive recycle will drop the synthesis gas H_2/CO ratio below the desired range. On the other hand, Yang *et al*. (2012) report CO_2 selectivity of less than 20 % for CO conversions exceeding 90 %. There is likely to be an optimum CO_2 selectivity to achieve the maximum product yield from a GTL plant gas loop configuration.

The target reactor inlet H_2/CO ratio should be close to the reactant consumption ratio (usage ratio) in order to achieve the best reactor productivity, i.e. a feed ratio between 1.0 and 1.5 for the catalyst of this study. Higher gas velocities and catalyst concentrations, than those previously reported in the public domain, and a two-stage reactor design approach are recommended.

Two potential approaches have been identified to get the carbon dioxide selectivity into the preferred range for GTL applications at 270 ˚C. Firstly, catalyst promoters can be investigated to suppress the water gas shift activity of the catalyst (which will then

increase the usage ratio). Secondly, a non-shifting catalyst could be used in one of the reactor stages.

Applying the adapted two-phase theory and the measured catalyst performance at the conditions tested (temperature - 260 and 270 ˚C; pressure - 30 and 40 bar and feed H_2/CO ratio – 1.0 and 1.5), it has been found possible to significantly improve on the previously proposed reactor productivity for the iron-catalysed slurry-phase reactor system for Fischer-Tropsch (FT) synthesis. An 8 m diameter first stage reactor for a two stage reactor configuration can produce 5350 tonnes/day of C_{2+} hydrocarbon product with an optimized productivity per reactor shell surface area of about 9 tonnes/day.m^2, corresponding to a plant capacity of 16000 tonnes/day (125 000 bbl/d) using two first stage reactors and one second stage reactor to achieve an overall synthesis gas conversion of 90 %.

Further progress for GTL applications will require suitable laboratory experimental data with an optimized catalyst formulation, using gas inlet compositions compatible with the desired optimum gas loop design for a GTL facility, including the use of a feed H_2/CO ratio approaching the reactant usage ratio.

It is further recommended to find the overall economic optimum, taking into account the value of the various hydrocarbon products for operating temperatures in the range from 250 to 270 ˚C, after also taking into account the feed gas composition and using an operating pressure between 30 bar to 40 bar which balances the slurry phase reactor productivity with considerations relating to the overall gas loop design.

Acknowledgements

I would like to thank the following people and organizations for their help, influence and support:

Prof. Jack Fletcher: for his patience, assistance and guidance as my supervisor.

Sasol Technology, Research and Development Division: especially Philip Gibson, for permitting me to undertake this project.

Sasol Technology, Research and Development Division: for access to relevant reports and information.

Dr. Ben Jager, Prof. Mark Dry and Dr. Terry Shingles: for their tremendous legacy at Sasol in the hydrocarbon synthesis technology field based on the Fischer-Tropsch synthesis.

The Iron Fischer-Tropsch group: for generating the requested micro-reactor data.

My wife: for her understanding and support.

I would also like to thank my colleagues at Sasol Technology for their support, especially Luis Dancuart, Pieter Venter, Don Hauman, Matthys Janse van Vuuren, Jack Vincent Fletcher, Wimpie Booysen and Berthold Breman.

I started this project to impress Craig and Kristen and I finished it because I think the outcome is important.

CONTENTS

List of Figures

List of Tables

Notation

AARE (Average Absolute Relative Error) $= \frac{1}{N}\sum_{i=1}^{N}\left|\frac{\varepsilon_{G,exp,i}-\varepsilon_{G,calc,i}}{\varepsilon_{G,exp,i}}\right|$

C constants used in equations (9), (11) and (16)
C_F fitted parameter in equation (17)
C_{cat} volumetric catalyst concentration
d_b diameter of a sphere having the same volume as a “large” bubble, m
$d_{b,max}$ maximum stable bubble size, m
d internal diameter of the reactor, m
D_c critical column diameter, m
g acceleration by gravity, m/s^2
GHSV gas hourly space velocity, ml_n/g-cat.h

h_o parameter determining initial bubble size, m
h* height above the gas distributor where the bubbles reach an equilibrium size, m
H bed height, m
MRE (Mean Relative Error) $= \frac{1}{N}\sum_{i=1}^{N}\frac{\varepsilon_{G},exp,i-\varepsilon_{G},calc,i}{\varepsilon_{G},exp,i}$
P pressure, bar
R the gas constant
T temperature, K or ˚C
u_g inlet superficial gas velocity, m/s
U superficial velocity, m/s
U_b dilute phase "large" bubble (gas void) velocity, m/s
U_{df} dense phase gas velocity, m/s
U_s saturation velocity above which no additional small bubbles circulate in the slurry
$V_{b,max}$ single bubble rise velocity of bubble at the maximum stable bubble size, m/s
V_R reactor volume, m^3
$\overset{o}{V}$ total volumetric gas flow rate into the reactor, m^3/s
W_{cat} catalyst mass, kg
$\chi_{per\ pass}$ per-pass conversion of synthesis gas, mole fraction

Greek letters
α constant in equation (4)
ε_d dense phase gas holdup
ε_b dilute phase gas holdup
ε total gas holdup
ε_G fraction of total bed volume excluding internals occupied by gas in equation (3)
ε_p fraction of bed excluding internals occupied by particles in equation (3)
$\varepsilon_{internals}$ fraction of bed occupied by internals in equation (3)
σ surface tension (N/m)
ρ_G gas density (kg/m^3)
ρ_L liquid density (kg/m^3)
ρ_p particle density (kg/m^3)
μ_L liquid viscosity (Pa.s)
μ_{sl} slurry viscosity (Pa.s)
ø Werther rise velocity constant
φ particle volume fraction in slurry

1. INTRODUCTION

1.1 Field of Application

Transportation fuels are mostly produced from fossil crude oil or bitumen resources and this is the main current use for crude oil. This oil is extracted from the ground and processed in oil refineries to liquid products which meet the specifications which make these products suitable for use in modern engines. Crude oil is also used for other purposes such as a feedstock for the production of chemical products and as the energy source for the production of electricity.

There are two other, more abundant, fossil resources which can be used to make the same final products, namely coal and natural gas. It is usually more costly to convert the alternative resources to the same products as those derived from crude oil, with the exception of electricity. Coal and natural gas are already more widely used for the production of electricity than crude oil, and there are several other sources of energy which can be used for electricity production such as nuclear, solar, wind, biomass, urban waste and hydropower. As crude oil supplies eventually decline and prices increase, alternative sources of energy, hydrocarbons, carbon or hydrogen will increasingly be used to supplement the products derived from crude oil.

Electricity is finding increasing use as an energy source for vehicles, particularly in the use of hybrid petrol-electric cars, but the preferred fuel for heavy duty transportation is diesel with hybrid diesel-electric engines used for train locomotive drives (and recently for the Mercedes Benz E-class). In addition to electricity, methanol, DME, LPG and liquefied or compressed natural gas (or even hydrogen) can also be considered as vehicle fuels although new investment in fuel distribution infrastructure and the required vehicle modifications needs to be justified.

Natural gas is increasingly being used for conversion to diesel and/or jet fuel together with some other hydrocarbon co-products. This is achieved in a three step process which first converts the natural gas to synthesis gas containing hydrogen and carbon monoxide, known as reforming, and then, in a second step, the synthesis gas is converted to liquid products in a hydrocarbon synthesis reactor and, finally, in the third step (product work-up), the primary liquid hydrocarbons undergo further reactions employing some hydrogen (i.e. hydroprocessing) to produce liquids which meet the product specifications. This is often referred to as a Gas-to-Liquids (GTL) process. Due to the immense size of the existing diesel fuel market, it can be expected that the market for diesel fuel will remain essentially unrestricted for natural gas conversion facilities for a very long time.

There has also been recent interest in the production of diesel fuel from coal in China due to their abundant coal resources and rapidly increasing demand for diesel fuel. The use of precipitated iron catalyst in slurry-phase reactors is preferred for Coal-to-Liquids (CTL) applications (Liu *et al*., 2010). Luo (2012) published a review article describing the development of China's CTL technology using Fischer-Tropsch (FT) synthesis.

A concept known as polygeneration or coproduction (Shen *et al.* 2003) involves the co-production of electricity and hydrocarbon products and is expected to be attractive when carbon dioxide capture and storage is required. This approach was studied by Yu *et al*. (2010) who concluded that the plant is more or less power neutral when feeding the

Fischer-Tropsch (FT) tail gas to a combined cycle gas turbine and also producing electricity from the various steam sources from the process. The preferred approach to export power is to decrease the FT unit conversion so that more FT tail gas goes to the gas turbine, as proposed also by Steynberg and Nel (2004), rather than bypassing synthesis gas from the gasifiers to the gas turbine.

Dry (1996) has explained the desirability to co-produce chemical products. The primary products, from the hydrocarbon synthesis step, contain olefinic components that can also be used as a desirable petrochemical feedstock. Jager and Espinoza (1995) reported a 50 % olefin fraction in the C_{13} to C_{18} cut and these olefins are particularly attractive for the production of surfactants. In addition, the fraction of the primary hydrocarbon product comprising carbon numbers of 25 or more are ideal for the production of high grade lubricant base oils.

Aasberg-Petersen *et al*. (2004) explain the features of relevant reforming technologies which may be used to prepare synthesis gas from natural gas for the GTL process. This is the most expensive of the three main process steps and is responsible for the largest part of the energy conversion in the plant. Dry and Steynberg (2004) describe how these technologies are used in commercial GTL applications which usually involves some form of adjustment of the relative amounts of hydrogen and carbon monoxide produced in the reforming process.

All current and expected future reforming of natural gas for GTL applications use both catalytic steam reforming (an endothermic reaction requiring an external heat source) and exothermic partial oxidation reforming in which the feed is reacted with oxygen in a flame at high temperatures. When the partial oxidation is combined with a catalyst prior to the reactor exit to bring the gas mixture close to equilibrium, the process is known as autothermal reforming (ATR).

Benham *et al*. (2003) compare the use of two reforming processes, non-catalytic partial oxidation (POX) and ATR, combined with both shifting FT catalyst at 250 °C and non-shifting FT catalyst in a GTL process.

Earlier, Gray and Tomlinson (1997) prepared a technical and economic comparison of natural gas and coal feedstocks for an iron-based catalyst investigated by the US Department of Energy (DOE). They also explored the effect of removing water gas shift activity from their iron-based catalyst.

More recently, Hao *et al*. (2008[c]) have also prepared a comparison for GTL plant designs with non-shifting (cobalt-based) and shifting (iron-based) FT catalyst for GTL facilities using ATR reforming. They concluded that the carbon efficiency for a GTL plant using iron-based catalyst would be 68 % relative to 73 % using cobalt-based catalyst. However, they assumed very high carbon dioxide selectivity (45 %). The result reported by Benham *et al*. (2003), that the carbon efficiency for both types of catalyst will be similar must be based on a lower carbon dioxide selectivity. In theory, the process efficiency should be determined by the energy balance considerations, provided that the carbon dioxide selectivity is not excessive, and can be similar for both types of catalyst. This will, however, require a different GTL process flowsheet structure for each type of catalyst.

It has been thought that ATR or non-catalytic partial oxidation (POX) costs less than

steam (and CO_2) reforming only for large scale applications because of improved economy of scale for oxygen plants relative to the tubular reformer (Rostrup-Nielsen, 2002). However, ATR technology has recently been selected for a small GTL plant with a capacity of 2000 bbl/day and may be preferred at small scale when oxygen is available for import as a utility. Bakkarud (2005) concluded that the ATR technology holds promises for significant, further improvements, both as a stand-alone technology and in combination with heat exchange reforming in a series arrangement (Haldor Topsøe exchange reforming in series (HTER-s)). According to Bakkarud, these technologies will be dominant, at least for the next 5–10 years (and probably for much longer given that it is already nearly 10 years after this prediction was made).

Steynberg *et al*. (2013) announced that Sasol Technology was ready to use heat exchange reforming technology for commercial application in GTL facilities. This is based on the latest technology developed by Haldor-Topsøe, and evaluated by Sasol using information provided by Aasberg-Petersen.

The topic of this work is a type of reactor used for hydrocarbon synthesis in the second step of this natural gas conversion process. The hydrocarbon synthesis usually proposed for GTL applications is typically referred to as the Fischer-Tropsch synthesis. It can also be used to convert any other source of synthesis gas to primary hydrocarbon products so it may further be used in a Biomass-to-Liquids (BTL) or Coal-to-Liquids (CTL) process for which the biomass or coal is converted to synthesis gas by means of gasification as a first step. However, coal gasification is more costly than natural gas reforming and is inevitably accompanied by higher carbon dioxide emissions in the absence of a carbon capture and storage solution (which, if available, would add to the capital cost disadvantage).

1.2 Aims and Objectives

The aim of this research is to explore alternative operating conditions for a generic alkali promoted precipitated iron catalyst in a slurry-phase reactor system. The objective is to find a combination of operating conditions providing increased reactor productivity for the hydrocarbon synthesis relative to previously published approaches. A target is set to increase the reactor productivity by at least 50 %. The achievement of this objective will decrease the cost for the production of hydrocarbon products with the aim to be competitive with a range of products, including fuels, which are today made from crude oil.

The relevant operating conditions to be selected are the operating temperature, pressure, catalyst concentration, gas velocity and feed gas composition. To be comparable to other alternatives, the reactor system productivity is determined for an overall synthesis gas conversion of at least 90 %. It is expected that this will be achieved with a two stage reactor configuration with a synthesis gas conversion of about 60 % in the first stage reactor. In addition, the conditions are to be selected to allow this conversion to be maintained for several weeks without catalyst replacement and to be sustainable for long campaigns by means of on-line catalyst removal and addition.

This iron-based catalyst produces more olefinic primary hydrocarbon products, relative to the cobalt catalysts, which may be more valuable for conversion to petrochemical

products. This may result in an attractive commercial option if competitive reactor productivity, in a cost effective GTL gas loop design, can be achieved.

The reactor productivity comparison to previously published reactor productivity information is confined to the first stage reactor. If the relative productivity is favourable for the first stage reactor then it is safe to assume that this will also be the case for the second stage reactor. For polygeneration applications starting with a solid feed, a second stage reactor may not be needed.

1.3 The Reactor Options for Hydrocarbon Synthesis

There are four types of hydrocarbon synthesis or Fischer-Tropsch (FT) reactors in commercial use at present. These are:

- Circulating fluidized-bed reactor
- Tubular fixed-bed reactor
- Fluidized-bed reactor
- Slurry-phase reactor

The industrial catalysts are either based on supported cobalt metal with noble metal promoters or alkali promoted iron carbide. Three different catalyst platforms are used:

- Fused iron catalyst with alkali metal promoters
- Precipitated iron catalyst with alkali metal promoters
- Supported cobalt catalyst

The latter two catalyst platforms are used in both tubular fixed-bed and slurry-phase reactors while the first is used in the two-phase fluidized bed reactors.

Commercial hydrocarbon synthesis in slurry-phase reactors occurs at the lower temperature range (220 to 250 °C) and these are collectively referred to as the Low Temperature Fischer-Tropsch (LTFT) synthesis. The two-phase fluidized-bed reactors are used commercially for High Temperature Fischer-Tropsch (HTFT) synthesis at temperatures ranging from 320 to 350 °C. This investigation explores the use of a slurry-phase reactor, in an intermediate temperature range above 250 °C and up to 270 °C, which is now being used in China.

Recently there has been an industrial focus on reactor intensification (Vogel *et al*., 2007) which implies the making of more hydrocarbon liquid products from a given reactor shell diameter and, consequently, to significant capital cost benefits. To-date the focus has been mainly on the reactors which use the supported cobalt catalyst and the fused iron catalyst. The precipitated iron catalyst was therefore selected for this investigation. This iron catalyst is used in a slurry-phase reactor which is also the approach used for the cobalt catalyst so that correlations developed to describe the gas fraction in the slurry (gas holdup) are applicable to processes which employ either of these catalysts.

1.4 Characteristics of the Selected Catalyst and Reactor System

The selected catalyst used to facilitate the Fischer-Tropsch or hydrocarbon synthesis reaction in this reactor is a precipitated iron catalyst. The catalytic material is in the form of a powder prepared by a spray drying process to produce spherical particles, typically smaller than 200 microns. This material is conditioned in the presence of carbon monoxide, and optionally hydrogen, to produce an iron carbide phase which is active for hydrocarbon synthesis.

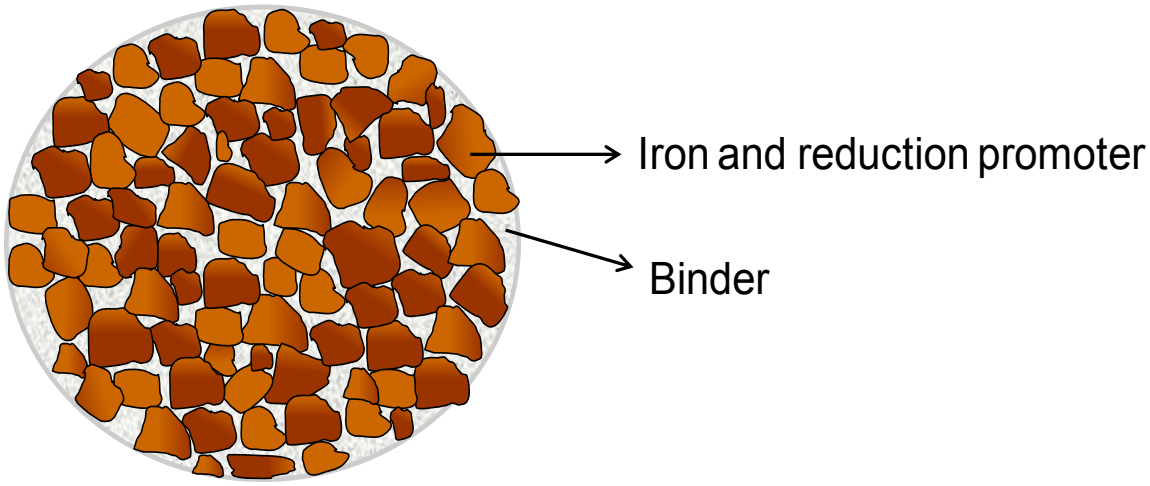

- **Iron as active metal (typically 60 - 65 wt.%)**
- **Second metal, often Cu, added as a reduction promoter (1 – 6 wt.%)**
- **Alkali metal (e.g. K) as promoter (1 – 6 wt.%)**
- **Structural promoter (e.g. SiO_2) as binder (1 – 20 wt.%)**
- **Co-precipitation of metals ⇒ binder addition ⇒ spray drying**

Figure 2: Schematic representation of a bulk iron catalyst for slurry-phase reactor application (Botes *et al*., 2013)

During hydrocarbon synthesis, the catalyst performance declines with time-on-stream and the rate of decline is important since catalyst consumption is a significant contributor to operating cost. Reactor intensification, to increase the reactor productivity, may be constrained, for the catalyst investigated, by the avoidance of operating conditions which lead to too rapid catalyst deactivation or to physical degradation of the catalyst.

The selected type of reactor, known as the slurry-phase reactor, slurry bed reactor or slurry bubble column reactor is characterised by the distribution of the synthesis gas through a gas distributor at the lower end of the reactor into a heavy hydrocarbon liquid in which the powdered catalyst is suspended to form a solid-liquid slurry.

It is envisioned that this reactor may be fed with synthesis gas derived from coal gasifiers or methane reformers to which carbon dioxide is recycled. These sources of synthesis gas have H_2/CO ratios which can be expected to range from about 0.5 to about 2.0. The

ratio may be adjusted upwards by reacting with steam or water vapour using the so-called water gas shift (WGS) reaction.

For purposes of understanding feed conversion, principal reactions of relevance are:

$CO + H_2O \rightarrow CO_2 + H_2$ - water gas shift (WGS)

$CO + 3H_2 \rightarrow CH_4 + H_2O$ - methanation

$2CO + xH_2 \rightarrow C_2H_{(2x-2)} + H_2O$ - Fischer-Tropsch (FT) commencement (x = 2 or 3)

$CO + C_nH_{2n+y} + 2H_2 \rightarrow C_{n+1}H_{2n+2+y} + H_2O$ - FT continuation for n > 1 (y = 0 or 2)

The overall usage ratio (or consumption ratio) is defined as the ratio at which hydrogen and carbon monoxide are consumed. The specific usage ratio for the Fischer-Tropsch reaction alone is slightly above 2, but with simultaneous water gas shift conversion, the consumption ratio decreases, as the WGS reaction consumes carbon monoxide and supplies hydrogen to the reacting system. Importantly, the WGS reaction also consumes part of the water produced by the FT reaction.

Iron catalysts generally are referred to as “shifting” catalysts to distinguish their performance from cobalt catalysts which have virtually no water gas shift activity and are therefore referred to as “non-shifting” catalysts. A further distinction needs to be made for the HTFT catalysts for which the reverse water gas shift reaction can, and usually does, occur since the CO reactant is consumed to low levels and the higher operating temperature encourages reaction of hydrogen with carbon dioxide and there is a reasonably close approach to water gas shift equilibrium at the reactor outlet. At temperatures of 270 ˚C or lower it is not possible for the reverse water gas shift reaction to take place, because the lower temperature favours the forward water gas shift reaction and the CO partial pressure in the reactor needs to be kept at a higher level to ensure competitive FT reaction rates. At these lower temperatures, the net rate of carbon dioxide production is determined by the kinetic performance of the catalyst and, unlike HTFT, equilibrium compositions are not attained at the reactor outlet.

There has been considerable investigation of similar catalyst systems in China over the last 10 years. Wang *et al*. (2003) tested an industrial Fe-Cu-K catalyst over a temperature range from 220 ˚C to 269 ˚C, pressure from 10.9 to 30.9 bar, H_2/CO feed ratio from 0.98 to 2.99. They reported the highest catalyst productivity at 30.9 bar, 1.52 feed H_2/CO ratio and 268 ˚C, similar to conditions explored in this study, but no information was provided on catalyst stability. Hao *et al*. (2008[a]) reported data which showed that their iron catalyst was unstable above 270 ˚C when the H_2 + CO conversion went above about 60 % (as temperature was increased with a constant space velocity). Much of the reported work was aimed mainly at improving both activity stability and catalyst strength (attrition resistance). This was apparently successful, but, in some cases, there has been a sacrifice of catalyst activity in order to achieve stable performance with time-on-stream.

For example, Wu *et al*. (2004) reported using a space velocity of 3200 ml_n/g-cat.h to achieve stable H_2 + CO conversion of 65 % at 20 bar, 260 ˚C with 0.67 feed H_2/CO ratio. This was with a precipitated iron catalyst containing low levels of sulphate. Due to the linear relationship with pressure, this corresponds to a space velocity of 4800 ml_n/g-cat.h

at 30 bar. This stable performance at higher conversions (but with a lower H_2/CO ratio feed gas), reported by Wu *et al*. (2004), was achieved after about 500 hours operation. Therefore, it may be necessary to run for relatively long periods to obtain data for design approaches targeting stable catalyst performance.

Nevertheless, it seems likely that stable catalyst performance at a reasonable space velocity, using the catalyst of Wu *et al*. (2004), is achievable by designing the reactor to operate with a greater bed height to accommodate more catalyst relative to more active catalyst options.

Besides low levels of sulphate, some metals have been investigated which are claimed to also contribute to activity stability, i.e. Zr (Qing *et al*., 2011 Qing *et al*., 2012), Mg (Yang *et al*., 2006) and Mn (Teng *et al*., 2005; Yang *et al*., 2005[a]; Yang *et al*., 2005[b]; Zhang *et al*., 2006; Li *et al*., 2006; Liu *et al*., 2007; Ding *et al*., 2009 and Li *et al*., 2009).

Molybdenum (Qin *et al*., 2011) is also used as a promoter but only when targeting a much lighter product spectrum and hence is not applicable to this work.

Shen *et al*. (2003) describe catalyst R&D supported by the US Department of Energy (DOE) as follows: “The objective of the slurry-phase Fischer-Tropsch catalyst work is to develop a family of iron catalysts with different alphas (probability of chain growth) that is capable of producing a broad slate of products for coproduction applications. The choice of iron over cobalt catalysts is based on its superior versatility in product selectivity, intrinsic water-gas shift (WGS) activity, and high tolerance for trace impurities in syngas. The low-alpha iron catalysts are primarily for light chemicals production, the intermediate-alpha ones for linear alpha olefins production in the C_{10} to C_{17} ranges, and the high-alpha ones for wax and fuel production.” Product selectivity considerations are discussed in section 2.2.

Hao *et al*. (2008[b]), on the other hand, reported synthesis performance, competitive with the Ruhrchemie SB3291 catalyst, at H_2 + CO conversion of 45 % for a fairly conventional 100Fe/5Cu/4.2K/25SiO_2 catalyst with impressive attrition resistance and stable activity and selectivity (for 500 hours). The key to this success appears to be the catalyst precursor preparation approach and optimized catalyst conditioning.

Yang *et al*. (2012) reported exceptional selectivity performance at CO conversion above 87 % when using one or more metal promoters selected from the group consisting of Mn, Cr and Zn. The carbon dioxide selectivity was less than 20 %, methane selectivity less than 5 %, C_{5+} selectivity greater than 90 % and C_2 to C_4 olefin plus C_{5+} selectivity potentially as high as 96 %.

1.5 Study Approach

The first aspect to be studied is the physical characteristics of the selected reactor system. In order to achieve higher reactor productivity, higher gas velocities and higher catalyst concentrations are required and it is necessary to determine whether available gas holdup predictions are reliable at the desired operating conditions. Previously published empirical correlations may be unreliable when extrapolating to higher gas velocities and catalyst concentrations, so it is considered important to try to find an

approach which is based on a more fundamental understanding of the influence of gas velocity and catalyst concentration on the gas holdup in the reactor. This fundamental understanding is also desired to identify the upper limit constraints.

Representative gas holdup data was generated by Koop (2003) for gas velocities up to 0.76 m/s and catalyst volume fractions in the slurry up to 0.415. This can be compared to the gas velocity upper limit of 0.69 m/s and the catalyst volume fraction upper limit of 0.4 for the data used to develop the correlation by Luo *et al*. (2009)). The intention is to show that it is possible to accurately predict the gas holdup data from Koop (2003) above 0.35 m/s using an adapted two-phase fluidization theory.

There are trade-offs required due to the fact that, for a given amount of catalyst, reactant conversion to products decreases as the gas feed rate is increased. The amount of catalyst in a given reactor volume is determined by the maximum practical catalyst concentration in the slurry and the amount of slurry which can be contained in a given reactor volume - which is influenced by the gas holdup in the slurry bed.

As reactants are consumed, the reaction rate declines due to the decreasing reactant partial pressures but if reaction products, particularly water and/or carbon dioxide, are removed then the reaction rate may be revived in a second stage reactor. A motivation is provided in support of the approach to use two reactor stages to achieve a commonly proposed target of 90 % overall reactant conversion. In the absence of recycle, this approach requires a reactant (H_2 + CO) conversion of at least 60 % for the first stage reactor.

Botes *et al*. (2013) explain why it has been considered necessary to limit per-pass conversion for the reason of catalyst stability. Quoting from Breman (2014): "…water (one of the products of the hydrocarbon synthesis process) causes deactivation of the catalyst. Consequently, a maximum per-pass conversion is normally specified that should not be exceeded in the design of a Fischer-Tropsch slurry bubble column reactor in order to limit the water partial pressure and thereby protect the performance and lifetime of the catalyst. The exact value of the per-pass conversion is catalyst dependent." Van Berge (1994) postulated that the upper limit may be influenced by operating at higher temperatures. Furthermore, water production can be decreased by operating at lower feed gas H_2/CO ratios. Feed gas H_2/CO ratios in the range from 1.3 to about 1.6 are lower than the values considered by Botes *et al*. (2013) and are expected to be compatible with gas-to-liquids (GTL) applications. Benham *et al*. (2003) describe how such a reactor can be used in a GTL process.

The most comparable previously proposed approach was modelled by Van der Laan *et al*. (1999), who recommended an optimum reactor feed H_2/CO ratio of 1.5 and also proposed a two-stage reactor design approach. Compared to the work by Van der Laan *et al*. (1999), it is considered that it may be possible to substantially further increase the reactor productivity, by at least 50 % by operating with a combination of higher temperatures, higher pressures, higher gas velocities and higher catalyst concentrations.

Relevant kinetic data is produced in a laboratory experiment for the selected catalyst in order to calculate the achievable reactor productivity for comparison to the reactor productivity reported by Van der Laan *et al*. (1999).

2. BACKGROUND & RELEVANT LITERATURE

2.1 Opportunity to Improve the Selected Reactor Productivity

New opportunities to improve the reactor productivity are possible when using an optimized H_2/CO ratio feed gas in GTL applications. It is also postulated that there exists scope to produce a desirable hydrocarbon product spectrum, at higher operating temperatures which is accompanied by higher reaction rates.

The desired final product in the fuels production mode is primarily diesel and/or jet fuel with naphtha and/or paraffins and/or olefinic petrochemical feedstock as significant co-products. It may be more desirable, depending on the circumstances, to target the C_{25+} material used for lubricant base oils as the desired primary product.

For a given product selectivity, Botes *et al*. (2013) have recently provided an elegant explanation of the factors determining the reactor capacity as follows: "*Regardless of whether a slurry bubble column FT reactor operates in a once-through mode or under recycle, the production rate of a single reactor can be expressed as follows:*

$$SRC = \overset{o}{V}\left(\frac{P_{syngas}}{RT}\right)\left(\chi_{per\ pass}\right), \tag{1}$$

where SRC *is the single reactor capacity,* $\overset{o}{V}$ *is the total volumetric gas flow rate into the reactor (i.e. fresh feed plus recycle),* P_{syngas} *is the partial pressure of synthesis gas at the reactor inlet, T is the absolute temperature in Kelvin, R is the gas constant and* $\chi_{per\ pass}$ *is the per-pass conversion of synthesis gas expressed as a mole fraction. The above equation can be further expanded as follows:*

$$SRC = u_g\left(\frac{\pi}{4}d^2\right)\left(\frac{P_{syngas}}{RT}\right)\left(\chi_{per\ pass}\right), \tag{2}$$

where u_g *is the inlet superficial gas velocity and* d *is the internal diameter of the reactor. Considering equation (2), it is clear that the following parameters determine the single reactor capacity of an FT slurry bubble column reactor:*

Inlet superficial velocity: As the gas velocity through a slurry bubble column increases, the gas holdup increases and eventually a flow regime transition will occur where gas becomes the continuous phase that is suspending slurry droplets, or the slurry will be transported out of the reactor. The superficial gas velocity is thus limited by hydrodynamic constraints, but this limit is to a large extent independent of the type of catalyst used.

Reactor diameter: By increasing the reactor diameter, the volumetric feed rate into the reactor can be increased without exceeding the limits on the gas velocity. However, large scale slurry-FT reactors are already manufactured at the limits of what is practically feasible in terms of factory construction, transportation and erection at site.

Syngas partial pressure at reactor inlet: The concentration of syngas in the total reactor feed is largely set by the gas loop design, and limited scope exists to increase this significantly. The more obvious way of increasing the inlet syngas partial pressure is to

increase the total pressure of the system, but the cost of a higher pressure reactor and other equipment will escalate. Furthermore, at the same per-pass conversion, higher operating pressures result in higher exit water partial pressures, which can be detrimental to the catalyst.

Per-pass conversion: Water damages the catalyst, which leads to faster deactivation or even an abrupt drop in activity. Since water is a product of the FT synthesis, the outlet water partial pressure increases with increasing per-pass conversion. This places a limit on the per-pass conversion that can be achieved in an FT reactor.

From the above analysis, it is clear that the catalyst property with the biggest influence on the single reactor capacity is its ability to withstand water. Cobalt catalysts can generally tolerate much higher water partial pressures than iron catalysts, so it is expected that cobalt would allow for much higher single slurry-FT reactor capacities than iron. Sasol has indeed announced new designs allowing for 24 000 bbl/day production capacity from a single reactor for its cobalt-based Sasol Slurry Phase Distillate (SSPD^{TM}) process and has indicated that there is still further potential for increased capacity. In other words, one would expect a cobalt-FT design to comprise a smaller number of tall reactors with a large capacity each and an iron-FT design to comprise a larger number of short reactors with a lower capacity each, given a certain required plant capacity.

One way of circumventing the capacity limitations of an iron-FT reactor is to feed a low H_2/CO ratio syngas to an iron catalyst having a high WGS activity. Since a significant portion of the water produced would be shifted to CO_2 under such conditions, high per-pass conversions can be achieved while limiting the maximum water partial pressure inside the reactor."

This analysis by Botes *et al*. (2013) was mainly based on the observed behaviour of iron catalyst at temperatures below 250 ˚C and did not consider the potential increased tolerance of the iron catalyst to water partial pressure with increasing temperatures. It should also be noted that the activity of the benchmark precipitated iron catalyst is higher than the benchmark supported cobalt catalyst at temperatures above 255 ˚C (see Figure 5). This means that a given per-pass conversion can be achieved using a relatively higher gas velocity at temperatures above 255 ˚C. The increased temperature driving force for heat removal is a further significant advantage when increasing reactor capacity. The iron catalyst system is also more responsive to operating pressure than the cobalt catalysts which again allows for higher molar flows to be used to reach a given per-pass conversion.

A 90 % overall synthesis gas conversion is a common target for an economically viable synthesis gas conversion facility. This can be achieved with two reactor stages (with intermediate water removal) if the first stage reactor is capable of operating at a 60 % per-pass conversion without recycle. So unless one catalyst system is capable of achieving the 90 % per-pass conversion in a single stage then either undesirable recycle or at least two reactor stages will be needed to achieve the target overall conversion. In the absence of first stage recycle, the relative plant capacities are a function of the relative molar flows to the first stage reactor/s.

Depending on the catalyst activity, it may be counter-productive to reactor productivity to operate at too high gas velocity due to the need to use excessively tall reactors. The

relative molar flows are determined by the combination of CO mole fraction, gas velocity, pressure and temperature. If similar gas velocity limits are reached for the desired, cost effective, reactor productivity then the iron catalyst should operate at a higher CO partial pressure in a shorter reactor relative to the cobalt catalyst to achieve improved productivity from a two-stage reactor system.

It is possible that the benefits of increased single reactor productivity for two reactor stages, when using iron catalyst at relatively higher temperatures and pressures, may be more economically beneficial than using fewer (but taller) reactors with cobalt catalyst, even if single stage operation with a 90 % conversion is achievable with the cobalt catalyst.

It is now clear that current commercial slurry-phase reactors are not yet at their capacity limits (Vogel *et al.*, 2007; Steynberg, 2010; Breman, 2014). There is now a need to demonstrate significantly higher reactor capacities compared to the current known benchmarks. The design of FT reactors is generally a compromise between competing trends which require optimization (Steynberg *et al.*, 2004 – p150). For example, higher operating temperatures, which increase the FT reaction rate, may increase the reactor capacity and productivity to the extent that there is scope to increase the feed gas velocity in proportion to the increased reaction rate. On the other hand, selectivity trends with increasing temperature may lead to a decline in the production of the desired products. The emphasis is on an understanding of the factors which constrain the reactor design so that the optimization process is not unnecessarily limited.

The use of a slurry-phase reactor with a gas velocity of at least 0.35 m/s has been patented (Steynberg, 2010). This patent applies to reactors with an aspect ratio of less than 5 using a non-shifting catalyst at H_2 + CO conversion of at least 60 %. Subsequently, Breman (2014) disclosed the advantages of applying a slurry-phase reactor for hydrocarbon synthesis in general with an inlet superficial gas velocity above 0.50 m/s.

Zhang and Wright (2006) explain quite nicely that maximum reactor productivity (or minimized reactor volume) is achieved with at least two reactor stages. They report a minimum reactor volume to achieve a total synthesis gas conversion of 90 % to be less than 0.02 cubic metres total reactor volume/(kg C_{5+}/h production). The C_{5+} production rate is claimed to exceed 50 kg/h.m^3 expanded catalyst bed. They target a synthesis gas conversion of less than 60 % in each reactor. Their example discloses a four stage design with a maximum superficial gas velocity of 0.655 m/s in the second stage and a minimum superficial gas velocity of 0.461 m/s in the first stage. However, it seems preferable to avoid more than two reactor stages by operating close to or slightly above 60 % conversion in each stage, to avoid adding the additional inter-stage cooling and condensing equipment, as there are significantly decreasing benefits to the reactor productivity when using more than two stages.

Zhang *et al*. (2005) explain that “at the intermediate conversion range, say conversion from 35 % to 75 %, the reactor volume required for the well-mixed gas flow is close to that for the plug flow regime.” The lower the conversion, the less the difference between inlet and outlet conditions and hence there is less difference resulting from the use of plug flow or well-mixed models. Reality is somewhere between these two extreme descriptions of the reactor mixing. This means that the mixing model used to calculate the reactor

performance is not particularly important for a design approach using two or more reactor stages. Bhatt *et al*. (1995) also reported that the well-mixed model used to match laboratory data could be used to predict their demonstration scale data with reasonable accuracy.

Fox (1990) also showed that for per-pass conversions of 60 % or less there is no significant difference in conversion prediction using a plug flow or fully mixed model. He also illustrates the rapid decline in reactor and catalyst productivity as the per-pass conversion is increased. Depending on the inert content in the feed, a 95 % overall conversion can be achieved with an internal recycle ratio of 1.0 or lower at a per-pass conversion of 60 %. The same overall conversion can be achieved using two reactor stages without recycle.

In the case of the alkalized precipitated iron catalyst, a catalyst precursor is typically conditioned (pre-treated) by reduction with hydrogen and, subsequently, carbon monoxide, or with mixtures of hydrogen and carbon monoxide (syngas), see for example Adeyiga (2003). At some point the catalyst precursor begins to exhibit FT activity and, once stable, it can then be exposed to the full normal synthesis conditions. Typically, externally conditioned catalyst is transferred to an operating reactor by on-line catalyst addition following the on-line removal of a portion of used catalyst (Steynberg *et al.*, 2004 - p72). Exposure of the catalyst precursor to FT conditions with high water formation results in the formation of inactive magnetite (O'Brien *et al.*, 1996; 1997).

For iron catalysts, it is generally accepted that iron carbide formation must occur before the active catalyst surface species for FT synthesis can form (Shroff *et al.*, 1995 - p205). According to Adeyiga (2003), at least five different forms of iron carbide are known to exist. Dry (2004[c]) has noted that maximum conversion corresponds to high levels of Hägg carbide (Fe_5C_2). Typical commercial LTFT synthesis conditions avoid the formation of graphitic carbon (Dry, 2004[c] - p. 567). The water formed during LTFT synthesis can react with the catalyst to form oxides (Dry, 2004[c] – p.569). Also, sintering which results in the loss of catalytic surface available for reaction is promoted by the presence of water (Dry, 2004[c] – p.569).

Upper limit per-pass conversions have been investigated for the slurry phase reactor (Janse van Vuuren, 2004) and rapid catalyst deactivation has been observed when a certain upper limit per-pass conversion is exceeded due to the resulting high water partial pressure, as explained by Breman (2014). For this reason an upper limit is set for the allowable per-pass conversion. This upper limit seems to be reasonably insensitive to the operating pressure so it is not sufficient to simply set an upper limit for the water partial pressure. For example, precipitated iron catalyst used in fixed bed Arge reactors was operated at up to 60 bar inlet pressure and similar per-pass conversion levels were achieved at all operating pressures when maintaining the same linear velocity (Steynberg *et al*, 2004 - p.68). Based on this result, an Arge reactor operating at higher pressure (45 bar inlet) was installed in 1987 (Dry, 1990).

Van Berge (1994) explored the performance of a representative precipitated iron catalyst at 250 ˚C and 20 bar with H_2/CO ratio inside the CSTR reactor ranging from 1 to 7 and concluded (p.3-60) that for syngas (H_2 + CO) conversions as high as 52 % significant catalyst deactivation does not occur. He also suggested (p. 7-1) that more insight into the absolute reactor water partial pressures that can be tolerated should be gained and that

the influence of reactor temperature on this phenomenon should be quantified. No subsequent publications were found which unambiguously explore this recommendation.

It is desirable to feed synthesis gas to the FT reactor with hydrogen and carbon monoxide close to the overall usage ratio (Dry, 2004[a] - p.201). For any reactor system, this approach makes the most effective use of the reactor volume since it avoids a loss of reaction rate due to the preferential depletion of one of the reactants.

If the water gas shift activity is high, e.g. at higher operating temperatures, then the overall H_2/CO usage ratio decreases and less water is produced. This may allow higher per-pass conversion levels because there is less water in the reactor to cause hydrothermal sintering. This hypothesis is supported by reported data (Adeyiga, 2003 – p.23) which indicated that reasonably stable catalyst performance can be achieved at an operating temperature of 260 ºC (with a total pressure of 21 bar and $H_2/CO = 0.67$) while achieving a methane selectivity of 2.0 ± 0.2 % and an overall usage ratio of about 0.55 (49 % CO_2 selectivity). The per-pass conversion declined from about 85 % to 60 % in about 450 hours and clearly more stable conversion is desired. It is unclear from this data whether or not the formation of graphitic carbon was causing problems and there was no explanation of the causes for the FT activity decline. It can be expected that higher operating pressure together with a higher (than 0.67) feed gas H_2/CO will lead to improved catalyst stability.

Interestingly, a similar postulate that graphitic carbon formation can be avoided by operating at higher pressure was made by Hall, Gall and Smith (1952) and they were able to demonstrate stable catalyst performance at a temperature of 305 ˚C and a pressure of 41.4 bar(g) using an iron based ammonia synthesis catalyst in a slurry phase reactor. The spent catalyst was found to comprise 42.3 % iron carbide, 45.3 % iron oxide and 4.4 % free (graphitic) carbon by weight after 192 hours. For this experiment the synthesis gas H_2/CO ratio was 2.0 and a recycle ratio of 3.7 was used to give an overall $H_2 + CO$ conversion of 97 % at a total feed H_2/CO ratio of 3.27. The present study aims to use a more active catalyst at a lower temperature (to completely avoid free carbon) and a selected moderate per pass conversion which, together with a lower feed gas H_2/CO ratio, avoids oxidation.

Chang *et al*. (2007) generated relevant data to fit a kinetic model mostly at a constant, relatively low, space velocity of 2000 ml_n/g-cat.h. The operating ranges were: feed H_2/CO ratio 0.67 to 1.5; pressure 10 to 25 bar and temperature 250 to 290 ˚C. The highest C_{5+} productivity was reported at the highest pressure and lowest temperature with a feed gas H_2/CO ratio of 1.24. The carbon dioxide selectivity for this data point was 37 % at a relatively high CO conversion of 72 %.

For this thesis it is considered that 25 bar and 250 ˚C should be at the lower end of the optimization range and that higher space velocities should be used while the feed H_2/CO ratio should be explored between 1.0 and 1.6.

The product selectivity for the precipitated iron catalyst is relatively insensitive to the feed gas pressure and the wax selectivity increases with decreasing H_2/CO particularly when the H_2/CO is below 1.9 (Dry, 2004[a]).

Fernandez (2006) constructed a mathematical model based on data reported by Raje and Davis (1997) and Donnelly and Satterfield (1989) and investigated reactor productivity optimization at 270 ˚C. A maximum pressure of 30 bar and a maximum superficial gas velocity of 0.45 m/s was considered. It was concluded that the reactor should be operated at the upper limit of the range considered for these parameters no matter what the desired products are. Volumetric solids fraction in the slurry in the range from 0.10 to 0.25 was considered for a fixed bed height of 30 m and it was found to be desirable to suppress the per-pass conversion in all cases by operating at the minimum solids fraction in this range. The reactor design by Van der Laan *et al*. (1999) was considered as the benchmark for comparison by Fernandez (2006) who found that the reactor specific volumetric productivity for the catalyst of Raje and Davis (1997) was 17 – 20 % lower than reported by Van der Laan *et al*. (1999) when using a similar approach to gas holdup modelling. This is not surprising considering the use of relatively low potassium content for the catalyst of Raje and Davis (1997) and the similar proposed operating pressure and gas velocity. For this catalyst, Fernandez found a similar optimum feed H_2/CO ratio (between 1.1 and 1.4) when targeting maximum gasoline (naphtha), diesel or C_{15+} olefin production but that the optimum is lower (0.9) for maximum wax production and higher (1.75) for maximum C_{4+} olefin production.

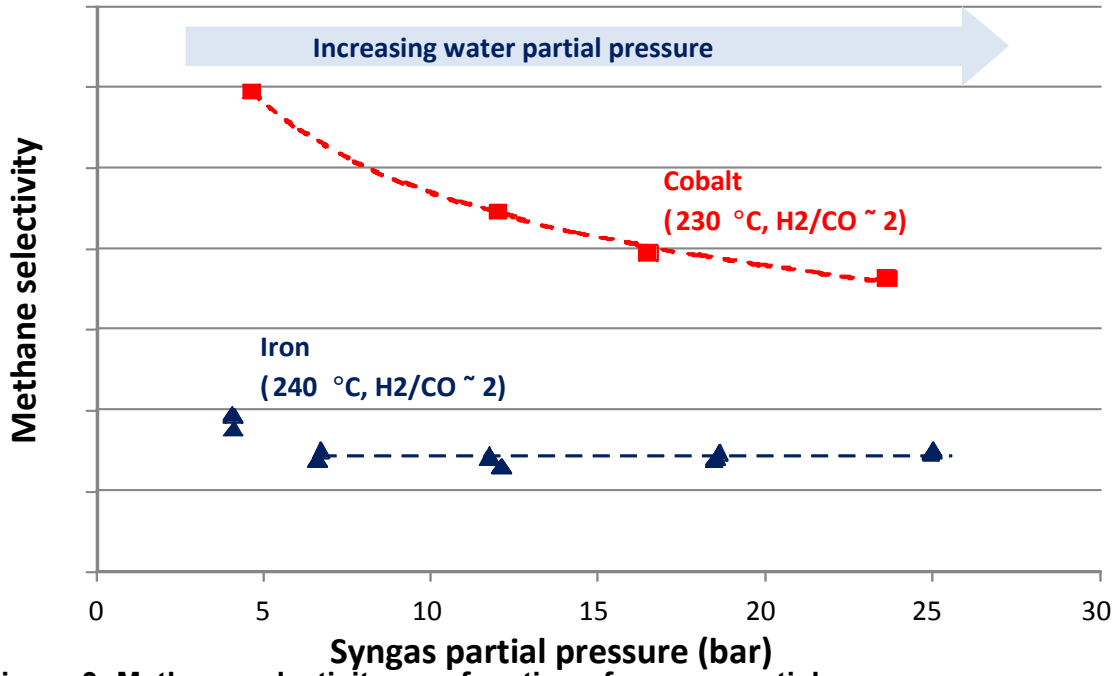

Figure 3: Methane selectivity as a function of syngas partial pressure as measured over an alumina-supported cobalt catalyst and a potassium-promoted iron catalyst at 230 °C and 240 °C, respectively, and constant H_2/CO ratio (Botes *et al.*, 2013).

Note the methane selectivity comparison as a function of the synthesis gas partial pressure shown in Figure 3 which indicates that the iron catalyst is far better than cobalt catalyst, especially at lower synthesis gas (H_2 + CO) partial pressures. Compared to other FT catalysts, the precipitated iron catalyst methane selectivity is relatively insensitive to all operating conditions, including temperature, as also pointed out by Schulz (2007). Nevertheless, the choice of operating temperature remains an optimization between competing activity and selectivity benefits while avoiding conditions which cause rapid catalyst degradation. In this regard, Shroff *et al.* (1995) explained that carbon formation at high temperatures leads to catalyst attrition in commercial slurry phase reactor systems. It

is expected, therefore, that there is scope to increase the optimum operating temperature provided that the onset of graphitic carbon formation can be avoided at the higher operating temperature by also increasing the operating pressure. Increased operating pressure is expected to retard the onset of graphitic carbon formation based on experience with fused iron catalysts operating at significantly higher temperatures (Dry, 1980) allowing stable operation with acceptable methane selectivity up to 270 ˚C.

Although Figure 4 indicates rapidly increasing catalyst activity for cobalt catalyst relative to the iron catalyst above 230 ˚C, operation at these higher temperatures is not desired for the cobalt catalyst due to the rapidly increasing methane selectivity.

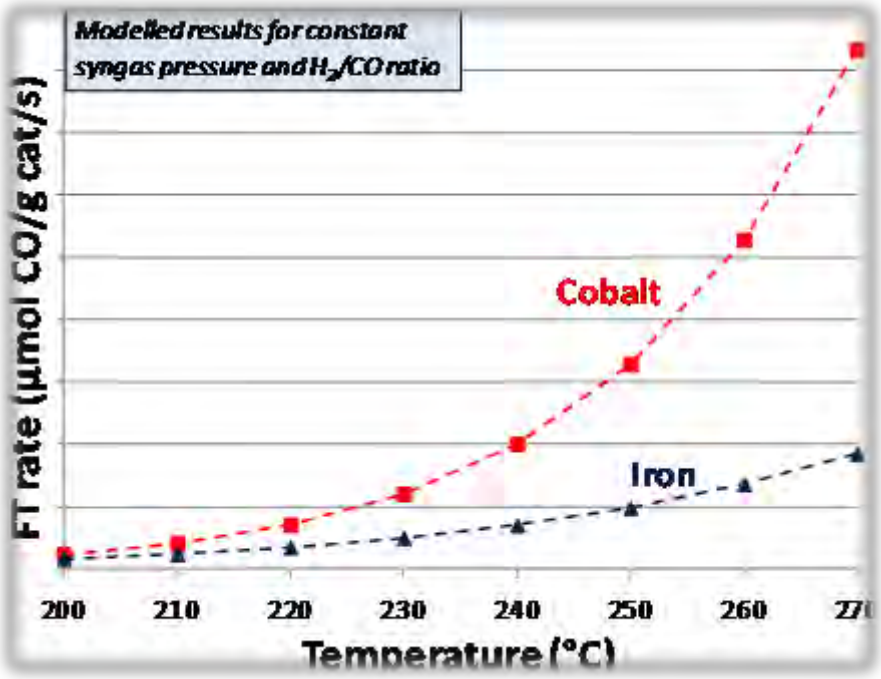

Figure 4: Model predicted effect of temperature on the FT reaction rate over cobalt and iron catalysts (Botes *et al*., 2013)

As can be seen from Figure 5 and Figure 6, higher pressure also has a beneficial effect on the relative reaction rate for the iron catalyst compared to the cobalt catalyst.

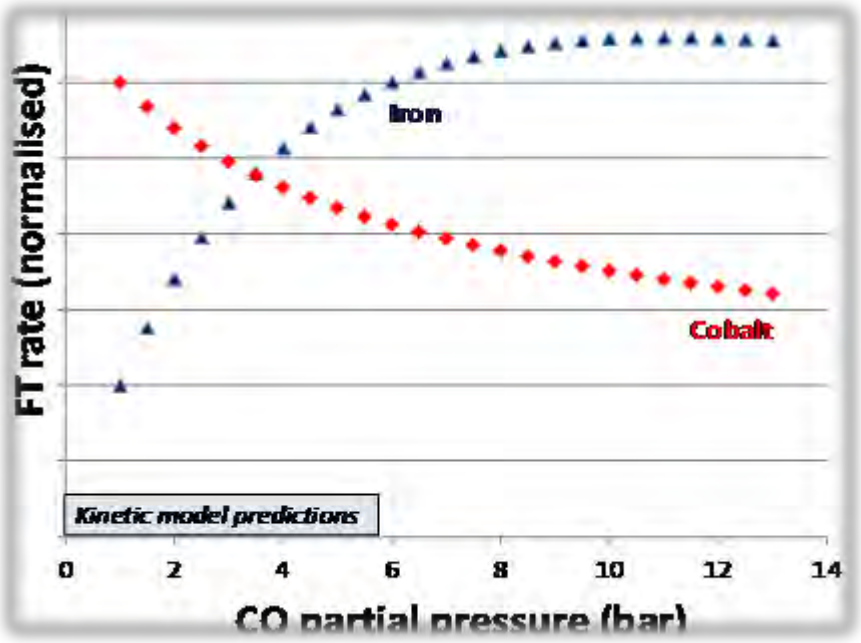

Figure 5: Effect of increasing CO partial pressure, while keeping other process conditions constant, on the FT reaction rate over cobalt- and iron-FT catalysts as predicted by macro kinetic models (Botes *et al*., 2013)

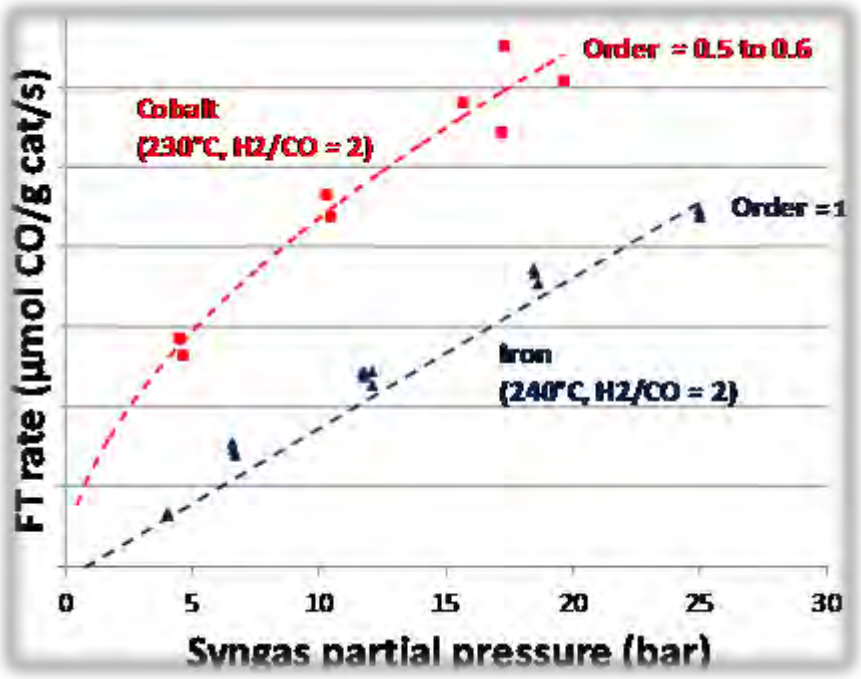

Figure 6: Measured increase in FT reaction rate with increasing syngas partial pressure at constant H_2/CO ratio for cobalt at 230 °C and iron at 240 °C (Botes *et al*., 2013)

Van Berge (1994) also explored the effect of operating pressure on the comparative performance for iron and cobalt catalysts. However, he confined this comparison to a feed gas H_2/CO ratio of 2.05. This feed H_2/CO ratio is close to the usage ratio for cobalt catalyst but far from the usage ratio for the iron catalyst (which was always less than 1.1) and this inevitably leads to an increasing accumulation of excess hydrogen in the reactor

with increasing conversion for the iron catalyst. This comparison should therefore be revisited using a feed gas composition which is more appropriate for the iron catalyst.

2.2 Primary Product Selectivity Considerations

If the values of the reaction rate constants for the repetitive stepwise addition of a C_1 monomer are regarded as being carbon number independent, the products of FT synthesis can be described with only one parameter, i.e. the probability of chain growth (PG) or alpha (α) (Schulz *et al*., 1988). When the molar content of a product compound xN with N carbon atoms is plotted logarithmically, straight lines are observed and the chain growth probability can be determined from the slope.

Real product distributions often show deviations from the ideal so called Anderson-Schulz-Flory (ASF) distribution. The four most commonly observed deviations are:
1) Higher than expected molar methane content.
2) Lower than expected molar C_2 content.
3) An increase in the chain growth probability with increasing carbon number.
4) Chain length dependent olefin content, decreasing as carbon number increases.

A number of researchers (König and Gaube,1983; Huff and Satterfield, 1984; Donnelly *et al*., 1988; Sarup and Wojciechowski, 1988; Vosloo, 1989; Egibor *et al*., 1995; Patzlaff *et al*., 1999) have fitted the C_{3+} carbon number distribution using two different chain growth probabilities (alpha1 and alpha2) and a third parameter (beta) that defines the positioning of the probability change. For the so-called double alpha model, the break from low alpha, usually near 0.7, to a high alpha, usually above 0.9, occurs between carbon numbers 8 and 12 on a semi-logarithmic plot of mole fraction versus carbon number.

Fletcher (2009) published the following data (Table 1) describing the expected influence of process parameters on product selectivity (Röper, 1983, Claeys, 1997, Van Dijk, 2001):

Table 1: Primary product selectivity trends

Increasing parameter	**Chain length**	**CH_4 selectivity**	**Olefin selectivity**	**Oxygenate selectivity**	**Olefin to Paraffin ratio**
Temperature	**-**	**+**	*	**-**	**+**
Pressure	**+**	**-**	*	**+**	**+**
H_2/CO (feed)	**-**	**+**	**-**	**-**	**-**
$P_{Hydrogen}$ (reactor)	**-**	**+**	**-**		
$P_{Carbon\ monoxide}$ (reactor)	**+**	**-**	**+**		
Residence time	**+***	**+***	**-**	**-**	**-**
Space velocity	*	**-**	**+**	**-**	
K (Fe catalyst)	**+**	**-**	**+**	**+**	

Note: Increases with increasing parameter **+**; decreases with increasing parameter **−**; complex relation *; differences in literature **+***.

The following approximate carbon atom selectivity performance can be inferred from the results published by Fletcher (2009) for operation at 260 °C:

Table 2: Carbon selectivity (260 °C; 20 % CO conversion; 2.1 feed H_2/CO ratio)

Component	% Carbon Selectivity
Methane	2.7
Ethane	0.4
Ethylene	1.2
Propane	0.5
Propylene	2.2
Butane	0.5
Butylene	2.1
C_5 to C_{10} paraffins	2.8
C_5 to C_{10} olefins	9.2 (hexene 1.7, octene 1.4)
C_5 to C_{10} oxygenates	4.0
C_{11+} hydrocarbons	74.4
Water soluble light oxygenates	3.0

Given that ethylene, propylene, butene, hexene and octene are all more valuable than diesel, there is potentially an incentive to increase operating temperature to increase the yield of these products.

It is unlikely that it would be worthwhile to recover the C_2 product so that, together with the methane, 4.3 % of the primary product is not recovered and is either used as fuel gas or recycled to the reformer. It may also not be desirable to recover the water soluble oxygenated products as final products and these may also either be used as fuel or recycled. The 74.4 % of the carbon in the C_{11+} cut, which mostly ends up as diesel, with optional co-production of kerosene and/or base oils, is attractive relative to alternative catalyst systems. The high olefin content of the kerosene cut may also make this cut a desirable feedstock for the manufacture of surfactants.

The conventional approach for the recovery of light hydrocarbons is described by Allem *et al*. (2013): "*Existing FT reactors have a post-reaction cooling step, followed by removal of condensed water and hydrocarbons. The final reactor vent gas following condensation contains a significant quantity of C_2 and higher hydrocarbon compounds that must be removed from the vent gas stream. The current general method of treatment is to cool the vent gas to a low temperature (typically - 90 ˚C to – 100 ˚C) following gas compression. The refrigeration system employed would typically be a cascade refrigeration system such as an ethylene-propylene cascade. Carbon dioxide removal (typically an amine scrubbing system) and a drying step (usually a desiccant drier with thermal regeneration) must be carried out prior to the cooling step for hydrocarbon removal*." A hydrocarbon wash is also sometimes proposed for light hydrocarbon recovery. It is energy intensive to cool to these very low temperatures so, when the C_2 hydrocarbon selectivity is low, then it may be preferable to operate at higher temperatures sacrificing this C_2 product to rather save energy and capital cost.

The carbon number ranges, C_3 to C_7 and C_8 to C_{14} were used by Fletcher (2009) to evaluate the chain growth probability as a function of the reaction temperature. Overall the chain growth probability in the range C_8 to C_{14} decreases with increasing temperature from 0.91 at 220 °C to 0.87 at 270 °C. Interestingly, the chain growth probability in the range C_3 to C_7 was observed to increase from 0.63 at 220 °C to 0.75 at 270 °C. In the two alpha models, alpha1 and beta (a parameter determining the carbon number at which the

alpha value changes) are highly correlated but it may be misleading to essentially fix beta by measuring alpha1 from C_3 to C_7 and a better fit might be obtained by allowing beta to vary. There is also significant curvature in the carbon number range from C_8 to C_{14} so it is expected that the alpha value at higher carbon numbers will be significantly higher than those reported for the C_8 to C_{12} range.

Patzlaff *et al*. (1999) show that the effect of potassium promotion is to increase the value of alpha2 and to move the transition from alpha1 to alpha2 to a lower carbon number.

2.3 Productivity Target Comparison with the Cobalt Catalyst Alternative

De Swart (1996) investigated a similar reactor system using a supported cobalt catalyst which provides a useful comparison to determine whether the precipitated iron catalyst system can be competitive. The plant capacity selected by De Swart was 5000 tonnes per day of liquid hydrocarbon product which corresponds to about 42 000 bbl/d which is a reasonable scale when compared to the ORYX GTL facility in Qatar which has a design capacity of about 32 000 bbl/d. The ORYX GTL plant uses two reactors with a somewhat larger diameter than the 7.5 m reactor diameter selected by De Swart who ended up with 4 reactors arranged in a 3 into 1 series configuration to achieve an overall conversion of 91 % using a bed height of 30 m. The selected operating temperature, pressure and the solids volume fraction in the gas free slurry were 40 bar, 240 ˚C and 0.25 respectively.

Subsequently, Sie and Krishna (1999) determined that a 5000 tonne/day plant may be built with only two reactor trains at a slurry concentration of 35 vol.% and using a superficial gas velocity of 0.35 m/s. Their capacity constraint was based on a maximum weight of 900 tonnes per reactor. The estimate by Sie and Krishna is used in this work for comparative purposes.

Based on the 7 m diameter reactor with a 30 m bed height producing 3000 tonnes/day of C_{1+} hydrocarbon products, reported by Sie and Krishna, this translates to a reactor productivity of 3.7 tonnes/day.m^2.

2.4 Previous Investigations and Applications using Iron Catalyst in a Slurry-Phase Reactor

Davis (2002) has provided an overview of slurry-phase reactor applications for Fischer-Tropsch synthesis. The terminology “liquid phase” is used instead of “slurry-phase” but these terms have the same intended meaning. He identifies three significant periods and we are now entering a fourth significant period due to the advent of new technology for the recovery of so-called shale gas which has resulted in the possibility for GTL plants to be viable in North America.

Also significant in this fourth modern period is the CTL developments in China. Luo (2013) has recently described the developments in China and estimated that by 2020 around 50 million tonnes/year of coal will be consumed by CTL facilities using FT technology developed in China. He also points out that, like the U.S., China possesses a large shale gas resource. Rentech Inc., in the USA, also claim to have demonstrated

precipitated iron catalysts in slurry phase reactor applications aimed at the production of liquid fuel products.

The conditions attempted by the US Department of Energy (DOE) were apparently influenced by the reported demonstration results from the Rheinpreussen operation (Kölbel and Ralek, 1980).

The Rheinpreussen operation targeted mainly gasoline production at 268 °C, but it is expected that the overall hydrocarbon yield will be enhanced by targeting a heavier product spectrum. Maximum diesel yield using a single parameter (so called single alpha) chain growth probability model (Dry, 2004 - p.215, Figure 5) indicates maximum straight run diesel yield with a probability parameter of at least 0.85. However, the heavier than diesel hydrocarbons are easily hydrocracked with a high diesel selectivity. Heavier hydrocarbons are also potentially valuable as feedstock to produce lubricant base oil products. So it is generally desirable, when aiming for diesel as the primary product, for the probability of chain growth to be as high as possible. Some compromise may be necessary to avoid negative impacts on the reactor conversion performance while attempting to improve selectivity performance.

2.4.1 Previous work at temperatures above 250 ˚C

The US DOE attempted to demonstrate operation for the production of fuels from feed gas with a H_2/CO ratio of about 0.67 (Fox, 1990; Abrevaya, 1993; Bhatt et al., 1995). The approach taken was to increase the operating temperature until the feed gas H_2/CO ratio is equal to the overall usage ratio so that H_2 and CO are consumed at equal rates. The activation energy of the WGS reaction is higher, so that this reaction rate increases relative to the FT reaction rate at higher operating temperatures (actual values are catalyst dependant). As a result, the overall usage ratio decreases with increasing temperature. A catalyst with a high WGS activity was also used.

The previous work at temperatures above 250 ˚C was, therefore, also aimed at a feed with a low H_2/CO ratio and this combination is very aggressive in terms of the propensity to form carbon. The bed height was also constrained to low values - by modern standards of what is practical from an engineering perspective.

Table 3 provides a comparison between the Rheinpreussen operation and the conditions investigated by the US DOE.

Table 3: Previous and proposed operating conditions for iron catalyst in a slurry-phase reactor

Application	Rheinpreussen Kölbel et al (1980)	US DOE Fox (1990)
Syngas H_2/CO	0.67	0.67
Pressure (bar)	12	28
Temp. (°C)	268	257
Bed height (m)	7.7	11.7
Recycle ratio	0	0.262
Conversion (%)	90	95
Velocity (cm/s)	9.5	11.5

2.4.2 Avoidance of catalyst physical degradation

Operating at the conditions used by the US DOE, it was initially not possible to avoid severe catalyst break-up (Abrevaya, 1993 - p.55), which in turn was probably due to graphitic carbon formation (Shroff *et al*, 1995 - p.206; Adeyiga, 2003 – p.2) according to:

$CO + CO \rightarrow C + CO_2$ - Boudouard reaction

On the other hand, Xu (2003 - p.56) speculated that catalyst attrition was due to insufficient mechanical strength of the precipitated iron catalyst and concluded that it is unlikely that even the strongest precipitated iron catalysts will have adequate attrition resistance. This is clearly not correct in view of the commercial slurry phase reactor operation in Sasolburg.

For the US DOE program, as a result of the rapid physical catalyst degradation for whatever reason, it was initially not possible to sustain the reactor operation due to problems with separation of the catalyst from the waxy liquid primary product (Abrevaya, 1993). Bhatt and Tijm (1998) reported that filtration issues were resolved during the F-T IV trial. It was further stated that: “The catalyst/wax filters performed well throughout the demonstration, producing a clean wax product. Use of a stronger catalyst along with some innovating filtration techniques helped achieve this significant milestone. For the most part, we needed only four filter housings. The filtration flux exceeded the design basis.”

In 1998, there was clearly still scope for further improvement and research continued into ways to improve the attrition resistance of these iron-based catalysts. For example, Adeyiga (2003) reported progress in this regard based on work sponsored by the US DOE and stated that the use of iron catalysts in a slurry bubble column reactor has been problematic due to severe attrition resulting in fines which plug the filter employed to separate the catalyst from the waxy product. It was further stated that iron catalysts undergo attrition not only due to the vigorous movement and collisions but also due to phase changes that occur during activation and reaction. It was also concluded that the attrition strength of the catalyst made out of largely spherical particles was considerably higher than that of catalyst consisting of irregularly shaped particles. It was further

reported that the amount of silica added to the catalyst formulation has to be optimized to provide adequate surface area, particle density and attrition resistance.

Zhao *et al*. (2002) investigated the effects of phase changes during activation and synthesis. They concluded that the type and concentration of silica that is incorporated during the preparation of spray dried iron catalysts have a much more significant impact on catalyst attrition than the iron phase change during activation. They proposed an optimum attrition resistant spray dried catalyst containing 9.1 wt.% of binder silica. The use of binder silica is preferred to precipitated silica for good attrition resistance. Ma *et al*. (2004) investigated the attrition resistance of the Ruhrchemie catalyst and found it to be adequate for slurry phase applications. Bukur *et al*. (2004[a,b]) also concluded that precipitated iron catalysts have suitable attrition resistance for slurry phase reactor applications (provided that the particles are spherical).

Bukur (2010) investigated catalysts with good synthesis performance prepared with different silica sources (colloidal silica, tetraethyl orthosilicate or potassium silicate) and found excellent attrition resistance under FT synthesis conditions with the catalyst comprising colloidal silica but severe attrition with the alternative silica sources. The 100Fe/3Cu/5K/16SiO_2 catalyst prepared using colloidal silica exhibited stable activity at 260 ˚C, 15 bar and about 70 % H_2 + CO conversion.

Lin *et al*. (2012) reported that an industrial catalyst did not have suitable attrition resistance so the best catalyst formulations are apparently not necessarily available yet from commercial manufacturers.

Further catalyst development is beyond the scope of this thesis but focus areas for further improvement are:

1) Optimization of the catalyst particle size;
2) optimization of the silica addition;
3) optimization of the spray drying technique;
4) optimization of the calcination;
5) optimization of the catalyst conditioning procedure to improve catalyst stability;
6) selection of appropriate catalyst formulations to avoid undesirable phase changes during the synthesis reaction.

A review of the literature over the past 10 years has revealed claims of improvements in all the above mentioned areas, mainly from China. It is reasonable to conclude that suitable catalyst attrition resistance is now achievable. This is also accompanied by reasonable catalyst activity stability with time on-line (which may require the sacrifice of some initial activity).

2.4.3 Stability of catalyst performance – avoidance of deactivation

An example of a stable catalyst (Wu *et al*., 2004) is a catalyst with the composition 100Fe/4.8Cu/2.6K/8.4SiO_2 and with residual sulphur due to the $FeSO_4.xH_2O$ starting material (present as SO_4 at a concentration of ~150 ppm).

Synthesis conditions reported for this catalyst were: 260 °C, syngas ratio 0.67, 2.0 MPa and GHSV of 3200 ml_n/gcat.h.

Variation in selectivity is reported as fairly constant – the reported methane selectivity is 2.5 - 2.9 wt.% with a slight increase in C_2-C_4 hydrocarbons after 350 hours on line and a slight decrease in C_{5+} selectivity. About 10 - 15 wt.% of all hydrocarbons are C_2-C_4 with a ~80 % olefin content.

Reported selectivities (based on total hydrocarbon product) for time on line 115 – 550 h are as follows: C_1 = 2.8 wt.%, C_{2-4} = 13.9 wt.%, C_{5-11} = 24.3 wt.%, C_{12+} = 59 wt.% for a syngas conversion of 65 - 72 % and a total hydrocarbon production of 0.35 - 0.48 gHC/gFe.h.

The reported GHSV is relatively low indicating that reactor productivity may not yet be optimized in these demonstration facilities.

The following illustrates the systematic approach for the research conducted in China for catalyst systems similar to the catalysts tested for this thesis:

Hao *et al*. (2005[a]) investigated the effect of calcination temperature and found that an increase of temperature decreased the catalyst activity but improved the catalyst stability and shifted the hydrocarbon products to higher molecular weight. Hao *et al*. (2005[b]) investigated the effect of reaction conditions on catalyst performance. Hao *et al*. (2005[c]) investigated the effect of conditioning/reduction conditions.

Wan *et al*. (2006) investigated various combinations of silica and alumina and it was found that the best performance was achieved with pure silica.

An *et al*. (2007[a]) reported on the negative impact of residual sodium on the catalyst performance, thus stressing the importance of quality control in the catalyst preparation. Stable operation for the baseline catalyst was demonstrated at a feed H_2/CO ratio of 0.67, 15 bar and at 250 ˚C for 500 hours. Steady 5 wt.% methane selectivity and 51 % CO conversion was reported. An *et al*. (2007[b]) performed a comparative study for potassium and sodium promotion.

Hao *et al*. (2007) explained the importance of the initial catalyst conditioning temperature with higher temperatures giving improved catalyst stability but, unfortunately, at the expense of less favourable initial activity and selectivity performance.

Zhao *et al*. (2008) demonstrated that silica was preferred to alumina and to ZSM-5 for potassium promoted iron catalysts without copper. The iron/K-SiO_2 catalyst was tested at a feed H_2/CO ratio of 2.0, 15 bar and 250 ˚C. Less than 4 wt.% CH_4 selectivity was measured at 34 % H_2 + CO conversion.

Hou *et al*. (2008) investigated the effect of silica content on catalyst stability. It was found that stability improved with increasing silica content but the product spectrum becomes lighter. The catalysts were tested at H_2/CO ratio of 0.67, 15 bar and 250 ˚C. The best catalyst, S25, had the composition 100Fe/5Cu/4.2K/25SiO_2. The catalyst precursors were calcined at 400 ˚C for 5 hours in a muffle furnace. No catalyst attrition was observed after 500 hours of operation in a 1 dm^3 continuously stirred tank reactor (CSTR). The catalyst was conditioned in-situ with syngas (H_2/CO ratio = 1.2) at 280 ˚C, 1 bar and GHSV = 2000 ml_n/g-cat.h for 24 hours. Photographs of the used catalyst show only spherical particles with a maximum diameter of about 100 microns. Reported selectivities (based

on total hydrocarbon product) are as follows: C_1 = 3.4 wt.%, C_{2-4} = ~15 wt.%, C_{5-11} = ~21 wt.%, C_{12+} = 61 wt.% at a synthesis gas (H_2 + CO) conversion of 45 % and CO conversion of 45 %.

Copper and potassium promoters were investigated by Wan *et al*. (2008) who reported stable operation of the K plus Cu catalyst at 0.67, 15 bar and 260 ˚C. 82 % CO conversion with about 4 wt.% methane selectivity was reported. It was concluded that, as compared to individual promotion of Cu and K, the double promotion of Cu and K keeps excellent stability and significantly improves the catalyst activity. This catalyst had the composition 100Fe/6Cu/5K and there was some indication that a slightly heavier product selectivity might be attained with less Cu. Farias *et al*. (2011) have recently revisited the effect of the potassium promoter for a silica supported iron catalyst at relevant operating conditions but the high silica content is clearly detrimental to the catalyst performance.

Hao *et al*. (2008[a]) investigated the phase transformations of a spray-dried iron catalyst for slurry FT synthesis during activation and reduction. The synthesis was conducted using a constant space velocity so conversions increased with operating temperature (at 15 bar and H_2/CO = 0.67). Re-oxidation was observed to dominate above 270 ˚C but it also appears that the catalyst (100Fe/5Cu/6K/16SiO_2) became unstable when the H_2 + CO conversion was above about 60 %. The catalyst precursor was calcined at 320 ˚C for 5 hours. The low calcination temperature may have contributed to the lack of activity stability at higher temperatures and conversions.

Ding *et al*. (2009) also reported on the topic of phase transformations during FT synthesis. Their tests were conducted at 15 bar, H_2/CO = 1.2, 260 ˚C and 29 % H_2 + CO conversion. The catalysts were calcined at 500 ˚C for 5 hours. Catalysts were conditioned for long periods of 12, 36 and 72 hours in the synthesis gas at a lower pressure of 5 bar.

Suo *et al*. (2012[a]) demonstrated stable synthesis performance at 280 ˚C with a catalyst prepared using tetraethoxysilane (TEOS) at 54 % CO conversion, 15 bar and 2.0 feed H_2/CO ratio. However, the methane selectivity was too high. Suo *et al*. (2012[b]) investigated various silica levels in the absence of promoters (e.g. K and Cu). Increasing silica content improved the catalyst stability and decreased methane selectivity. The catalyst activity first decreased then passed through a minimum and then increased with increasing silica content.

Yang *et al*. (2012) reported exceptional selectivity performance at CO conversion above 87 % when using one or more metal promoters selected from the group consisting of Mn, Cr and Zn. The carbon dioxide selectivity was less than 20 %, methane selectivity less than 5 %, C_{5+} selectivity greater than 90 % and C_2 to C_4 olefin plus C_{5+} selectivity potentially as high as 96 %.

2.4.4 Selection of operating conditions favouring both catalyst stability and reactor productivity

The focus for this thesis is the selection of synthesis operating conditions which improve catalyst stability by avoiding undesirable phase changes during reaction.

Carbon deposition is usually associated with catalyst particle swelling, and the formation of graphitic nuclei, within catalyst crystallites, that create stresses which disintegrate the

particles (Dry, 1980). With fixed bed Fischer-Tropsch reactors such swelling and disintegration inevitably leads to bed plugging, mal-distribution of the gas flow and hot spots. For this reason fixed bed Fischer-Tropsch reactors are usually run at temperatures sufficiently low to avoid carbon deposition.

Catalyst disintegration is equally undesirable in slurry-phase reactors, but due to their isothermal operating characteristic, they can run at a higher average temperature than fixed bed reactors which exhibit a significant axial temperature profile.

Poutsma (1980) reviewed the highly influential results from the Rheinpreussen demonstration and Table 4, extracted from this publication, shows product distributions from slurry runs aimed at “low”, “medium” and “high” average carbon numbers. It appears that most of these changes were achieved by changes in catalyst composition and operating temperature. Chain growth is enhanced by lower temperatures but particularly by higher alkali (K_2O) content in the catalyst.

Table 4: Rheinpreussen data

Molecular Weight Goal	**Low**	**Medium**	**High**
Single pass product yield (g/m_n^3 H_2 + CO feed)[a]	166	175	182
Distribution of C_{3+} products (%)			
C_3-C_4	18	7	2
Gasoline (C_5 – 190 ˚C)	68	40	7
Diesel (190 – 310 ˚C)	11	26	8
310 – 450 ˚C	2.5	18	33
> 450 ˚C	0.5	9	50

[a]Theoretical yield of all organic products is 208 g/m^3 if the usage ratio equals the feed ratio.

It was further reported that two-stage operation with inter-stage scrubbing of CO_2 product was also demonstrated. With first stage conversion of about 60 %, a total conversion of 96 – 97 % was reported with a 50 % increase in catalyst productivity and a two-fold increase in catalyst lifetime compared with single stage operation. This provides a compelling motivation to use the two-stage approach aimed at producing high molecular weight products.

Deckwer (1985) produced an influential analysis of the Rheinpreussen demonstration plant performance. He calculated an optimum inlet superficial gas velocity of 0.088 m/s which compared well with the reported experimental operating velocity of 0.095 m/s. However, this experimental optimum was for a relatively low catalyst concentration of 12 wt.% iron, a relatively short 8 m column and targeting a high synthesis gas (H_2 + CO) conversion of 90 %. Furthermore, he used a gas holdup prediction that correlated gas holdup with gas velocity to the power of 1.1 and which created a false prejudice to operation at higher gas velocities. It is now clear that there is scope to target much longer reactors with modern fabrication technology and it is now also known that kinetic control remains dominant at very high slurry concentrations with attrition resistant catalysts, such that a much higher optimum gas velocity can be expected. This is particularly so when targeting a lower conversion per reactor in two-stage reactor designs.

Shah *et al*. (1982) reviewed the available published gas holdup data which only included one set of data (Ueymada and Miyauchi, 1979) for a column diameter larger than 0.15 m (0.6 m) and their analysis yielded a gas holdup nearly proportional to gas velocity to the power of 0.5. The gas holdup was less than 50 % at 0.9 m/s gas velocity. Shah *et al*. (1982) were under the mistaken impression at that stage that the presence of solids does not affect the gas holdup significantly. General impressions were biased for a long time by the much larger amounts of data available for smaller columns at low gas velocities.

The most comparable design approach, for the selected iron catalyst system, to be found in the literature is that by Van der Laan *et al.* (1999). There are many similarities with the approach used by De Swart (1996) for the cobalt catalyst system. Van der Laan *et al.* found that the reactor productivity was highest at the highest catalyst volume fraction considered of 0.35 (to be compared to the value of 0.25 used by De Swart and the same maximum value of 0.35 considered by Sie and Krishna (1999)). It was further calculated that the reactor productivity was not particularly sensitive to the gas inlet H_2/CO ratio in the range from 1.0 to 2.0 but the productivity at a ratio of 1.5 was higher than at 1.0 or 2.0 and this is stated to be the optimum feed gas H_2/CO ratio.

The selected operating temperature, pressure and the solids volume fraction in the gas free slurry were 30 bar, 250 ˚C and 0.35 respectively. A reactor was selected with a diameter of 8 m and a bed height of 24 m. It was found that the reactor productivity increased with increasing gas velocity from 0.15 m/s to the maximum value investigated of 0.4 m/s. At the lowest velocities (less than 0.15 m/s) the synthesis gas conversion reached a constant level of 80 % with the kinetic expression used for this study by Van der Laan *et al.* (1999).

The results indicate that it should be possible to reach an overall conversion of 91 % in a two stage reactor configuration at a gas velocity close to 0.4 m/s in the first reactor stage. This can be compared to only 0.14 m/s selected by De Swart for the first reactor stage.

Benham *et al*. (2003), from Rentech, also fitted the product distribution using two chain growth parameters - one for carbon numbers from 1 to a transition carbon number of 9 and a second from the transition carbon number onwards. Using this approach they give a value of 0.69 for the first parameter and a value of 0.95 for the second parameter at a temperature of 249 °C and a pressure of 15.5 bar for a feed gas H_2/CO ratio which ranged from 0.7 to 2.0.

Fletcher (2009) reported a first probability parameter value of about 0.73 and a second probability parameter of about 0.90 at 245 °C. As mentioned previously, the second parameter was fitted by Fletcher over the carbon number range of C_8 to C_{14} and it is likely that there is further curvature towards higher numbers with increasing carbon number. The conclusion from the comparative example, provided by Benham *et al*. (2003), is that similar maximum yields are achievable with the two different catalyst systems in a slurry phase reactor as part of a gas-to-liquids (GTL) process.

Interestingly, Benham *et al*. (2003) proposed a two-stage reactor design for the cobalt catalyst and a single stage for the iron catalyst while a single stage is used commercially by Sasol with a cobalt catalyst and a two stage approach is often proposed by others for the iron catalyst.

Govender *et al*. (2006) explored the importance of the inlet H_2/CO ratio and carbon dioxide build-up with recycle at 240 ˚C and 20 bar. They found that the usage ratio was about 1.4 and that the level of carbon dioxide did not significantly change the CO_2 selectivity, hence, CO_2 is regarded as an inert component at these conditions.

Fletcher (2009) studied the impact of temperature on selectivity on a precipitated iron catalyst in a temperature range from 220 to 270 ˚C. The partial pressures in the laboratory reactor were kept relatively constant by varying the space velocity to keep the conversion to hydrocarbon products close to 20 %. This target conversion may be on the low side for commercial applications but can be expected to ensure a relatively stable catalyst performance. However, no catalyst performance data was reported as a function of time on-stream so it is unclear whether the performance is sustainable for long runs. It is also unfortunate that the data at 270 ˚C may be unreliable due to unexplained catalyst deactivation since the following is reported: “The space velocity used at 270 ˚C is lower than that at 260 ˚C and only slightly higher than the space velocity for the experiment at 250 ˚C. This might indicate that the catalyst has deactivated before the data obtained at 270 ˚C were collected.” The data at 270 ˚C is therefore not considered to be reliable.

Table 5: Average conversions and space velocities as a function of temperature, Fletcher (2009)

Temperature (°C)	**Average $X_{CO\ to\ FT\ prod}$ (%)**	**Average $X_{CO\ to\ CO_2}$ (%)**	**Average space velocity measured, (ml_n/g-cat.h)**
220	20	16	5100
230	21	16	8000
245	18	17	16600
250	22	22	17000
260	20	14	22400

Note the significantly higher space velocities in Table 5 compared to those reported by Hou *et al*. (2008).

Data from operation at 260 ˚C gives favourable results with respect to achievable reactor productivity while also exhibiting excellent selectivity to useful hydrocarbon products.

Table 6: Average partial pressures of kinetically relevant components, Fletcher (2009)

Component	Average (bar)	Maximum (bar)	Minimum (bar)
Hydrogen	10.2	11.4	9.6
CO	4.8	5.1	4.2
Water	1.2	1.6	0.9
CO_2	0.5	1.0	0.2

The methane selectivity reported by Fletcher (2009) based on on-line FID analysis was 3.4 wt.% at both 250 and 260 ˚C which is in line with the data reported by Hou *et al*. (2008) in spite of the much lower feed gas H_2/CO ratio used in the latter case. A feed gas H_2/CO ratio of 2.1 was used by Fletcher (2009) and this resulted in a considerable accumulation of hydrogen in the reactor, as shown in Table 6. It seems that methane selectivity is relatively insensitive to H_2/CO ratio.

Other iron catalyst based modelling work (Wang *et al*., 2007; Iliuta *et al*., 2008) has approached the optimization from the perspective of selecting a constant reactor height of 30 m and selecting conditions based on the variation in conversion and product selectivity with temperature, pressure and feed gas H_2/CO ratio. Wang *et al*. (2007) show that reactor productivity increases with gas velocity and catalyst concentration but only show results up to 0.4 m/s and 0.30 volumetric solids fraction. Wang *et al*. (2007) concluded that an optimum selectivity for intermediate distillates (gasoline and diesel) can be obtained between 260 ˚C and 290 ˚C, 20 to 30 bar and 1.0 to 1.5 inlet H_2/CO ratio.

2.4.5 Application in GTL facilities

When using an autothermal reformer (ATR) in a GTL flowsheet, the example provided by Benham *et al*. (2003) with the highest C_{6+} hydrocarbon production was reported to be with a feed gas H_2/CO ratio of 1.99. This ratio was achieved by removing hydrogen from the FT tail gas (after 90 % CO conversion) for recycle to the FT reactor and then recycling 84.5 % of the remaining tail gas back to the ATR. The carbon selectivity to C_{6+} product is calculated as 73 % but it is unfortunately not possible to calculate the carbon dioxide selectivity.

The approach described by Benham *et al*. (2003) illustrates that the optimum H_2/CO ratio for the integrated GTL flowsheet may differ from the optimum productivity point considering the FT reactor in isolation, as reported by Van de Laan *et al*. (1999).

Earlier, Gray and Tomlinson (1997) calculated that by removing water gas shift activity (from their iron-based catalyst performance description), the required selling price for the hydrocarbon products decreased by 7 %. However, they did not report the impact at intermediate carbon dioxide selectivity levels or explore flowsheet optimisation opportunities such as hydrogen recycle to the FT reactor as proposed by Benham *et al*. (2003). The use of a catalyst with water gas shift activity also lends itself to the recovery of hydrogen from the FT tail gas for use in the downstream hydroprocessing of the primary liquid products. Neither Benham *et al*. (2003) nor Gray and Tomlinson (1997) considered this advantage for a shifting catalyst in their comparison.

More recently, Hao *et al*. (2008[b]) have also prepared a comparison for GTL plant designs with non-shifting (cobalt-based) and shifting (iron-based) FT catalyst for GTL facilities

using ATR reforming. They concluded that the carbon efficiency for a GTL plant using iron-based catalyst would be 68 % relative to 73 % using cobalt-based catalyst. However, they assumed very high carbon dioxide selectivity (45 %). It is conceivable that the carbon dioxide selectivity can be somewhat decreased for GTL applications so that the carbon efficiency for both types of catalyst will be determined by the energy balance and can be similar for both types of catalyst. This will require a different optimum GTL process flowsheet structure for each type of catalyst.

When applying a shifting catalyst in a GTL configuration, it is expected that a two-stage FT reactor configuration will be used with the removal of both water and carbon dioxide between stages as described by Poutsma (1980). The separated carbon dioxide will be recycled to the reforming unit. After the second stage reactor, it is expected that some tail gas will also be recycled to the reforming unit while the balance of the tail gas will be processed to make hydrogen and to provide fuel gas for a power plant.

Increased GTL flowsheet complexity relative to the approach for the non-shifting catalyst needs to be justified by improved FT reactor productivity and a more valuable hydrocarbon product spectrum.

2.5 Background on Slurry Bubble Column Hydrodynamics

Four types of flow regime have been observed in bubble columns, as depicted in Figure 7. At low gas velocities the homogeneous (bubble) flow regime is observed. In small diameter columns slug flow can be observed at higher gas velocities but this regime is not encountered in large industrial bubble columns. The regime of interest for the selected applications is the heterogeneous or churn-turbulent flow regime. The annular flow regime is generally avoided for chemical synthesis applications due to the low liquid or slurry holdup and, strictly speaking, there is no longer a bubble column in this regime since there are no remaining bubbles.

The homogeneous bubble flow regime is characterized by uniformly sized small bubbles traveling vertically with minor transverse and axial oscillations. There is practically no coalescence and break-up, hence there is a narrow bubble size distribution. The gas holdup distribution is radially uniform; therefore bulk liquid circulation is insignificant. This regime is not of interest for the large scale industrial hydrocarbon synthesis applications due to the low reactor productivity associated with operating at low gas velocities.

Heterogeneous flow occurs at high gas superficial velocities. Due to intense coalescence and break-up, small as well as large bubbles appear in this regime, leading to a wide bubble size distribution. The large bubbles (or gas voids) churn through the liquid, and thus this is called the churn-turbulent regime. The non-uniform gas holdup distribution across the radial direction causes bulk liquid circulation in this regime.

Depending upon the operating conditions, the homogeneous and heterogeneous regimes can be separated by a transition regime. Using chaos analysis of pressure fluctuation signals, Letzel *et al*. (1997) observed that an additional transition occurs within the boundaries of the heterogeneous regime for increased gas densities (ρ_G > 5 kg/m^3) and at a superficial gas velocity being typically 2 - 3 times the 1st homogeneous regime-heterogeneous regime transition velocity. This “pseudo” transition is characterized by two

classes of large bubbles of which the sizes mainly overlap at low gas densities but are substantially different at increased gas densities.

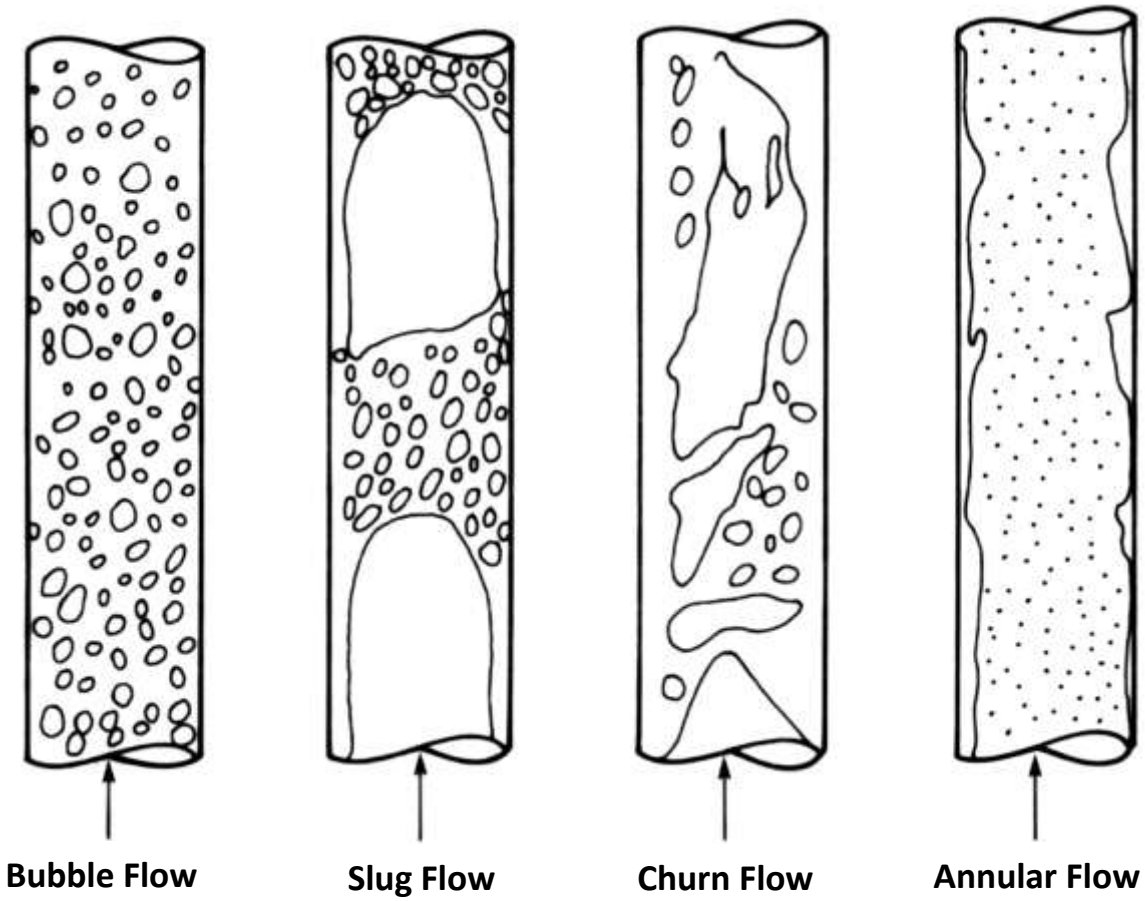

Figure 7: Flow regimes for bubble columns (Shaikh and Al-Dahhan, 2007)

A gradual transition occurs from a gas-in-liquid dispersion to a liquid-in-gas dispersion (phase inversion) at superficial gas velocities above the 2nd transition velocity as shown in Figure 8 (Hills, 1976; Botton *et al*., 1978). Notice from Figure 8 that this phase inversion occurs smoothly over a rather broad range of superficial gas velocities. The on-set of this transition is characterized by a gas holdup in excess of 0.65 – 0.7. The upper value is not far from the interstitial liquid voidage of a dense 'packed bed' of spherical bubbles (Kunii and Levenspiel, 1991). Increasing the superficial gas velocity beyond the upper limit of this transition regime results in the occurrence of a transported bed regime (so called scump bed regime in Figure 8), where a true dispersion zone with a constant holdup of dispersed liquid slugs occurs up to a certain column height above which the liquid holdup (1 – gas holdup) decreases exponentially with height (Hills, 1976).

The transition velocities depend on the physical liquid properties (especially surface tension and viscosity), the gas density and the presence of catalyst particles in the liquid.

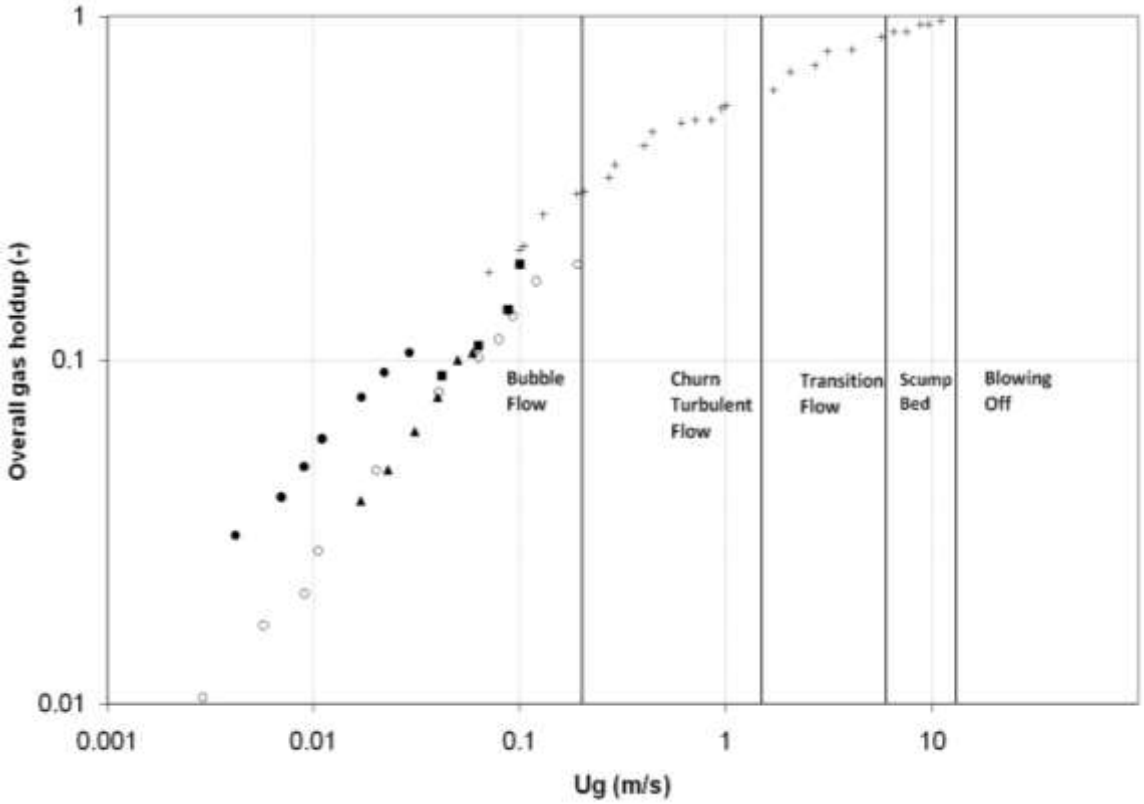

Figure 8: Flow regimes and gas holdup as a function of superficial gas velocity for the air-water system at ambient pressure and temperature (Botton *et al*., 1976). Column diameters: 0.02 (●), 0.075 m (+), 0.25 m (o), and 0.48 m (▲).

Due to the economic incentive to maximize reactor capacity, for the selected applications, the upper end of the gas velocity range, at high solids concentrations, in the churn-turbulent regime is of particular interest. In order to be able to predict the overall gas holdup in this range of gas velocities, various empirical and semi-empirical correlations have been developed. A modified two-phase theory, discussed in the next section, is a more theory based approach. This modified two-phase theory relies on the identification of the regime transition, from the homogeneous (bubble flow) regime to the heterogeneous (churn turbulent flow) regime, to define the "small bubble" contribution to the overall gas holdup.

Unfortunately, the conclusion from the recent review by Shaikh and Al-Dahhan (2007) is as follows: "In short, it still remains a challenge to '*a priori*' predict flow regime transition (from bubble to churn-turbulent flow) without resorting to extensive experimentation or a judicious estimate based on experience." This creates a problem to predict the "small bubble" contribution to the total gas holdup.

To avoid this problem, an *adapted two-phase theory* is now proposed to enhance gas holdup predictions at higher velocities in the churn turbulent regime. The proposed adaptation is to change the definition of "small bubbles" to be those bubbles which remain in circulation in the slurry and therefore, by definition, these small bubbles do not contribute at all to the gas flow through the slurry.

2.6 The Reactor Modelling Approach

Octave Levenspiel published a lovely article with the title “modeling in chemical engineering” (Levenspiel, 2002). He states the following in the abstract: “Chemical engineering has changed our accepted concepts and our ways of thinking in science and technology. Here modelling stands out as the primary development.”

He goes on to quote Denbigh, “In science it is always necessary to abstract from the complexity of the real world, and in its place to substitute a more or less idealized situation that is more amenable to analysis.”

According to Levenspiel, this statement applies directly to chemical engineering, because each advancing step in its concepts frequently starts with an idealization which involves the creation of a new and simplified model of the world around us. The acceptance of such a model changes our world view.

When modelling the selected reactor system the approach is taken to only add model complexity when this produces a significantly better prediction of reality.

The steps in the reaction process which consumes the reacting gases are:

1) Mass transfer from the gas phase to the liquid phase
2) Mass transfer through the liquid phase to the catalyst particles
3) Diffusion through boundary layer and pores to the surface of the catalyst
4) Reaction of the surface species

The pioneering work by Deckwer *et al*. (1981) produced the following summarized result: “An analysis of FT studies in the slurry phase with 8 different catalysts and reactor geometries, respectively, has been carried out on the basis of reliable hydrodynamic data and the assumption of first-order consumption kinetics for hydrogen. Contrary to the conclusions of Satterfield and Huff (1980), the present analysis shows that the FT slurry process in bubble column reactors is governed mainly by reaction resistance. Mass transfer limitations are negligible for the known catalysts and operating conditions.”

Steps 1, 2 and 3 above can therefore be neglected and the reactor modelling problem is then reduced to predicting the quantity of catalyst in the reactor and the mixing in the slurry and gas phases. Furthermore, while the mixing cannot be neglected for detailed reactor design work, it is less important when the reactant conversion is restricted to relatively low levels to avoid catalyst degradation. This is the case with the system selected for investigation. This means that, after selecting the catalyst and the reactor operating temperature and pressure, the primary determining features for the best reactor performance are the gas velocity (u_g) through the reactor and the mass of catalyst (M) in the reactor. If the reactant per-pass conversion is constrained to a maximum target value then this conversion will be achieved at a given value for M/u_g. This reduces the reactor design approach to the selection of the catalyst concentration in the slurry, the gas velocity and the slurry bed height required to achieve the maximum allowable per-pass conversion.

For a selected target conversion when using the maximum practical catalyst concentration, the required reactor bed height is determined by the gas holdup in the

slurry bed. It is therefore important to be able to predict the gas holdup at the potentially desirable combinations of gas velocity and catalyst concentration.

A new approach to the description of the relevant hydrodynamic regime and the prediction of gas holdup is proposed in section 5.1.2. This approach is similar to the approach pioneered by Krishna and Ellenberger from 1993 to 1996 (Krishna, Ellenberger and Sie, 1996) and applied by both De Swart (1996) and Van der Laan *et al.* (1999).

The earliest recorded formulation of a gas distribution theory is credited to Toomey and Johnstone (1952) and is known as the two-phase theory of fluidization as used in models by May (1959) and Van Deemter (1961). This two-phase theory, developed to describe the gas distribution in conventional gas-powder fluidized beds, can also be of use in describing the gas distribution in a slurry bubble column. Simply stated, the theory specifies that all gas in excess of that needed to bring a fluidized bed to minimum fluidization conditions passes through in the form of bubbles. This simple theory has been modified, for a slurry bubble column, by defining a dense phase which consists of the slurry aerated by small bubbles. Gas in excess of that required to maintain the dense phase (homogenous regime) passes through in the form of large “bubbles” or gas voids and these large gas voids are referred to as the dilute phase (in the heterogeneous or churn-turbulent flow regime).

In the case of slurries, there is a velocity at which a transition occurs between a homogeneous bubble regime and the heterogeneous churn-turbulent regime. This transition determines the dense phase transition to a combination of dense and dilute phases as defined by this modified two-phase theory. This approach has been widely adopted to describe slurry bubble columns. An important feature of the churn-turbulent regime is that the circulating slurry entrains smaller bubbles into circulation with the slurry.

According to Vermeer and Krishna (1981), it is important to differentiate the dense phase gas holdup from the dilute phase gas holdup because the dense phase gas holdup, for smaller diameter columns, is not affected by the column diameter while, the dilute phase gas holdup is significantly affected (i.e. decreases with increasing column diameter). In the case of liquids and slurries, prediction of the gas holdup in the dense phase may be unreliable because of the sensitivity to the liquid surface tension which can be affected by small amounts of impurities.

The gas holdup is an essential parameter that needs to be known in order to design a slurry bubble column reactor (Wang *et al*., 2008).

The gas holdup also influences the reactor pressure profile and the amount of catalyst which can be held in a given reactor volume. The catalyst concentration C_{cat} is related to the gas hold-up via:

$$C_{cat} = W_{cat}/V_R\,(1-\varepsilon_{internals}) = \varepsilon_p(1-\varepsilon_G)/\rho_p \qquad (3)$$

Using the modified two-phase theory, the dilute phase gas holdup can be described using the equation:

$$\varepsilon_b = (U - U_{df})/\,U_b \qquad (4)$$

Using the correlation proposed by Werther (1983) of $U_b = \varphi(g\ d_b)^{½}$ and substituting into equation (2) gives:

$$\varepsilon_b = (U - U_{df})/\ \varphi(g\ d_b)^{½} \qquad (5)$$

Following the Darton *et al.* (1977) approach, the diameter of a sphere having the same volume as the actual bubble, for dispersion heights exceeding h* (where h* is the height above the gas distributor where the bubbles reach an equilibrium size), is given by :

$$d_b = \alpha\ (U - U_{df})^{2/5}\ (h^* + h_o)^{4/5}\ g^{-1/5} \qquad \text{for } h^* \leq h \leq H \qquad (6)$$

Ellenberger and Krishna (1994) derived the following equation for $H \geq h^*$:

$$\varepsilon_b = (U - U_{df})^{4/5}/\ \alpha^{1/2}\ \varphi\ g^{2/5}\ (h^* + h_o)^{2/5} \qquad (7)$$

Substituting for d_b from equation (6) into equation (5) gives equation (7). This shows that the approach of Ellenberger and Krishna is consistent with the modified two-phase theory.

It is also known that h* is a function of $(U - U_{df})$ which may lead to some errors in simply lumping constants to determine the effect of gas velocity on the dilute phase gas hold-up, ε_b. This is particularly important if data is taken from relatively short mock-up columns for use to design industrial reactors which would typically have bed heights in the range from 15 to 40 m. According to Krishna *et al*. (1996), the equilibrium height (h*) lies in the range from 0.2 to 1.2 m for industrial operations.

The column design can influence the gas holdup in bubble columns. The type of gas distributor can be especially important. However, several researchers (Lee and Foster, 1990; Wilkinson, 1991; Radoš, 2002) showed that this effect is only significant in the homogeneous regime at low gas velocities. In the churn-turbulent regime, the gas distributor effects can be neglected due to the intensive bubble coalescence in this regime. Moreover, the effect of gas distributor design on bubble formations is less pronounced at pressures above atmospheric (Wilkinson, 1991). Since the focus is now on high throughput columns at elevated pressures, gas distributor effects are of less significance and are not discussed further.

In the churn-turbulent regime, the overall gas holdup, according to the modified two-phase theory postulated by Vermeer and Krishna (1981), consists of two components namely a dense phase void fraction and a dilute phase void fraction. Expressed mathematically –

$$\varepsilon = \varepsilon_b + \varepsilon_d(1 - \varepsilon_b) \qquad (8)$$

If the constants in equation (7) are lumped together into one constant, C, then the equation (7) reduces to –

$$\varepsilon_b = CU^{0.8} - C(U_{df})^{0.8} \qquad (9)$$

Figure 9 illustrates the modified two-phase theory approach for the two regimes encountered in bubble columns. The homogeneous regime occurs in bubble columns at relatively low superficial gas velocities. The transition from the homogeneous regime to

the churn-turbulent regime occurs at the so-called 1st transition velocity. This churn-turbulent regime is characterized by the occurrence of two types of gas phases, i.e. the small bubble gas phase or dense phase and the large bubble gas phase or dilute phase. The small bubbles are homogeneously dispersed over the entire column, whereas the large bubbles rise preferentially away from the walls and other surfaces where slurry down flow occurs (Deckwer, 1985; 1992).

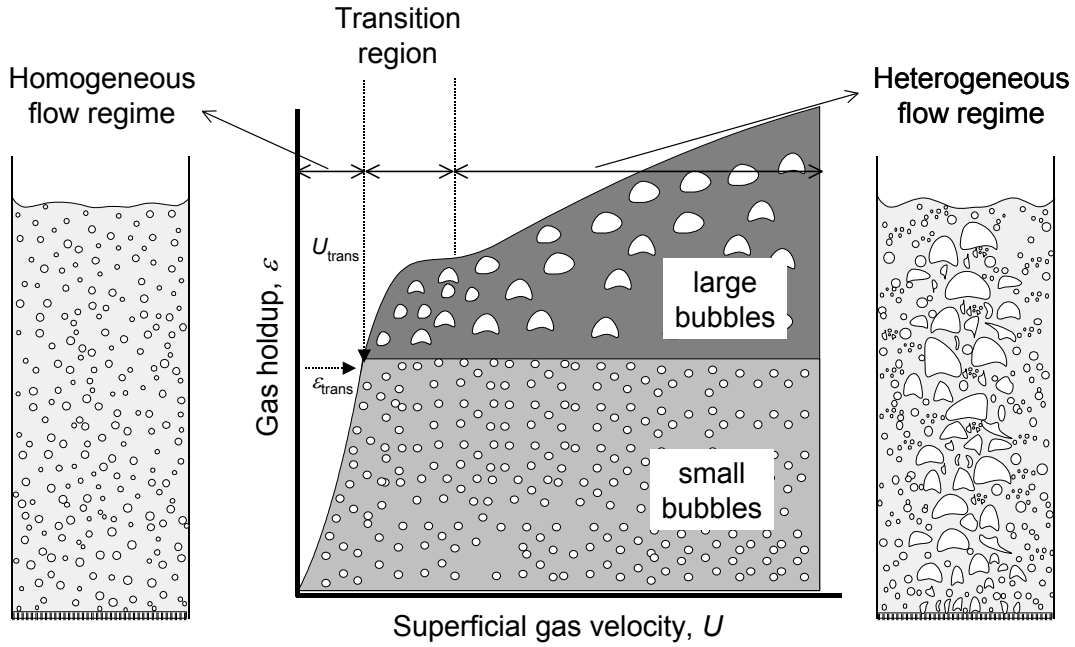

Figure 9: Homogeneous (bubble flow) and heterogeneous (churn-turbulent) flow regimes in gas-liquid bubble columns (Krishna, 2000).

The gas holdup in the dense phase can also be determined by means of a bed collapse experiment (Rietema, 1967). For the bed collapse experiment, the gas feed is rapidly interrupted and the bed height drops rapidly initially as the large bubbles disengage. Then there is a subsequent period of much slower bed height reduction as small bubbles disengage. The decay of the residual slurry circulation, after the dilute phase bubbles have left the slurry, will influence the decline in the dense phase gas holdup during the bed collapse experiment. The determination of the dilute phase gas holdup by means of a bed collapse experiment gives a more precise result than the approach of tracking the gas holdup from the bubble regime through a transition regime to the churn-turbulent regime.

Ellenberger and Krishna (1994) reported results from bed collapse experiments in support of their proposed unified approach to the design of fluidized bed and gas-liquid bubble column reactors. Krishna and Sie (2000) discuss results from bed collapse experiments with slurries. They found that the decrease in gas holdup in more concentrated slurries is primarily caused by the decrease in holdup of the small bubbles. The small bubble population is virtually destroyed as the slurry concentration approaches 30 vol.%. They considered a 40 vol.% slurry concentration to be the maximum which can be used in commercial practice without motivating their conclusion. They also proposed operation at gas velocities below 0.3 m/s in order to operate at 90 % single pass conversion.

Bukur *et al.* (1987) reported a good fit to gas holdup data with a correlation proposed by Bach and Pilhofer (1978) with refitted parameters for solids free waxes at relevant operating temperatures for gas velocities less than 0.15 m/s. They make the following comment on the effect of solids on page 14: "The addition of solids reduces the gas holdup (Deckwer *et al.,* 1980; Kuo *et al.* 1985). This may be viewed as a viscosity effect, since the viscosity of the slurry increases with solids concentration. The gas holdup is expected to decrease as the viscosity of the medium increases."

Based on an extensive set of experimental data, both own work and data from literature, Luo *et al.* (1999) fitted an empirical correlation that can be used for the prediction of the gas holdup in liquid and slurry bubble columns. This correlation is referred to hereafter as the Ohio State University (OSU) correlation.

The range of applicability for this correlation is shown in Table 7:

Table 7: Range of applicability for the OSU correlation

Parameter	**Units Range**
ρ_L (kg/m^3)	668 – 2965
μ_L (mPa s)	0.29 – 30
σ (mN/m)	19 – 73
ρ_G (kg/m^3)	0.2 – 90
ϕ (-)	0 – 0.4
d_p (µm)	20 – 143
ρ_s (kg/m^3)	2200 – 5730
u_G (m/s)	0.05 – 0.69
D_c (m)	0.1 – 0.61
H/D_c (-)	> 5

Distributer type: perforated plate / sparger / bubble cap

Note that extrapolation is required for gas velocities exceeding 0.69 m/s.

Behkish *et al.* (2006) reviewed available gas holdup correlations and proposed a new correlation which was fitted to data with gas velocities up to 0.574 m/s. Booysen (2013) compared the correlations from Behkish *et al.* (2006) and the OSU correlation to the measured gas holdup data from Koop (2003) for gas velocities above 0.35 m/s. The comparison was based on a calculation of the Average Absolute Relative Error (AARE) and the Mean Relative Error (MRE).

The OSU correlation has AARE = 10.1 % and MRE = - 5.5 %

The Behkish *et al.* (2006) correlation has AARE = 20.7 % and MRE = - 6.9 %

Therefore the OSU correlation appears to be the most appropriate prior art correlation at higher gas velocities.

3. OBJECTIVES OF RESEARCH

3.1 Conclusions from the Background Review

From the preceding review, it can be concluded that the slurry-phase reactor for hydrocarbon synthesis has significant potential for improved productivity relative to previously published approaches. There is scope for a novel contribution to the understanding of the iron-catalysed slurry-phase reactor system. Although the emphasis for this investigation is on the use of an iron-based catalyst, the gas holdup prediction is also applicable to the cobalt based catalyst in a similar reactor system and a performance comparison between these catalyst options is also relevant.

It is established practice to design the slurry-phase reactor by aiming for a target reactant per-pass conversion. For some catalysts there is evidence that the catalyst performance degrades at an unacceptable rate if an upper limit per-pass conversion is exceeded. This upper limit may depend on various operating conditions. Overall reactant conversion exceeding 90 % is a common target and there are economic benefits to achieve this target with a two-stage reactor design without first stage recycle. This approach provides a target first stage reactor per-pass conversion of at least 60 %.

The literature indicated that the system is kinetically controlled so it was necessary to obtain kinetic data at the new proposed operating conditions. Experiments were therefore proposed to be performed at the Sasol Research laboratories in Sasolburg to obtain the required kinetic data at relevant new operating conditions.

The primary determining features for the best reactor performance are the gas velocity (u_g) through the reactor and the mass of catalyst (M) in the reactor. If the reactant per-pass conversion is constrained to a target value then this conversion will be achieved at a given value for M/u_g. This reduces the reactor design approach to the selection of the catalyst concentration in the slurry, the gas velocity and the slurry bed height required to achieve the maximum allowable per-pass conversion. The calculation of the slurry bed height requires the prediction of the gas holdup as a function of gas velocity and catalyst concentration at the desired operating conditions.

The best available correlation to predict the gas holdup in the slurry-phase reactor is an empirical correlation which should therefore not be extrapolated to higher gas velocities. The two-phase modelling approach provides scope for improved gas holdup prediction at higher gas velocities, above 0.69 m/s, up to a “safe” upper limit fractional gas holdup of about 0.65 (avoiding phase inversion to a continuous gas phase).

3.2 Hypotheses

It is hypothesized that it is possible to significantly increase the slurry-phase reactor productivity, used for hydrocarbon synthesis, by operating closer to the identified constraints, i.e. that operating at higher temperatures, pressures, gas velocities, catalyst concentrations and per-pass conversions, and at optimized feed gas H_2/CO ratios, compared to the previous proposal by Van der Laan *et al*. (1999), will enhance the reactor productivity.

It is further hypothesized that some previous attempts to demonstrate higher temperature operation with low feed gas H_2/CO ratio failed due to catalyst break-up and subsequent declining conversion resulting from the formation of graphitic carbon, and that this can be avoided by increasing the operating pressure and operating at an intermediate feed gas H_2/CO ratio. The literature review indicates that the choice of alternative promoters may also be effective in suppressing both graphitic carbon formation and catalyst oxidation but catalyst development is beyond the scope of this thesis. Higher operating pressures remain desirable due to the positive effect on reactor productivity.

3.3 Proposed New Operating Conditions to Explore

The new set of feasible and desired operating conditions, for the selected precipitated iron catalyst, which it is recommended to explore is summarized as follows:

Temperature between 250 and 270 ˚C
Pressure between 30 and 40 bar
Feed H_2/CO close to the usage ratio
Superficial inlet gas velocity above 0.69 m/s
Solids volume fraction above 0.3

The proposed gas velocity would require an extrapolation for the most appropriate prior art correlation for gas holdup prediction so it is considered necessary to explore a more theoretical approach to gas holdup prediction at higher gas velocities. Reactor productivity calculations in this thesis are limited to a maximum solids volume fraction of 0.4 which is the upper limit used to develop a published gas holdup correlation.

3.4 Objectives

The objective of the proposed research was to establish a new set of feasible and desired operating conditions for a generic precipitated iron catalyst similar to the catalyst originally developed by Ruhrchemie, suitably prepared and conditioned for use in a slurry-phase reactor system. In particular, these new operating conditions target the cost effective application of a significantly higher slurry-phase reactor capacity for the production of hydrocarbon products.

It is expected to be possible to demonstrate a significant improvement to the reactor design proposed and modelled by Van der Laan *et al.* (1999) while taking into account catalyst stability issues which were not considered for their proposed design. A target is set to increase the reactor productivity by at least 50 %.

It is proposed to adapt the two-phase theory to better describe the gas holdup at higher velocities in the churn-turbulent regime. A characteristic of the churn-turbulent regime is that small bubbles are dragged into circulation and it is postulated that there is a limit to the gas holdup contribution from small bubbles that are circulating with the slurry. The velocity above which no further small bubbles are dragged into circulation is described as the saturation velocity, U_s. It is proposed to adapt the two-phase theory to reclassify the dense phase and the dilute phase. In this adaptation, all bubbles which contribute to flow

through the slurry are deemed to constitute the dilute phase while all bubbles which remain in circulation are deemed to constitute the dense phase.

To use the bed collapse method to determine the small bubble holdup is effectively the same as defining small bubbles as those bubbles which are in circulation in the slurry. The bed collapse method is therefore better aligned with the adapted two-phase theory rather than the original modified two-phase theory.

It is proposed to select a temperature higher than that used for the investigation by Van der Laan *et al.* (1999) at equal or higher pressures.

A first laboratory experiment was proposed using a well-mixed laboratory slurry micro reactor, at the selected higher temperature (260 ˚C) and pressure (40 bar) relative to the conditions selected by Van der Laan *et al.* (1999) (i.e. 250 ˚C and 30 bar). The intention was to determine the FT reaction rate constant and the reactant usage ratio, using a feed gas H_2/CO ratio slightly below the usage ratio, at one boundary for the proposed new operating space. Both the higher temperature and the higher CO partial pressure are expected to have a positive impact on the reactor productivity. In addition, it has been observed that a higher temperature decreases the selectivity to organic acids which can be detrimental to catalyst stability. On the other hand, higher temperatures are more prone to result in the formation of graphitic carbon which disintegrates the catalyst. The higher pressure is expected to counteract this tendency and suppress the onset of graphitic carbon formation.

A second experiment was then proposed at the selected higher temperature (270 ˚C), but at a pressure (30 bar) and feed H_2/CO (1.56) similar to the values considered by Van der Laan *et al.* (1999). The single pass conversion was set to match the typically proposed first stage reactor conversion. The intention is to demonstrate stable catalyst performance at the selected conditions and to quantify the improved reactor productivity with the higher temperature.

The overarching objective is to directly use the experimental results to calculate potential reactor productivity for comparison to prior reactor productivity claims.

3.5 Key Questions

In formulating the key questions, certain findings from the literature review are assumed to be valid. The first assumption is that that there exists an upper limit per pass conversion which should not be exceeded if a stable catalyst performance is to be maintained. Secondly, it is assumed that problems previously encountered with graphitic carbon formation, which leads to unacceptable physical degradation of the catalyst, were due to operation at lower pressures. Attempting to determine precise boundaries for these constraints of minimum operating pressure and an upper limit per pass conversion, for a variety of operating conditions, would require a massive experimental effort. The approach used is rather to build on previous work by incrementally modifying the relevant operating parameters in a direction which will further enhance the reactor productivity while also being compatible with likely commercial applications. The per pass conversion is set at a level which is compatible with a two stage reactor design and the conditions investigated by Van der Laan *et al*. (1999) are used as the departure point to explore feed H_2/CO ratios closer to the usage ratio; higher operating pressures and higher operating temperatures. The acceptability of the catalyst stability and the product selectivity trends are then evaluated and, if acceptable, then the impact on the reactor productivity is determined.

The key questions to be answered with this approach are:

1) Can catalyst break-up (previously observed at higher operating temperatures and low feed gas H_2/CO ratios) be avoided at the selected operating conditions (by increasing the operating pressure and operating at a feed gas H_2/CO ratio between 1.0 and 1.5)?

2) Can the favourable methane and carbon dioxide selectivities reported by Fletcher (2009) and others be repeated but with a stable FT conversion at a level high enough to be competitive with the cobalt catalyst?

3) Can reasonable catalyst activity stability be maintained at the proposed new operating conditions?

4) What is the potential further improvement in reactor productivity achievable by operating closer to the usage ratio with a feed gas H_2/CO ratio between the values used for the two experiments performed for this study?

5) What is the achievable reactor productivity at the target 60 % per-pass conversion when using a higher gas velocity and catalyst concentration relative to the values used by Van der Laan *et al.* (1999) when combined with new proposed operating conditions tested in the laboratory?

It is important to understand the maximum allowable catalyst concentration at commercial synthesis conditions but this is beyond the scope of this thesis since this would need to be determined experimentally in large scale equipment. Potential negative consequences, such as excessive temperature gradients due to poor thermal mixing and heat transfer, may occur at higher concentrations. In answering question 5, concentrations up to 40 vol.% are considered since this is the upper limit for the range of applicability of the OSU correlation. Prior to engaging in large scale experiments it may be useful to use

computational fluid dynamic (CFD) simulations to understand the slurry mixing trends with increasing catalyst concentration.

3.6 Experimental Data Acquisition and Modelling Approach

The approach to addressing the key questions is to first determine the catalyst synthesis performance at the selected operating conditions in a laboratory micro reactor. Stable performance allows questions 1, 2 and 3 to be addressed.

A simple well-mixed reactor model is set up to calculate the relative reactor productivity in terms of the hydrocarbon production per unit of reactor shell surface area (which is directly proportional to the reactor shell mass and cost). This model requires a prediction of the mass of catalyst in the reactor as a function of the bed height - which depends on the gas holdup. The gas holdup data of Koop (2003) is used to develop a suitable gas holdup prediction. This model is then used to address questions 4 and 5.

4. EXPERIMENTAL

4.1 Laboratory Reactor Experiments

Two laboratory experiments were performed, the first at 260 ˚C and the second at 270 ˚C. Both experiments used standard alkali-promoted precipitated iron catalyst precursor with the reactor stirrer speed set at 450 rpm. The catalyst precursor is conditioned in situ to produce the active catalyst. 10 g of catalyst precursor was used for the experiment at 260 ˚C and 5 g of catalyst precursor was used for the experiment at 270 ˚C.

The experimental equipment used, at the Sasol Technology R&D facilities in Sasolburg, has been well established to provide reliable kinetic data for various catalysts used for Fischer-Tropsch synthesis and no new approaches were required, other than to select an appropriate amount of catalyst and the appropriate space velocity to explore the proposed new operating conditions.

To eliminate internal and external transport limitations, small catalyst particles were used (particle diameter < 190 micron) and the reacting phases were well mixed.

Because the reactor contents are well mixed, the catalyst sees the exit gas composition. This simplifies the application of the kinetic expressions to calculate the activity coefficients for the reaction of CO and H_2 on the catalyst surface. Unless otherwise stated, the kinetic expressions proposed by Botes and Breman (2006) and motivated in detail by Botes (2008) are used.

4.1.1 Experimental setup

The experimental system used consists of mass flow controllers controlling the feed to a stirred tank reactor (constructed in-house at Sasol Technology R&D) followed by a hot pot, a cold pot and a back pressure regulator. On-line gas chromatographs (GC's) are used for the tail gas and the synthesis gas analyses. Synthesis gas is fed from gas cylinders, one containing H_2 and another containing CO.

The reactor has a total volume of 500 ml and an operational slurry volume of approximately 300 ml at 250 °C. Reactor internals such as the stirrer, thermowell and gas feed line take up the remaining volume thereby increasing the slurry level to the filter.

The reactor has a double-blade stirrer to ensure good mixing of the slurry (liquid and solid) and the gas phase under reaction conditions. The feed line enters at the top of the reactor and ends below the bottom stirrer in order to ensure good gas mixing. Both the gaseous and liquid products leave the reactor through a filter to ensure that all the catalyst remains in the reactor. The temperature in the reactor is measured by two thermocouples placed in a thermowell. The mixed (liquid and vapour) product from the reactor passes into the hot pot which is kept at 200 °C. In the hot pot all the liquid ("wax") is collected along with some condensed vapour. The remaining vapour stream then passes through a cold pot which is chilled to 25 °C. The temperature is measured at the outlet of the cold pot by a thermocouple in contact with the gas phase.

In the cold pot, water and organic product compounds are condensed out. The liquid products were not analysed for this investigation which focussed primarily on the gas

phase conversions; the selectivity to the unwanted methane product and the carbon dioxide selectivity.

The remaining tail gas is sampled from a point before the back-pressure regulator with the remainder of the gas passing through the back pressure regulator and out to the vent. The composition of the tail gas is determined by on-line gas chromatographs. Reactant conversions are calculated from the measured flow and compositions of the feed gas and the tail gas.

Further details of a similar experimental set-up can be found in the thesis of Van Berge (1994). The so-called ampoule-sampling technique (developed by Shulz's group) is described in this thesis but was not required for this work since on-line GC measurements of the tail gas composition were sufficient for the necessary results. Govender *et al*. (2006) also describe a similar experimental set-up.

In order to establish the conversion of the reactants and the methane and carbon dioxide selectivities, it is only necessary to consider the gaseous streams. Measurement of the selectivity of the higher carbon numbers was not attempted for this work and only the yield of the wax and hydrocarbon condensate products, from the hot and cold pots respectively, are reported based on the measured liquid flows. Determination of the wax carbon number distribution is often complicated by the need to run with steady performance for a long time period in order to displace the liquid wax inventory present in the reactor from the starting wax material or to displace wax produced under other operating conditions. It has also been pointed out previously by Raje and Davis (1996) that the measured product selectivity up to C_{15} may be distorted by the stripping of previously accumulated dissolved lighter hydrocarbons if the catalyst is deactivating towards a lighter product spectrum. For the experiments performed for this work there was no such catalyst deactivation towards a lighter product spectrum.

The analysis of the "permanent" gases and the Fischer-Tropsch products up to C_{15} are performed using different GC methods.

The analysis of the permanent gases (i.e. H_2, Ar, N_2, CO, CH_4 and CO_2) was performed on a GC which was equipped with two identical thermal conductivity detectors (TCD's). The reason for the two TCD's is that no single suitable carrier gas is available that will allow the simultaneous determination of the listed gases. H_2 is therefore exclusively analysed on the one TCD channel with Ar as carrier gas, whilst the other "permanent" gases are analysed using a second TCD channel with H_2 as carrier gas.

For the analysis of the hydrocarbon gases other than methane, it is necessary to preheat the sample line to about 200 ˚C in order to ensure that all the sampled hydrocarbons are vaporized for analysis using a flame ionization detector (FID) GC analysis.

The quantification of the catalyst performance in terms of conversion, methane selectivity and catalyst activity requires the use of a calibration gas mixture consisting of H_2, Ar, N_2, CO, CH_4 and CO_2.

The consumption rate of carbon monoxide to form hydrocarbon products by Fischer-Tropsch synthesis is easily determined by a carbon balance in which the molar tail gas

flow rate of carbon monoxide plus carbon dioxide is subtracted from the molar feed flow rate of carbon monoxide plus carbon dioxide (usually zero). Thus,

r_{FT} = moles/s $(CO + CO_2)_{in}$ – moles/s $(CO + CO_2)_{out}$

$$r_{FT} = A_{FT} \frac{p_{CO}(p_{H_2})^{0.5}}{(1+0.09p_{CO})^2}$$

A_{FT} is referred to as the catalyst activity and may be further expressed as a pre-exponential rate constant k_{FT} and an Arhenius term describing the temperature dependence, thus:

$$A_{FT} = k_{FT} \left(e^{E_A/RT}\right)$$

Where E_A is the activation energy.

$$\text{The methane selectivity} = \frac{\text{moles/h } (CH_4)_{out} - \text{moles/h } (CH_4)_{in}}{\text{moles/h } (CO + CO_2)_{in} - \text{moles/h } (CO + CO_2)_{out}}$$

$$\text{The carbon dioxide selectivity} = \frac{\text{moles/h } (CO_2)_{out} - \text{moles/h } (CO_2)_{in}}{\text{moles/h } (CO)_{in} - \text{moles/h } (CO)_{out}}$$

The (H_2 + CO) conversion, also referred to as the synthesis gas conversion, is calculated as follows:

$$(H_2 + CO) \text{ conversion} = \frac{\text{moles/h } (H_2+CO)_{in} - \text{moles/h } (H_2+CO)_{out}}{\text{moles/h } (H_2+CO)_{in}}$$

The feed gas hourly space velocity (including inert gases) is calculated by dividing the feed flow in ml_n/h by the catalyst mass (g). The synthesis gas hourly space velocity is determined by multiplying the feed gas hourly space velocity by the mole fraction of (H_2 + CO) in the feed gas.

The moles/h (H_2 + CO) in the feed gas can be calculated by multiplying the measured feed gas flow in ml_n/h by the mole fraction of (H_2 + CO) in the feed gas and dividing by the conversion factor of 22414.

4.1.2 The experiments

4.1.2.1 Experiment 1 (260 ˚C, 40 bar(g), feed H_2/CO = 1)

For the experiment at 260 ˚C, the pressure was 40 bar(g) with a synthesis gas feed H_2/CO ratio of 1.0. The space velocity was set high enough to safely avoid the catalyst deactivation. Experimental conditions (temperature, feed H_2/CO and gas hourly space velocity) with time-on-line are presented in Figures 10, 11 and 12 respectively.

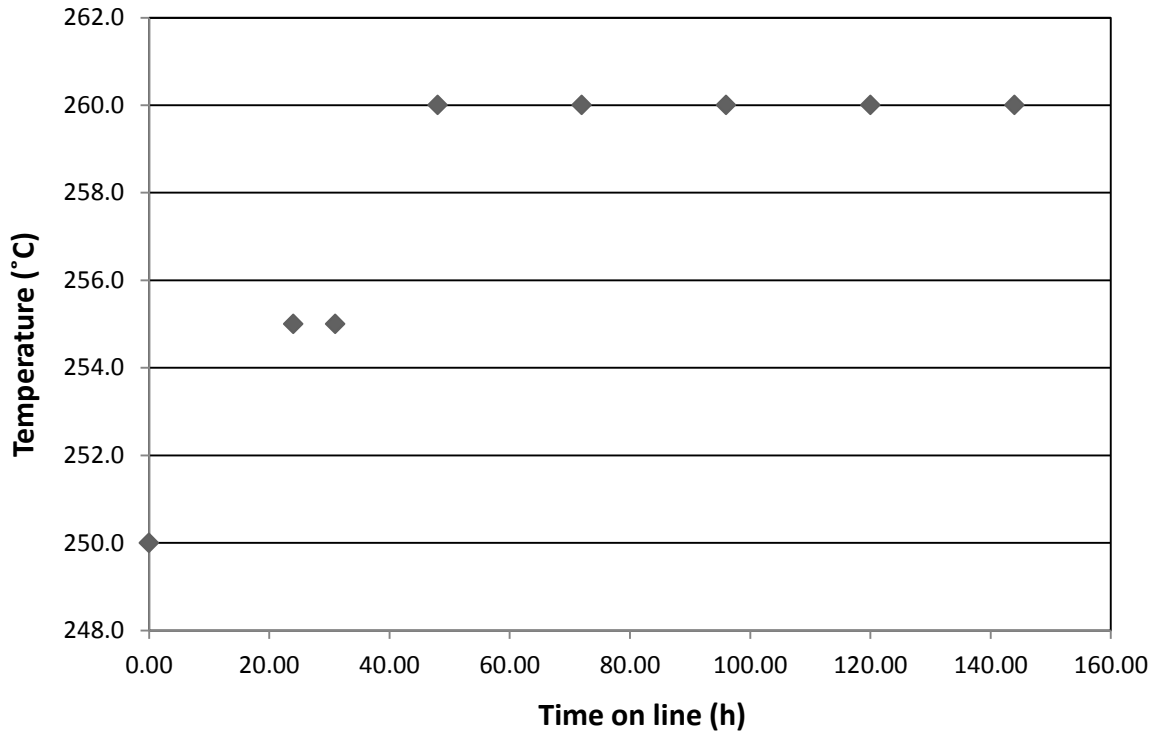

Figure 10: Temperature ramp up to 260 ˚C

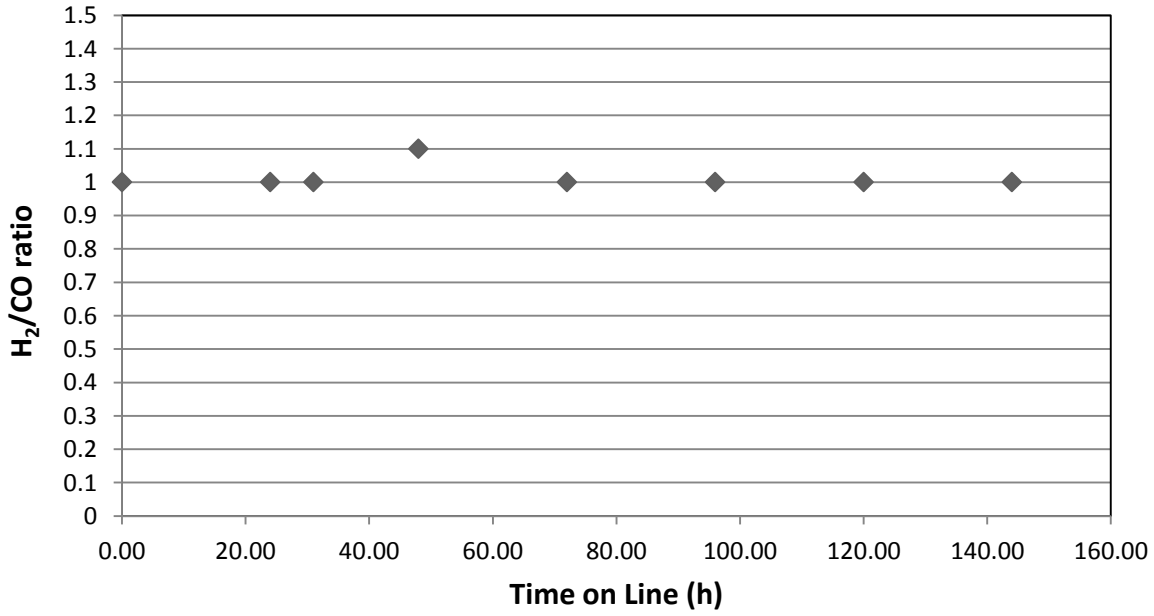

Figure 11: Feed gas H_2/CO ratio for the 260 ˚C experiment

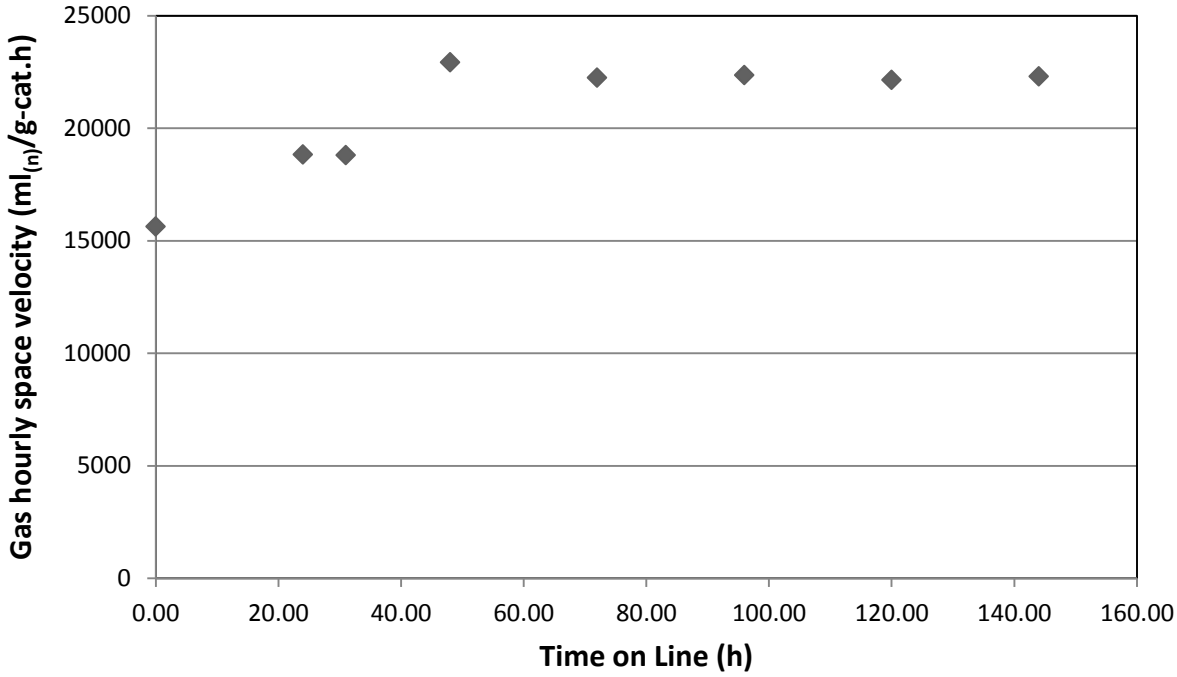

Figure 12: Synthesis gas hourly space velocity ($ml_{(n)}(H_2 + CO)$/g-cat.h) for the 260 ˚C experiment

4.1.2.2 Experiment 2 (270 ˚C, 30 bar(g), feed H_2/CO ratio = 1.56)

For the run at 270 ˚C, the pressure was 30 bar(g) and the synthesis gas feed H_2/CO ratio was 1.56. The space velocity was selected to achieve a target synthesis gas (H_2 + CO) conversion of 60 %. Experimental conditions (temperature, feed H_2/CO and gas hourly space velocity) with time-on-line are presented in Figures 13, 14 and 15 respectively.

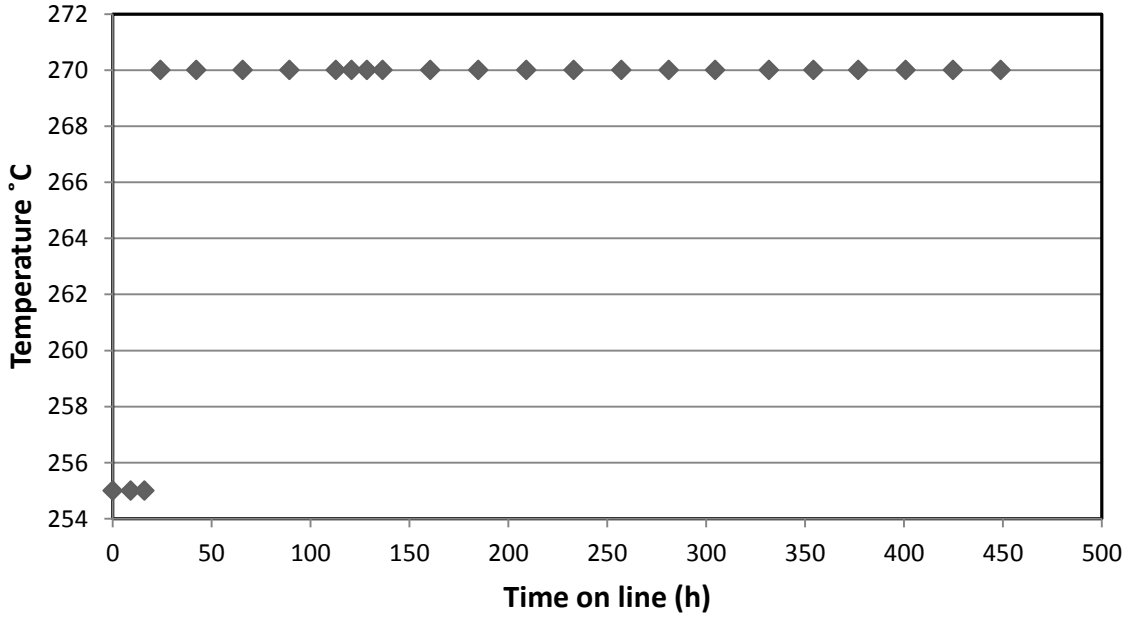

Figure 13: Temperature ramp up to 270 ˚C

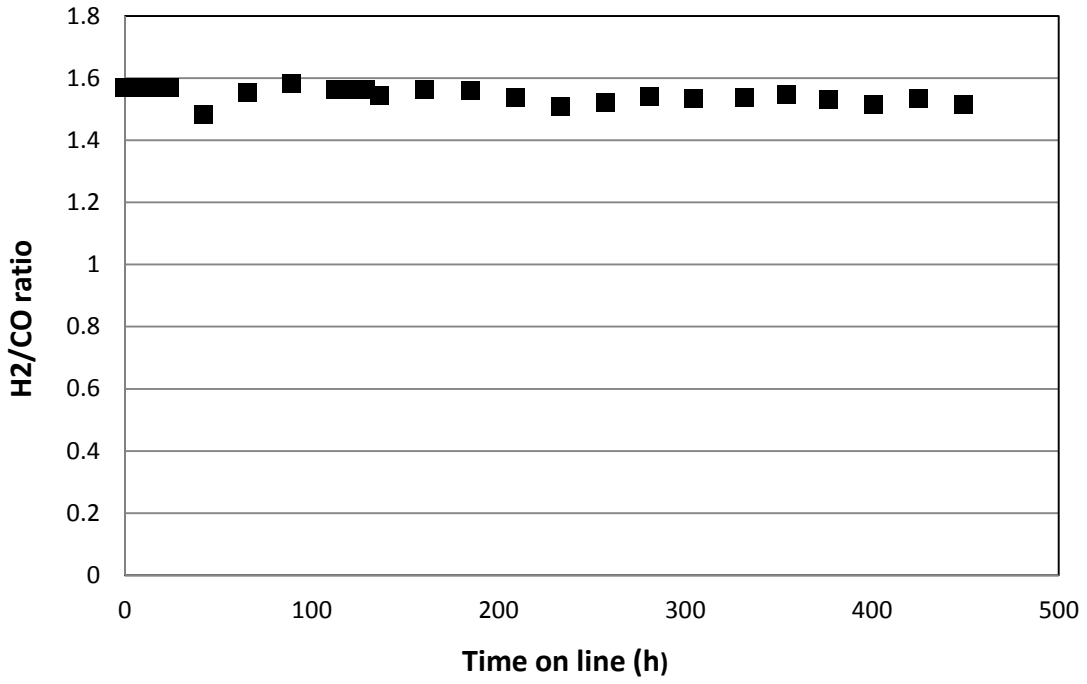

Figure 14: Feed gas H_2/CO ratio for the 270 ˚C experiment

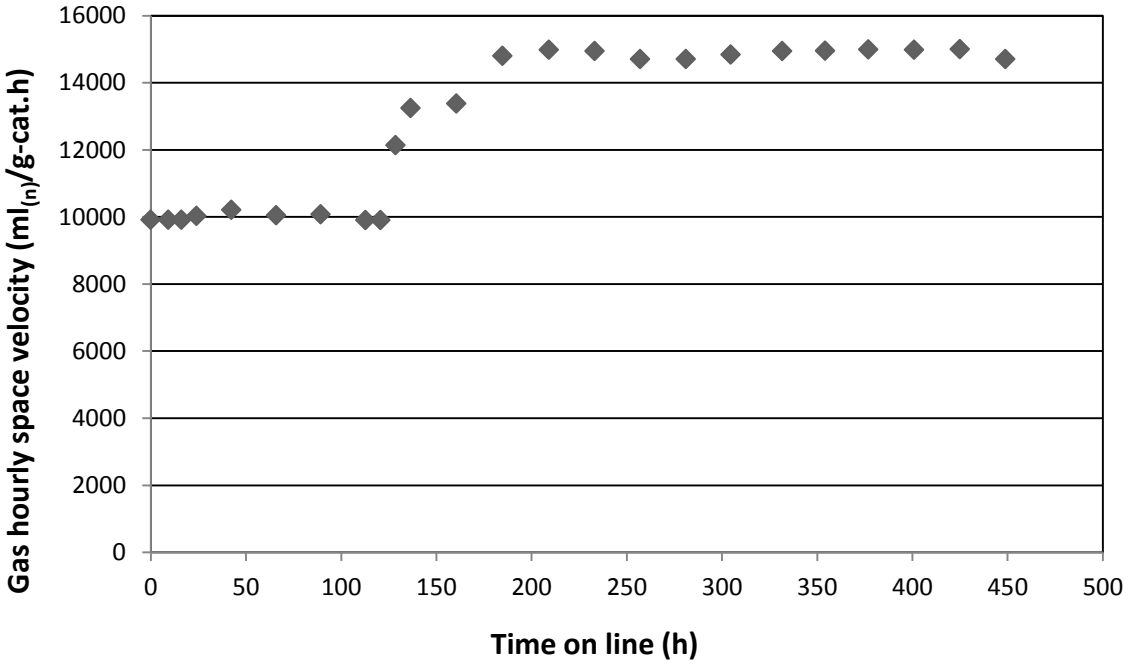

Figure 15: Gas hourly space velocity for the 270 ˚C experiment

5. RESULTS

5.1 Development of Adapted Two-Phase Theory for Gas Holdup Prediction

The departure point was to first examine the constraints relating to the catalyst concentration and gas velocity in a commercial reactor. This was aimed at key questions (5) and (6). Experimental results for gas holdup at a range of relevant operating conditions were fitted to a well-accepted empirical correlation from the literature and a new correlation was proposed using an adapted two-phase theory.

5.1.1 Relevant gas holdup data

Relevant data was available from the hydrodynamic experiments carried out by Koop (2003) with compressed air at room temperature and are reproduced below for convenience. Table 8 compares the gas densities of air under experimental conditions and typical synthesis gas (syngas) under Fischer-Tropsch reactor conditions considered by Koop (2003). The densities are reported at 230 ˚C (503 K) and in the range of 25 - 40 bar, which are typical Fischer-Tropsch conditions envisaged for cobalt catalyst. Given that a range of gas densities was used, it is considered that the density effect can be evaluated and extrapolated, if necessary, to also apply to the gas densities considered for use with the iron catalyst system. 5, 8, 10 and 11 bar air pressures correspond to the pressures used in the hydrodynamic experiments.

Table 8: Gas densities of syngas and air

Syngas Pressure (bar)	Syngas[a] Density at 230 ˚C (kg/m^3)	Air Pressure (bar)	Air[b] Density at 25 ˚C (kg/m^3)
25	7.7	5	5.8
30	9.3	8	9.4
35	10.8	10	11.7
40	12.3	11	12.9

[a] Composition: 60 % H_2, 30 % CO, 6 % CO_2 and 4 % CH_4

[b] Composition: 78 % N_2, 21 % O_2 and 1 % Ar

Relevant physical properties of the paraffins are given in Table 9.

Table 9: Relevant physical properties of paraffins at 25 ˚C

	ρ (kg/m^3)[a]	μ (Pa.s)[b] x 10^3	σ (N/m)[b] x 10^3
n-heptane	679.5	0.387	19.65
n-octane	698.5	0.508	21.14
n-nonane	713.8	0.665	22.38
n-decane	726.4	0.838	23.37
n-undecane	736.5	1.098	24.21

[a]Taken from Lide (2002)

[b]Taken from Hesse *et al*. (1996)

The compositions of the liquid mixtures are given in Table 10. The mixtures' density and viscosity are computed as a simple weighted average from the pure component properties. This approach is also applied for the surface tension, i.e. the composition at

gas-liquid interfaces is assumed to be similar to that of the bulk fluid. Table 11 shows these calculated properties.

Table 10: Composition of the two paraffin mixtures (wt.%)

C_7-C_8 mixture	**C_9-C_{11} mixture**
C_6 and lighter <0.1	C_8 and lighter 3.3
C_7 hydrocarbons 39.8 (40)	C_9 hydrocarbons 36.3 (38)
C_8 hydrocarbons 58.6 (60)	C_{10} hydrocarbons 34.5 (37)
C_9 and heavier 0.2	C_{11} hydrocarbons 23.8 (25)
	C_{12} and heavier 1.9

Numbers between brackets: used for calculating mixture properties; see Table 9. In some of the experiments 5 vol.% (5 vol.% of the gas and solids free liquid) of alcohol was added. The alcohol was 1-propanol.

Table 11: Comparison of physical properties FT-wax and mimic fluids

	FT-mixture[a]	C_7-C_8 Paraffin	C_9-C_{11} Paraffin
T (˚C)	230	25	25
ρ (kg/m^3)	679	691	724
μ (Pa.s) x 10^3	0.741	0.460	0.837
σ (N/m) x 10^3	18.04	20.54	23.20

[a]average C_{30} paraffins/olefins

For the liquid, it is important to select a liquid with representative density, viscosity and surface tension. All experiments were performed with relevant mixtures of normal paraffins. The properties of the solids used are provided in Table 12.

Table 12: Relevant physical properties of alumina particles

Manufacturer	Sasol
Particle diameter range (μm)	≈ 50–150
Particle pore volume fraction	0.639
$\rho_{skeleton}$ (kg/m^3)	3420
$\rho_{particle}$ (kg/m^3)[a]	1700

[a]Liquid filled pores (ρ_L = 724 kg/m^3)

5.1.2 Gas holdup prediction

A new approach to gas holdup prediction is developed in order to provide more confidence to extrapolate prior art empirical correlations, such as the OSU correlation, to higher gas velocities. This new approach, explained in this section, is referred to as the 'adapted two-phase theory'. This is considered to be the scientific result underlying the ability to predict the selected reactor performance at higher capacities with improved confidence for the accuracy of the prediction.

The OSU correlation was compared to the data from Koop (2003) and found to match the data well in the range of applicability for this empirical correlation. It was then accepted that this correlation can be used to accurately predict gas holdup for the solids-free paraffin liquids in the churn-turbulent regime.

Wilkinson (1991) concluded that the only experimental data relevant for design of commercial scale bubble columns are those obtained in bubble columns with a diameter larger than the critical column diameter, an aspect ratio H/D > 5 or H > 1 – 3 m and perforated plate or single nozzle with hole diameters in excess of 1 – 2 mm as gas distributor. The critical column diameter above which the gas holdup is not influenced by the diameter is usually close to 15 cm and can be expected to decrease to some extent with increasing gas density and decreasing surface tension. Wilkinson gives the following correlation to estimate the critical column diameter D_c:

$$D_c = 20\left(\frac{\sigma^2}{g^2(\rho_L - \rho_G)\rho_G}\right)^{0.25} \quad (10)$$

Equation (10) gives a critical column diameter of 0.09 – 0.11 m for gas densities of 6 and 10 kg/m^3 respectively. It is clear that the column diameter of 16.15 cm used by Koop (2003) is sufficient in the pressure range of 5.8 to 12.9 kg/m^3.

In order to extrapolate gas holdup predictions to higher gas velocities and higher solids concentrations, a more theoretical approach is developed which is referred to as the adapted two-phase theory.

5.1.2.1 Theoretical basis for the adapted two-phase theory

The modified two-phase theory approach from the literature is described in section 2.6. For any two-phase theory the dense phase gas holdup, ε_d, is taken as the predicted gas holdup at the dense phase saturation and this is added to the dilute phase gas holdup, ε_b using equation (8) to get the total gas holdup:

$$\varepsilon = \varepsilon_b + \varepsilon_d(1 - \varepsilon_b) \quad (8)$$

The adapted two-phase theory differs from the modified two-phase theory approach in that the small bubbles are defined as the bubbles which only remain in circulation rather than as the bubbles present at the transition from bubble flow to churn-turbulent flow.

Equation (9) from the modified two-phase theory is then replaced by equation (11) for the adapted two-phase theory, i.e.

$$\varepsilon_b = CU^{0.8} - C(U_{df})^{0.8} \quad (9)$$

replaced by:

$$\varepsilon_b = CU^{0.8} \quad (11)$$

It is postulated that there is a saturation gas holdup of small bubbles which remain in circulation at high superficial gas velocities for bubble columns operating in the churn-turbulent flow regime.

To predict the total gas holdup with the proposed approach, it is required to first predict the small bubble saturation (dense phase) gas holdup and then the dilute phase gas holdup.

The rationale for the new approach used to predict the small bubble saturation (dense phase) gas holdup is as follows:

A comparison of the gas holdup matched to the experimental data at the upper end of the velocity range when fitting equation (11) (as shown in Figure 16) shows a divergence between the measured and predicted gas holdup at some lower velocity (at about 0.3 m/s in Figure 16). It is postulated that the gas holdup at which this divergence occurs corresponds to the small bubble saturation gas holdup, such that further increases in gas holdup above this point of divergence are entirely due to the contribution of the larger bubbles.

It has been observed that the ratio of saturation gas holdup for various solids concentrations relative to the pure liquid is inversely proportional to the relative viscosity of the slurry.

Prediction of dense phase gas holdup therefore begins with prediction of the slurry viscosity.

Thomas (1965) suggested an equation to predict the relative slurry viscosity based on an extensive set of experimental data with several types of particles in the range of 0.1 to 500 micron and solids concentrations up to 60 % by volume:

$$(\mu_{sl}/\mu_L) = 1 + 2.5\varphi + 10.05\,\varphi^{2} + 0.00273e^{16.6\varphi} \qquad (12)$$

The maximum error was 13 % at 50 % solids. Barnea and Mizrahi (1973) used Thomas' data to find:

$$(\mu_{sl}/\mu_L) = \exp(2.66\,\varphi/(1-\varphi)) \qquad (13)$$

This correlation is used in this thesis to predict the slurry viscosity.

There are several correlations that have been proposed over the years for predicting the slurry viscosity based on the liquid properties and the volume fraction of solids. It should be noted that many of the correlations were fitted for low solids concentrations. The correlations of Barnea and Mizrahi (1973), Krieger and Dougherty (1959), Thomas (1965) and Graham (1981) are in good agreement.

With this approach, a new insight has been identified that the saturation of the dense phase with small bubbles in the churn-turbulent regime occurs at lower gas holdups as the slurry viscosity increases. The value of ε_d at the saturation gas holdup remains constant at higher velocities.

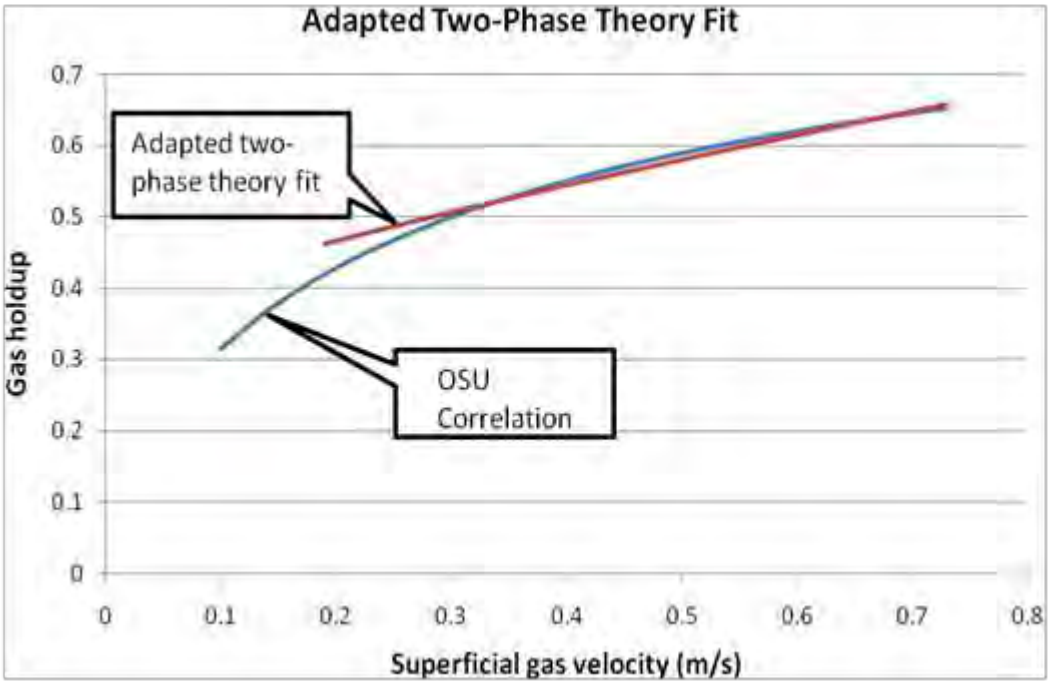

Figure 16: Gas holdup (ε) adapted two-phase theory fit to Ohio State University (OSU) correlation (Luo et al., 1999) for 5 bar air and C_9 – C_{11} paraffin liquid for C = 0.6 and U_{df} = 0

Similar best fits were prepared for a wide variety of catalyst concentrations and gas densities. The value of C = 0.6 from the reference case experiment, modified for pressure effects, was used successfully to fit data for all the solids concentrations for which the OSU correlation was developed.

Considering now the effect of pressure on the dilute phase, i.e. the large gas bubbles, it is noted that the following relationships have been proposed to describe the maximum stable bubble size:

$$d_{b,\max} \approx 2.53\sqrt{\left(\frac{\sigma}{g\rho_G}\right)} \tag{14}$$

for gas-liquid systems, and

$$d_{b,\max} \approx 3.27\sqrt{\left(\frac{\sigma}{g\rho_G}\right)} \tag{15}$$

for gas-slurry systems

As a consequence, the rise velocity of a bubble at its maximum stable bubble size is proportional to $(1/\rho_G)^{0.25}$ as can be deduced by substituting into the Taylor-Davies correlation to give:

$$V_{b,\max} \approx \sqrt{\left(\frac{C\,g^{0.5}\sigma^{0.5}}{2\rho_G^{\,0.5}}\right)} \approx \sqrt{\frac{C}{2}}\left(\frac{g\sigma}{\rho_G}\right)^{0.25} \tag{16}$$

Hence, the large bubble sizes decrease at higher pressures. The postulated result is a dependence of ε_b on the gas density to the power of 0.25.

The effect of pressure on the dilute phase gas holdup is predicted by multiplying the coefficient, C, from equation (11) by the relative pressure to the power 0.25. It should be noted though that it was proposed by Krishna *et al.* (1997) that the mean bubble velocity is proportional to $(1/\rho_G)^{0.5}$ because the bubble size distribution is observed to narrow at higher gas densities. Gas density is the only gas phase physical property of interest; hence, experiments conducted using air, at pressures giving a representative gas density, are likely to be relevant to synthesis gas applications.

To apply this new theory, the first step is to find a value for the constant C in equation (11). This constant was determined by selecting a value for this constant which matches the OSU correlation gas holdup prediction for solids-free paraffin liquid - a value for C of 0.6 gives a good fit for the gas velocities $U > U_s = 0.3$ m/s (see Figure16). This fit then provides a constant value for the dilute phase gas holdup, ε_b of 0.36 when applying equation (8) (repeated below for convenience).

$$\varepsilon = \varepsilon_b + \varepsilon_d(1 - \varepsilon_b) \quad (8)$$

The results of the predicted dense phase saturation properties are shown in Table 13. It is therefore possible to predict the saturation gas holdup for a variety of solids volume fractions and gas densities from the known saturation gas holdup for the solids-free liquid at any given gas density.

Table 13: Predicted saturation gas holdup using the reference case data

Solids volume fraction	Calculated relative slurry viscosity[1]	Predicted saturation dense phase gas holdup[2]
0.23	2.21	0.163
0.335	3.82	0.094
0.415	6.60	0.055

[1]The viscosity was calculated by inserting the solids volume fraction into equation (10).
[2]Calculated by dividing the solids free best fit saturation gas holdup of 0.36 by the calculated relative slurry viscosity.

In order to predict the total gas holdup, the dense phase gas holdup, ε_d is taken as the predicted gas holdup at saturation and the total gas holdup is then obtained using equation (8) with the dilute phase void fraction calculated from equation (11) – with $C = C_F(\text{relative density})^{0.25}$ and with $C_F = 0.6$.

Expressed as a single equation, the total gas holdup is calculated using:

$$\varepsilon = C_F(\rho_G/5.8)^{0.25}U^{0.8} + (0.36/(\exp(2.66\ \varphi/(1-\varphi))))(1-0.6(\rho_G/5.8)^{0.25}U^{0.8}) \quad (17)$$

When the “new” prediction from equation (17) is compared to the experimental data from Koop (2003) for gas velocities above 0.35 m s^{-1}, the mean square error is 0.00169 which is less than the mean square error for the OSU correlation prediction of 0.00332.

Expressed in the same terms as the fit to prior art correlations described in section 2.6:

For the adapted two-phase theory approach, AARE = 9.81 % and MRE = -4.90 %.

For the OSU correlation, AARE = 10.11 % and MRE = -5.51 %.

Where AARE (Average Absolute Relative Error) $= \frac{1}{N}\sum_{i=1}^{N}\left|\frac{\varepsilon_G,exp,i-\varepsilon_G,calc,i}{\varepsilon_G,exp,i}\right|$ (18)

and

MRE (Mean Relative Error) $= \frac{1}{N}\sum_{i=1}^{N}\frac{\varepsilon_G,exp,i-\varepsilon_G,calc,i}{\varepsilon_G,exp,i}$ (19)

In general, the predicted gas holdup closely follows the experimental data points at higher gas velocities for gas holdup values below 0.7.

5.2 Laboratory Reactor Experimental Results

5.2.1 Experiment 1 (260 ˚C, 40 bar(g), feed H_2/CO = 1)

The following results apply to the laboratory experiment at 260 ˚C, 40 bar(g) and feed gas H_2/CO ratio of 1.0. Figures 17, 18, 19 and 20 show the synthesis gas conversion, the H_2/CO usage ratio, methane selectivity and wax/oil yields, respectively with time on line.

The space velocity, operating temperature and conversion were only stable for the last 5 data points shown in all the Figures relating to this experiment. The reactant consumption ratio or usage ratio lined out at a value of between 1.2 and 1.3 during this stable operation which is above the feed ratio of 1.0. The CO_2 selectivity was 24 %.

Prior to ramping up to the stable operating temperature of 260 ˚C, the usage ratio was higher at between 1.4 and 1.5 when operating at 245 ˚C indicating slightly enhanced water gas shift reaction activity relative to hydrocarbon synthesis activity at the higher temperature. The impact of operating temperature on the usage ratio relative to the theoretic predictions from relevant literature is examined in the discussion section.

For the last 5 data points in Figures 17, 18, 19 and 20, the average partial pressures (bar) in the reactor are given in Table 14:

Table 14: Reactor average gas partial pressures for the 260 ˚C experiment

Components	Partial pressures (bar)
Hydrogen	14.31
Carbon monoxide	15.79
Water vapour	2.67
Carbon dioxide	1.35
Methane and higher hydrocarbons	1.51
Argon	4.37
Nitrogen	0.45

A very positive result for the operation at 260 ˚C was the low and stable methane selectivity of below 3 % (Figure 19) which is lower than can be achieved with cobalt

catalysts even when the cobalt catalyst is operated at the lowest practical operating temperature of around 220 ˚C.

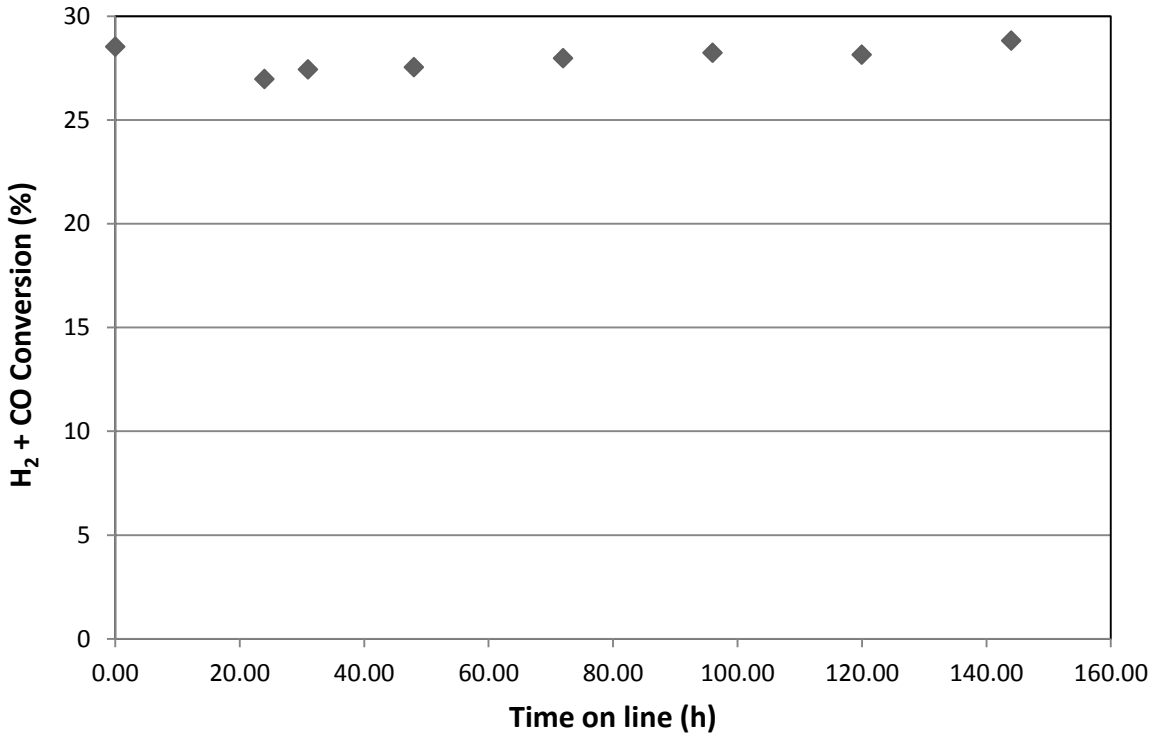

Figure 17: Synthesis gas conversion for the 260 ˚C experiment

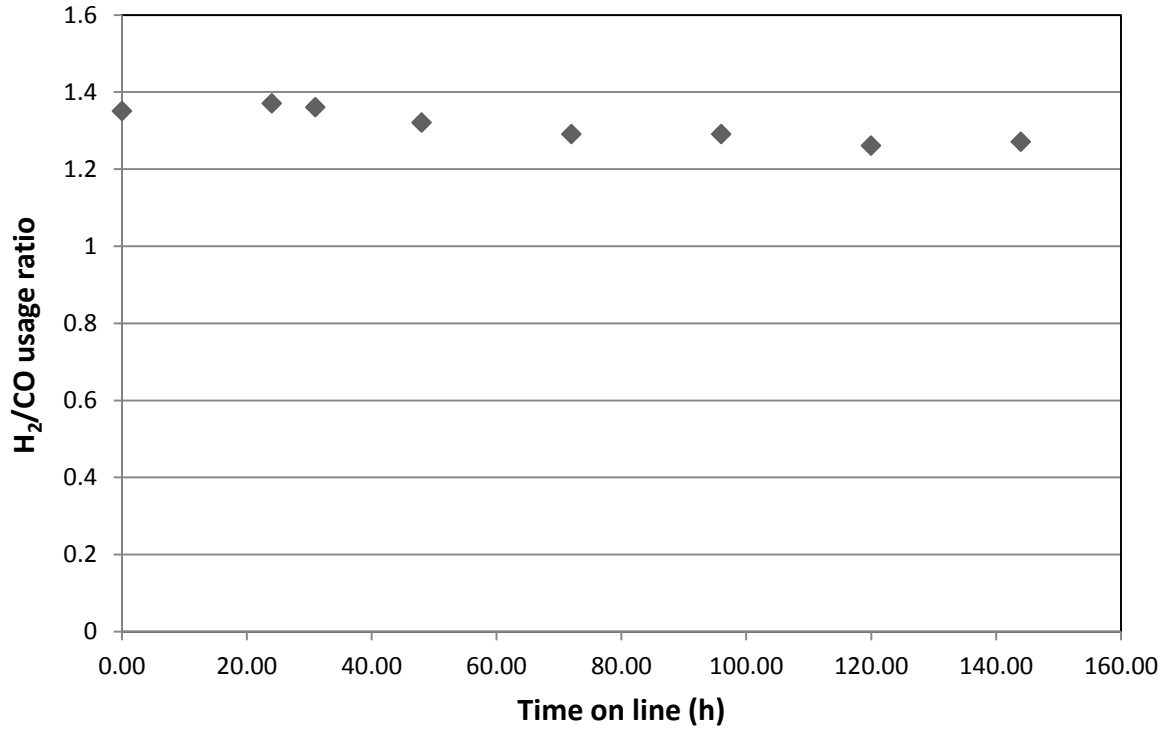

Figure 18: Measured usage ratio for the experiment at 260 ˚C, 40 bar and with feed H_2/CO ratio = 1.0

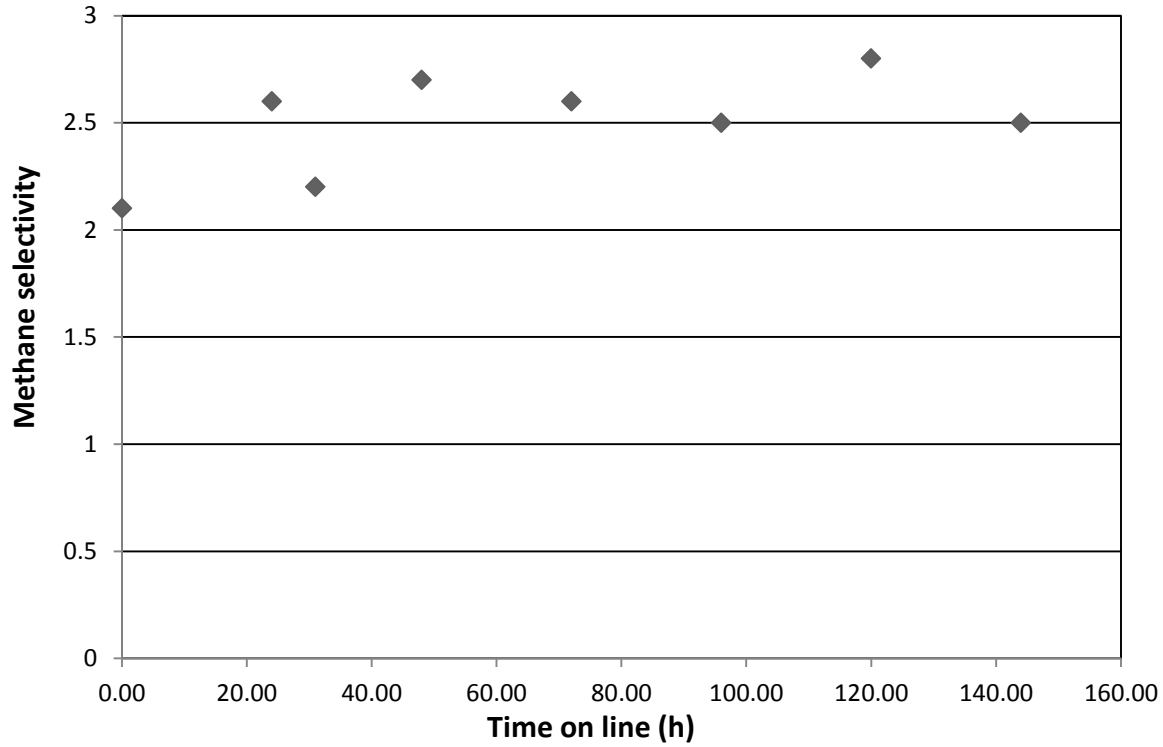

Figure 19: Methane selectivity for the experiment at 260 ˚C

The following liquid hydrocarbon product yields were obtained:

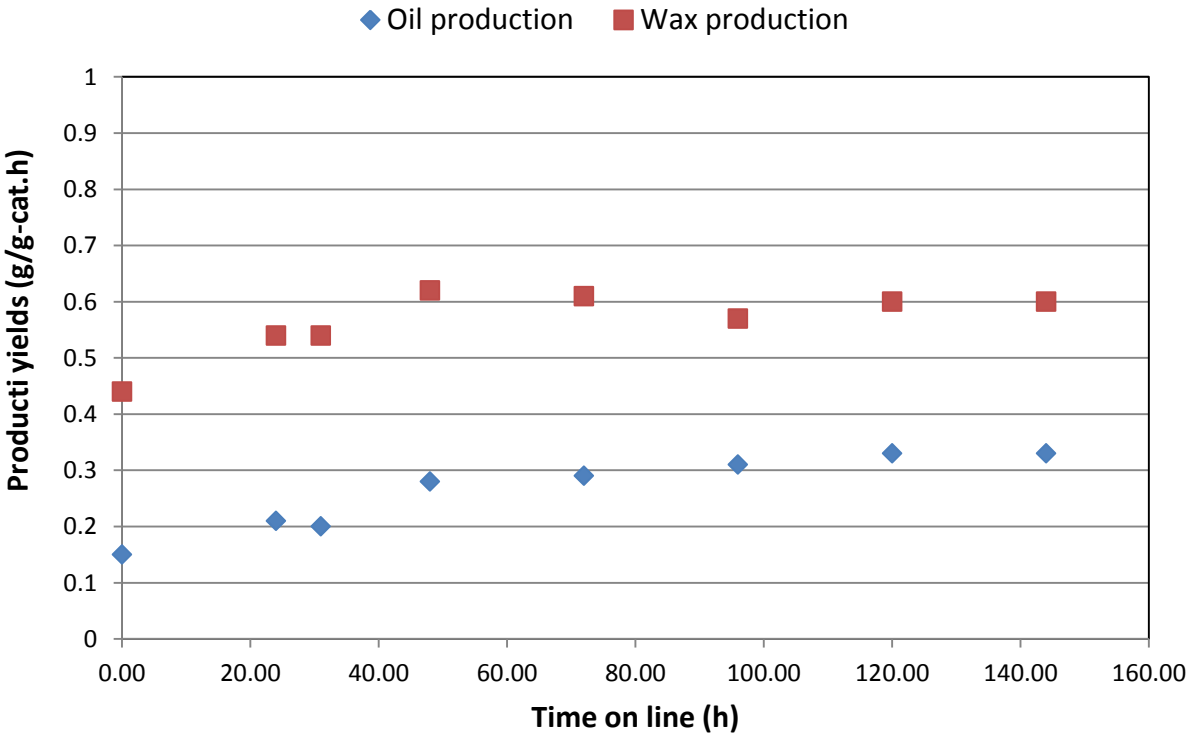

Figure 20: Product yields for the experiment at 260 ˚C

5.2.2 Experiment 2 (270 ˚C, 30 bar(g), feed H_2/CO ratio = 1.56)

From the fact that it was possible to establish a stable reactant conversion level with a very low methane selectivity at 260 ˚C, it was decided that more aggressive conditions could be attempted in a 270 ˚C experiment targeting desirable commercial operating conditions. The conditions for the 270 ˚C experiment were similar to conditions proposed by Van der Laan *et al*. (1999) other than that they used 250 ˚C.

The following results apply to the laboratory experiment at 270 ˚C, 30 bar(g) and feed gas H_2/CO ratio of 1.56. Figures 21, 22, 23 and 24 show the synthesis gas conversion, the H_2/CO usage ratio, methane selectivity and wax/oil yields, respectively with time on line.

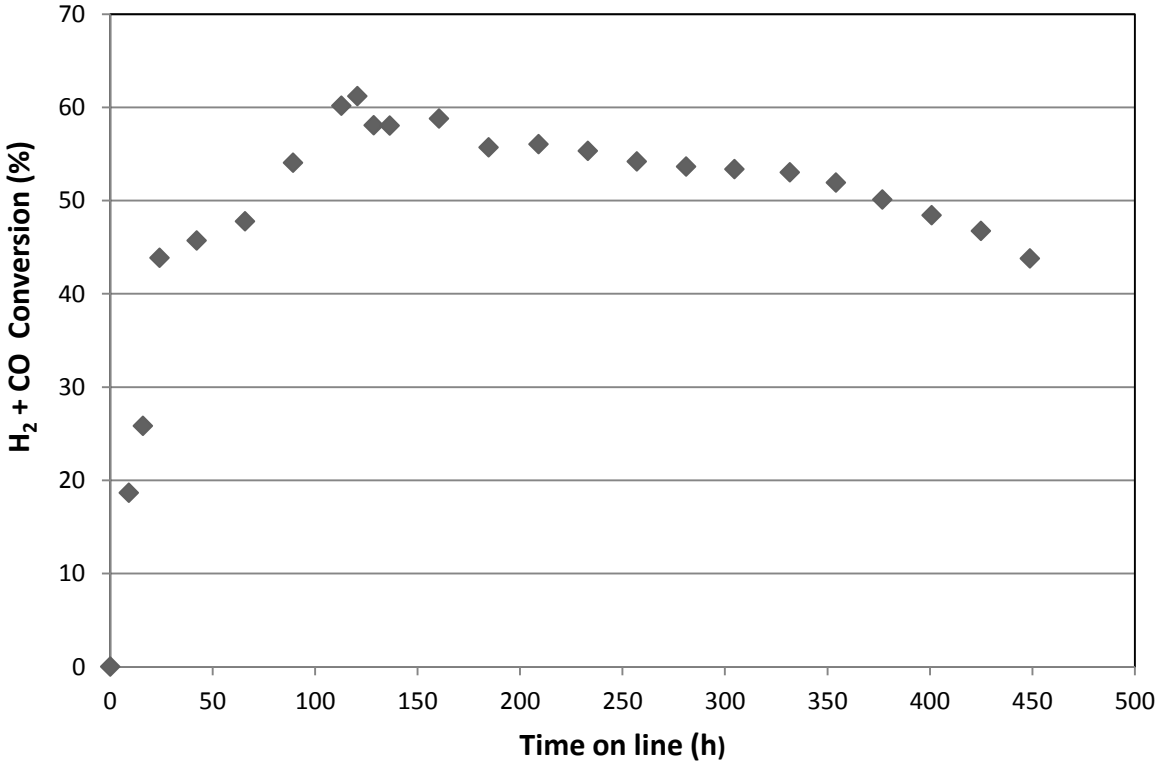

Figure 21: Synthesis gas conversion for the 270 ˚C experiment

Note, from Figure 22, that the usage ratio was between 1.2 and 1.3 initially for 3 data points after the temperature was at 270 ˚C. The usage ratio then decreased to between 1.0 and 1.1 corresponding to an increase in CO_2 selectivity from about 26 % to 33 %. The CO_2 selectivity remained steady as the synthesis gas conversion declined from the peak value indicating similar rates of decline for the water gas shift and hydrocarbon synthesis activity.

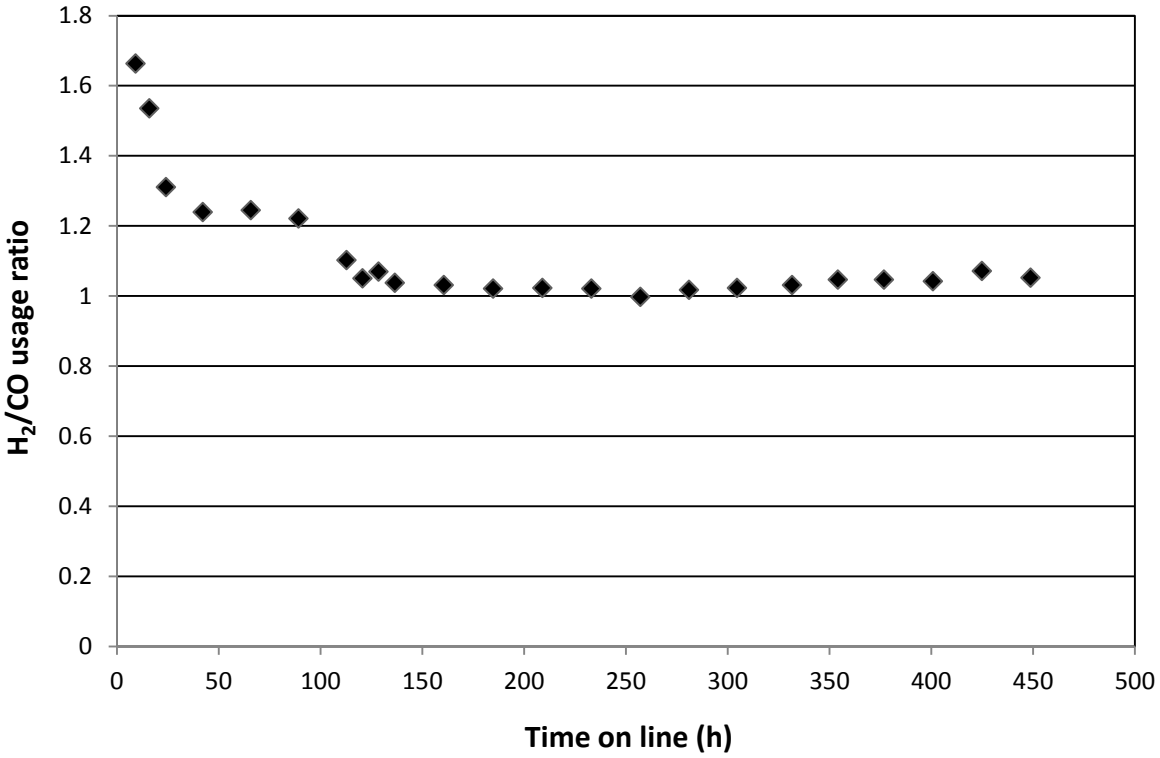

Figure 22: H_2/CO usage ratio for the experiment at 270 ˚C with feed H_2/CO ratio = 1.56

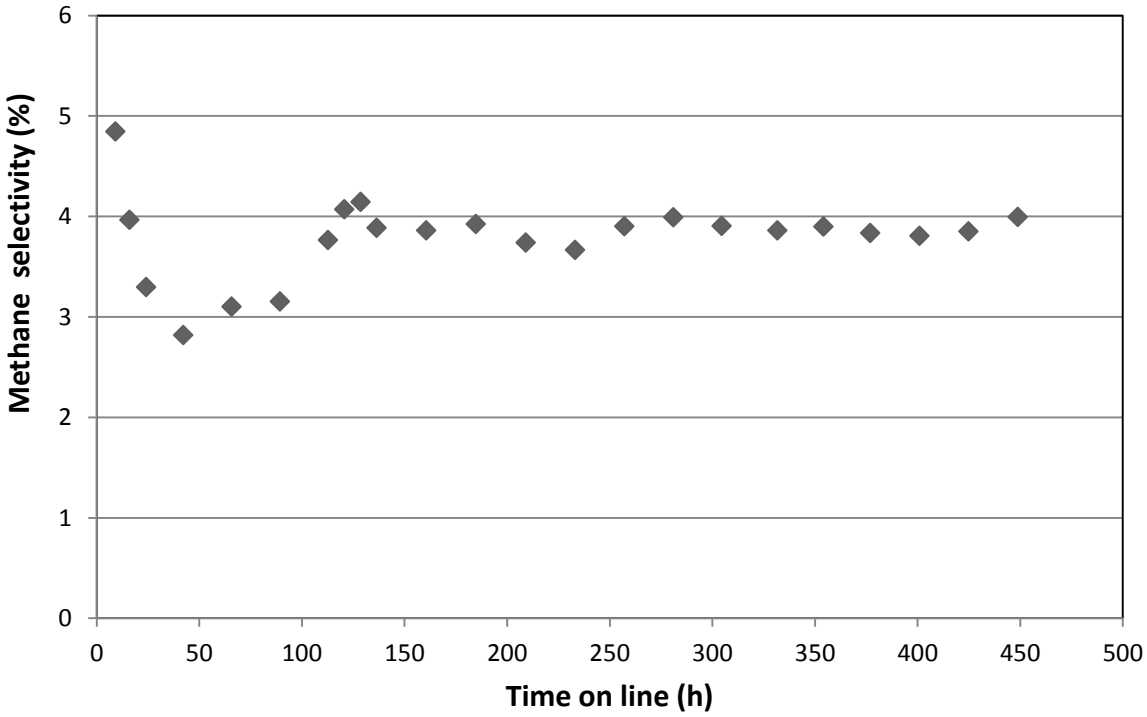

Figure 23: Methane selectivity for the experiment at 270 ˚C

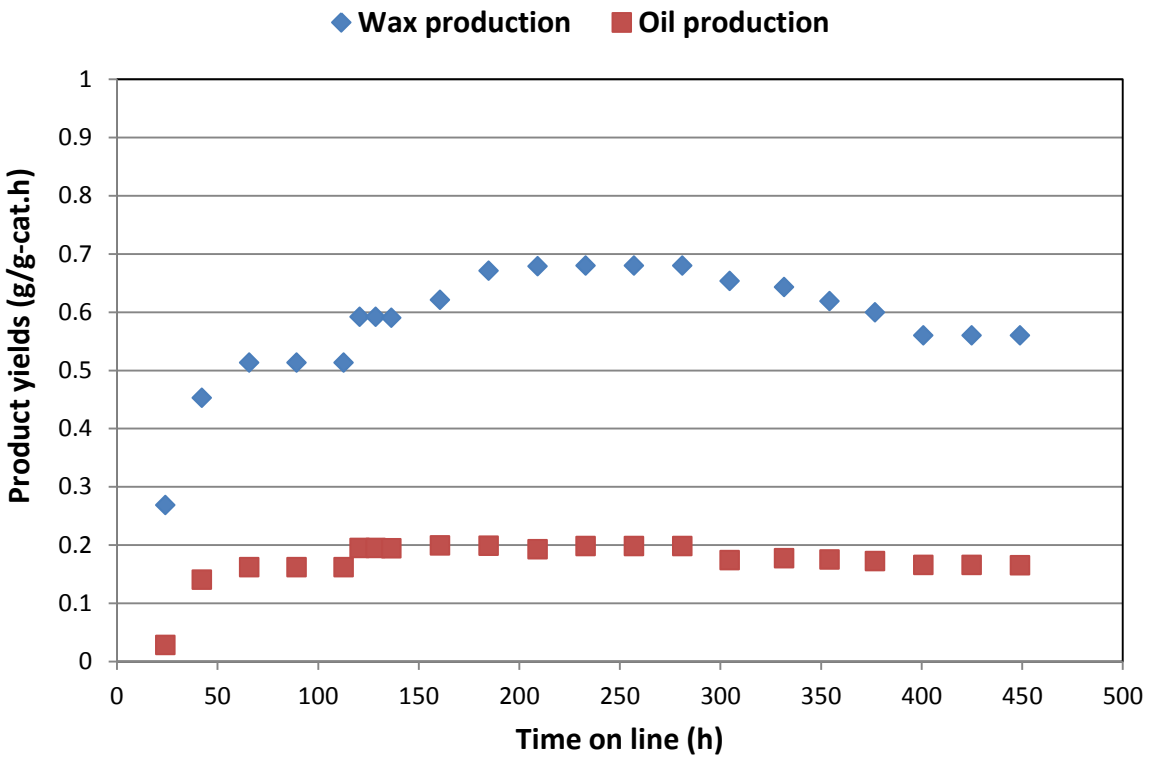

Figure 24: Product formation rate for the experiment at 270 ˚C

The selectivity for C_2 to C_4 hydrocarbons was 25 % (including oxygenated hydrocarbons) and the C_{5+} selectivity was 71 % for the periods when the methane selectivity was 4 %. Table 15 shows relevant gas partial pressures used in the performance calculations.

Table 15: Reactor average gas partial pressures for the 270 ˚C experiment

Component	3 day average partial pressure at peak catalyst activity (bar)	Average partial pressure for the last 3 days (bar)
Hydrogen	11.9	13.2
Carbon monoxide	4.0	6.2
Water vapour	3.9	2.9
Carbon dioxide	3.75	2.6
Methane and higher hydrocarbons	2.8	2.0
Argon	4.5	3.9
Nitrogen	0.06	0.06

Using the rate equation proposed by Botes, the catalyst activity for the FT reaction was calculated to be 3.65×10^{-6} moles/s.g-catalyst.bar on average for a 12 day period after the peak catalyst activity was reached for the experiment at 270 ˚C.

The calculated value of the FT catalyst activity for the 3 days at the peak catalyst activity is 4.06×10^{-6} and the average for the last 3 days at the end of the run was 2.75×10^{-6}, twelve days after the peak activity was attained. The catalyst is more active than expected from previous work – see Appendix 1.

6. DISCUSSION

6.1 Avoidance of Excessive Catalyst Attrition

The first key question is essentially: Can catalyst break-up be avoided at the selected operating conditions?

The literature review provided evidence that excessive catalyst attrition in a slurry phase reactor can be avoided. There were no observed problems with catalyst attrition for the recommended operating conditions of 270 ˚C, 30 bar(g) and feed H_2/CO between 1.5 and 1.6 in the second laboratory reactor experiment over a period of 450 hours. When severe catalyst attrition occurs, this is usually also accompanied by difficulties in maintaining the feed and product flows and this was not observed in this experiment. However, laboratory experiments do not generally provide conclusive results regarding catalyst mechanical integrity. Therefore demonstration in larger scale equipment will be needed to answer this key question conclusively. The performance stability in the laboratory experiment can merely be regarded as an indication that larger scale test work is warranted.

Lin *et al*. (2012) reported (See Chapter 2) that an industrially available iron catalyst, from an undisclosed source, did not exhibit suitable attrition resistance. It is therefore important to prepare the catalyst using the latest available knowledge relating to catalyst composition, preparation method and conditioning procedure when preparing catalyst for further demonstration work.

6.2 Methane and Carbon Dioxide Selectivity at the Selected Conditions

The second key question is: Can the favourable methane selectivity reported by Fletcher (2009) and others be repeated but with a stable FT conversion at a level high enough to be competitive with the cobalt catalyst?

The second laboratory experiment demonstrated steady methane selectivity of 4 % while achieving a 60 % synthesis gas conversion compatible with the first stage conversion required for a two stage reactor design approach. There was no significant hydrocarbon selectivity change for the 450 hour run. This is better than the methane selectivity typically achieved with cobalt catalysts. Therefore the answer to the second key question is affirmative. However, the selectivity to carbon dioxide is relatively high and, at the measured level of 33 % for the 270 ˚C experiment, this is expected to have a detrimental effect on the hydrocarbon yield for GTL applications. Based on the following analysis, this is too high for GTL applications.

In order to understand the significance of the carbon dioxide selectivity for GTL applications, some background discussion is appropriate. The most cost effective methane reforming technologies will use oxygen, steam and carbon dioxide reagents in a reaction with methane derived from natural gas. The reforming can be considered to be a combination of partial combustion, steam reforming and reverse water gas shift reactions:

Partial combustion $CH_4 + \frac{3}{2} O_2 \rightarrow CO + 2\ H_2O$ $\quad -\Delta H^0_{298}$ = + 519 kJ/mole

Steam reforming $CH_4 + H_2O \rightleftarrows CO + 3\ H_2$ $\quad -\Delta H^0_{298}$ = - 206 kJ/mole

Reverse-shift $CO_2 + H_2 \rightleftarrows CO + H_2O$ $\quad -\Delta H^0_{298}$ = - 41 kJ/mole

The goal is to balance these reactions such that the ratio of hydrogen and carbon monoxide is close to the usage ratio required for the FT synthesis and simultaneously to make the minimum use of the partial combustion exothermic reaction to provide the heat needed for the remaining endothermic reactions. A significant amount of high grade heat is needed to provide the energy for air compression to produce the oxygen used for reforming and the air separation unit is expensive so it is generally desirable to minimize the amount of oxygen used.

It has been proposed; by Steynberg *et al.* (2001) that achievable overall carbon efficiency is potentially up to 82.5 % which implies that there must be a net production of carbon dioxide to close the energy balance.

.

It should be noted that the reforming reactions which minimize oxygen consumption will require the co-feeding of carbon dioxide (recycled in FT tail gas and/or by separation from gas streams downstream of the reformer). If insufficient carbon dioxide is recycled then the synthesis gas contains too much hydrogen relative to the Fischer-Tropsch synthesis requirements. Separation of excess hydrogen from the synthesis gas implies that oxygen is unnecessarily consumed to provide the additional heat for hydrogen production from the highly endothermic steam methane reforming reaction.

When using autothermal reforming (ATR), Benham *et al*. (2003) have shown that similar hydrocarbon product yields can be obtained with a synthesis gas H_2/CO ratio ranging from 1.3 to 2.0. Oxygen consumption is minimized at the lower end of this range when the H_2/CO ratio is decreased by recycling carbon dioxide.

The CO_2 selectivity which consumes the reactants in stoichiometric balance at a synthesis gas H_2/CO ratio of 1.3 is 23.3 % while the desired carbon dioxide selectivity for the synthesis gas H_2/CO ratio of 1.56, tested in experiment 2, is about 15 %.

The 33 % CO_2 selectivity for experiment 2, at 270 ˚C, is high compared to the desired value for applications with a natural gas feed. To put this in perspective, carbon dioxide selectivity can be calculated from Table 16 which was published by Fletcher (2009).

Table 16: Space velocity used to keep CO conversion constant with increasing temperature

Temperature (°C)	Average $X_{CO\ to\ FT\ prod}$ (%)	Average $X_{CO\ to\ CO2}$ (%)	Average space velocity measured, (ml_n / g-cat.h)
220	20	16	5100
230	21	16	8000
245	18	17	16600
250	22	22	17000
260	20	14	22400

The carbon dioxide selectivity is $X_{CO\ to\ CO2}$ / ($X_{CO\ to\ CO2}$ + $X_{CO\ to\ FT\ prod}$) so that the carbon dioxide selectivity at 260 ˚C is 41 %.

In comparison to the 260 ˚C results from Fletcher (2009), with partial pressures shown in Table 17, the new experimental data at 260 ˚C from experiment 1, with partial pressures shown in Table 18, resulted in a carbon dioxide selectivity of 24 %. This carbon dioxide

selectivity would require confirmation in a longer run with a higher CO conversion level and a feed H_2/CO ratio increased from 1.0 to 1.3.

The new comparative higher pressure, lower H_2/CO ratio experiment at 260 ˚C used an average space velocity of 25022 $ml_{(n)}$/g-cat.h resulting in a conversion of CO to hydrocarbon products of 19 %. This means that the reactor productivity is substantially improved given that the feed rate of CO is increased by a factor of about 3 due to the higher operating pressure (40 bar compared to 20 bar) and the lower H_2/CO feed ratio (1.0 compared to 2.1) relative to the data from Fletcher (2009).

Table17: Reactant partial pressures reported by Fletcher (2009) at 260 ˚C

Component	Average (bar)	Maximum (bar)	Minimum (bar)
Hydrogen	10.2	11.4	9.6
CO	4.8	5.1	4.2
Water	1.2	1.6	0.9
CO_2	0.5	1.0	0.2

Table 18: Reactant partial pressures for experiment 1 at 260 ˚C

Component	Average (bar)	Maximum (bar)	Minimum (bar)
Hydrogen	14.5	15.1	14.3
CO	15.8	15.95	15.35
Water	2.7	2.75	2.6
CO_2	1.25	1.1	1.35

The higher pressure (40 bar) and lower feed H_2/CO ratio (1.0 versus 2.1) for the new comparative data at 260 ˚C (experiment 1) was expected to result in a decrease in methane selectivity, yet a surprisingly similar methane selectivity (2.6 % versus 2.7 %) was obtained at these significantly different component partial pressures at 260 ˚C. This indicates that non-oxygenate light hydrocarbon selectivity is insensitive to the component partial pressures and is determined primarily by the catalyst (preparation method and promoter content) and the operating temperature. Methane formation is, however, also not very temperature sensitive, i.e. 3.7 % - 4.1 % at 270 ˚C which is only slightly higher relative to the values measured at 260 ˚C.

Average (for 5 days at the beginning of the run) partial pressures of kinetic ally relevant components for the new experimental data at 270 ˚C are presented in Table 19.

Table 19: Reactant partial pressures for experiment 2 at 270 ˚C

Component	Average (bar)	Maximum (bar)	Minimum (bar)
Hydrogen	12.0	12.3	11.71
CO	4.05	4.3	3.65
Water	3.9	4.15	3.55
CO_2	3.75	3.6	3.9

The measured usage ratio was initially between 1.2 and 1.3 at 270 ˚C, declining to about 1.05 after four days, hence the accumulation of hydrogen relative to CO in the reactor.
This reasonably stable run (experiment 2), at the feed H_2/CO ratio of 1.56, a pressure of 30 bar and a temperature of 270 ˚C, had no carbon dioxide in the feed gas. Govender *et*

al. (2006) discuss the influence of CO_2 in the feed gas on the CO_2 selectivity at 240 ˚C and 20 bar.

Wang *et al*. (2007) and Yang *et al*. (2012) indicate that stable catalyst performance is achievable without carbon dioxide removal from the synthesis gas. However, carbon dioxide removal elevates the reactants' partial pressure which makes the hydrocarbon synthesis reactors more cost effective. So it should, nevertheless, be cost effective to remove some carbon dioxide prior to the second stage reactor even if this is not required for reasons of catalyst stability.

Yang *et al*. (2012) reported exceptional selectivity performance at CO conversion above 87 % when using one or more metal promoters selected from the group consisting of Mn, Cr and Zn. The carbon dioxide selectivity was less than 20 %, methane selectivity less than 5 %, C_{5+} selectivity greater than 90 % and C_2 to C_4 olefin plus C_{5+} selectivity potentially as high as 96 %. This result indicates that the appropriate selection of catalyst promoters is a potential option to achieve the desired carbon dioxide and methane selectivity performance.

There is a trade-off between space velocity and conversion to hydrocarbon products. High space velocity leads to high reactor productivity but lower conversion so, if the percentage conversion in each stage is set too low, this leads to an excessive number of reactor stages. The second experiment (at 270 ˚C and 30 bar) explored this trade-off by targeting a space velocity and conversion compatible with a two-stage reactor configuration. The feed H_2/CO ratio was set to be directly comparable with a first stage reactor design proposed by Van der Laan *et al*. (1999) thus demonstrating productivity improvement with increased operating temperature. Unfortunately this approach resulted in unacceptably high CO_2 selectivity for GTL applications. The CO_2 selectivity of 24% measured at 260 ˚C is more promising.

Potential approaches to get the CO_2 selectivity into the preferred range at 270 ˚C are firstly, to suppress the CO_2 selectivity by the use of suitable catalyst promoters and, secondly, to use a non-shifting catalyst in one of the reactor stages.

The measured product selectivity at 260 ˚C and 270 ˚C indicates that operation at a temperature between 250 and 270 ˚C may be desirable from the perspective of producing a larger proportion of the desired products. Interestingly, the wax production rates were similar for the new experiments at 260 ˚C and 270 ˚C but oil production is about 50 % higher at the lower temperature. This indicates that the optimum temperature, for the catalyst investigated, will depend on the relative value of the hydrocarbons condensed to form liquids at about 40 ˚C and those that must be recovered by chilling the reactor product gas to below ambient temperatures, i.e. the propylene, butylene and LPG products. At 270 ˚C there is a significant portion of the hydrocarbon product (about 25 wt.%) in the C_2 to C_4 range (inclusive of oxygenated products) so the effective recovery of these products will be essential when targeting this operating temperature.

6.3 Catalyst Stability at the Target Per-pass Conversion

The third key question is: Can reasonable catalyst activity stability be maintained at the proposed new operating conditions?

This question assumes that there is an upper limit per-pass conversion which cannot be exceeded without causing too rapid an oxidation of the catalyst which, in turn, causes the catalyst to lose activity. The upper limit requires further investigation but the approach can be illustrated by using the catalyst activity determined from the second laboratory experiment.

Experiment 2 at 270 ˚C exhibited reasonably stable catalyst activity with a peak (3 day average) value of 4.06×10^{-6} moles/s.g.bar for the reaction rate constant and declining to 2.75×10^{-6} moles/s.g.bar for the last 3 days at the end of the run. The average water partial pressure over this period was 3.3 bar.

The catalyst stability is acceptable but catalyst consumption will be relatively high, to maintain the catalyst activity measured after 450 hours so it may be preferable to increase the average catalyst age beyond the maximum age reached in experiment 2. There is therefore an incentive to generate more data with longer runs. The final FT activity, after 450 hours, was similar to the initial activity at 270 ˚C with an intermediate activity peak. It is unclear how the catalyst will respond after this initial period of activity enhancement and decline.

The use of small quantities of sulphate in the catalyst has been claimed to have positive effect with respect to improved activity stability (Wu *et al*., 2004). The sulphate promoted catalyst was compared to the Ruhrchemie catalyst in a slurry phase reactor by Wu *et al*. (2004). The sulphate promoted catalyst achieved stable performance at 260 ˚C with H_2 + CO conversion at 65 % (at 20 bar with 0.67 feed H_2/CO ratio). The catalyst productivity was comparable to a Ruhrchemie SB-2886 catalyst at a higher H_2 + CO conversion of 79 % (which may have severely deactivated this Ruhrchemie catalyst due to the high water partial pressure). The reported productivity by Wu *et al*. (2004) at the lined out conditions after 500 hours on-line is 0.35 g-HC/g-Fe/h. This could be increased to 0.53 gHC/g-Fe.h at a 30 bar operating pressure. In comparison, the catalyst productivity at a H_2 + CO conversion of 60 %, with the catalyst activity measured after 450 hours in experiment 2 of this thesis, is significantly higher, at 1.0 g-HC/g-catalyst.h.

To explore the reactor design implications for catalyst performance corresponding to experiment 2, a catalyst replacement interval is set at 14 days. With linear extrapolation, this corresponds to an end of run reaction rate constant of $2.2 \text{ X } 10^{-6}$ moles/s.g.bar. To keep the conversion performance constant over this period, the reactor catalyst inventory needs to increase by about 84 % during this 14 day period.

Calculations were made to determine the bed height needed for a commercial scale reactor design to maintain a 50 % per-pass CO conversion to hydrocarbons (60 % H_2 + CO conversion), demonstrated in experiment 2. This was done using the assumption of perfect mixing with the spreadsheet described in Appendix 2, which will slightly overestimate the true bed height and catalyst mass needed. The result is that by starting with a catalyst volume fraction in the slurry of 0.3, at the peak catalyst activity, and ending with a value of 0.4, the required initial bed height is 15.4 m and the ending bed height is

20.1 m for a superficial gas velocity of 0.75 m/s. The start-of-run catalyst mass is about 151 tonnes increasing to about 279 tonnes after 14 days. The resulting annual catalyst consumption is about 7250 tonnes (assuming no reactor down time). It may be desirable to use a taller reactor with a lower catalyst activity, associated with older catalyst, to decrease catalyst consumption but, as mentioned previously, this approach would require data at an increased run length.

In practice, on-line catalyst removal and addition would be used to maintain the desired reactor performance (Espinoza *et al*., 1999). This approach results in a slightly higher catalyst consumption which is more than compensated by the improved reactor on-stream factor.

A systematic approach has been followed with respect to the optimization of the typical promoters used with the iron catalyst at the Chinese Academy of Sciences. Wan *et al*. (2008) reported attractive selectivity performance for a potassium promoted iron catalyst with silica as the structural promoter (Fe/K-SiO_2) relative to alternative structural promoters. Hao *et al*. (2008)[a] reported that catalyst stability improves with increasing silica content but the product spectrum gets lighter. Wu *et al*. (2008) showed that, as compared with individual promotion of Cu and K, the double promotion of Cu and K effects excellent stability (attributed to Cu) and significantly improves the FT synthesis activity without significantly impacting on the selectivity benefits attributed to the K promoter.

From the literature review, it can be concluded that there is still scope to improve the catalyst activity stability relative to the catalyst tested for this thesis. Hao *et al*. (2008)[b] reported data which showed that their iron catalyst was unstable above about 270 ˚C when the H_2 + CO conversion went above about 60 % (as temperature was increased with a constant space velocity). Zirconia (Qing *et al*., 2011; Qing *et al*., 2012), magnesium (Yang *et al*., 2006) and manganese (Teng *et al*., 2005; Yang *et al*., 2005[ab]; Zhang *et al*., 2006; Li *et al*., 2006; Liu *et al*., 2007; Ding *et al*., 2009; Li *et al*., 2009) promoters have been investigated to improve the catalyst stability.

As mentioned in the previously, Yang *et al*. (2012) reported exceptional selectivity performance at CO conversion above 87 % when using one or more metal promoters selected from the group consisting of Mn, Cr and Zn.

It will be worthwhile to perform a longer run using an adjusted space velocity at the proposed operating conditions to determine whether improved catalyst stability can be achieved at a somewhat lower synthesis gas per-pass conversion than 60 %. If improved catalyst stability (at a lower per-pass conversion) is found to be cost effective then it will be necessary to use a third stage reactor to achieve the target 90% synthesis gas conversion. Alternatively, two reactor stages could still be used with some recycle added. It is also worthwhile to explore catalyst promoters which have been claimed to improve activity stability at synthesis gas conversion levels at or above 60 % (which are compatible with a two-stage reactor configuration without recycle).

6.4 Prospects for Operation with Feed H_2/CO Ratio at the Usage Ratio

The fourth key question is: What is the further improvement in reactor productivity potentially achievable by operating closer to the usage ratio with a feed gas H_2/CO ratio between the values used for the two experiments performed for this study?

The usage ratio is somewhat of a moving target since the CO_2 selectivity which determines the usage ratio is both catalyst dependant and also depends on the feed gas composition and the reactor operating conditions. The measured CO_2 selectivity at 270 ˚C lined out at about 33% at the selected first stage reactor operating conditions tested in experiment 2. The resulting H_2/CO usage ratio was between 1.0 and 1.1. This means that, by decreasing the feed H_2/CO ratio to the usage ratio, the CO content in the feed gas could be increased by 25 %. For a given CO conversion (and assuming no significant selectivity performance differences) the reactor productivity will then increase by 25 %. However, as discussed in section 6.2, it is desirable to decrease the carbon dioxide selectivity which will increase the usage ratio.

There may be other considerations determining the feed gas composition in a GTL gas loop but there is a significant incentive to attempt to match the feed gas composition to the value which will lead to the lowest cost reactor design. It is therefore worthwhile to explore lower feed H_2/CO ratios than 1.5. From the discussion in section 6.2, it seems that a good target would be to aim for about 23 % carbon dioxide selectivity at a feed H_2/CO of about 1.3.

From the analysis of the water gas shift reaction rate in Appendix 1, it is clear that the nature of the catalytic activity for this reaction changed under the synthesis conditions in a rather unpredictable way, increasing with run time over a nine day period. It would be beneficial, for GTL applications, if the activity for the water gas shift could be stabilized close to the initial activity. This may require significant catalyst development work.

6.5 Prospects to Demonstrate Higher Reactor Productivity

The fifth key question is: What is the achievable reactor productivity at the target 60 % per-pass conversion when using a higher gas velocity and catalyst concentration relative to the values used by Van der Laan *et al.* (1999) when combined with new proposed operating conditions tested in the laboratory?

To illustrate reactor productivity trends, a simple, fully mixed, reactor model is used. As mentioned previously, the use of a model based on the other extreme mixing assumption of plug flow does not significantly affect the results for a per-pass conversion of 60 % or less. The mass of catalyst required to achieve the target conversion is calculated as a function of the velocity in the reactor. The calculation procedure is described in Appendix 2. For experiment 2 at 270 ˚C, the tail gas flow was 60 % of the feed gas flow for a synthesis gas conversion of 60 %. The average gas velocity in the open reactor shell is therefore 80 % of the inlet gas velocity when taking into account the volumetric contraction due to the hydrocarbon synthesis reaction. Using the simplifying assumption of 20 % of the reactor cross-section being occupied by internals, the average velocity can then be taken to be the same as the inlet velocity. It will be necessary to revisit this

simplifying assumption regarding the fraction of the cross-sectional area occupied by internals for more detailed reactor design work.

As the velocity is increased, for a constant reactor diameter, the fluidized slurry bed height must be increased to accommodate the amount of catalyst needed to achieve the target conversion. Using equation (17) with C_F = 0.6 to determine the gas holdup and the catalyst activity for the last 3 days up to 450 hours, of 2.75 × 10^{-6} moles/s.g.bar, from the experiment 2 (with CO partial pressure = 4.12 bar and H_2 partial pressure = 11.71 bar), the required bed height is shown in Figure 25.

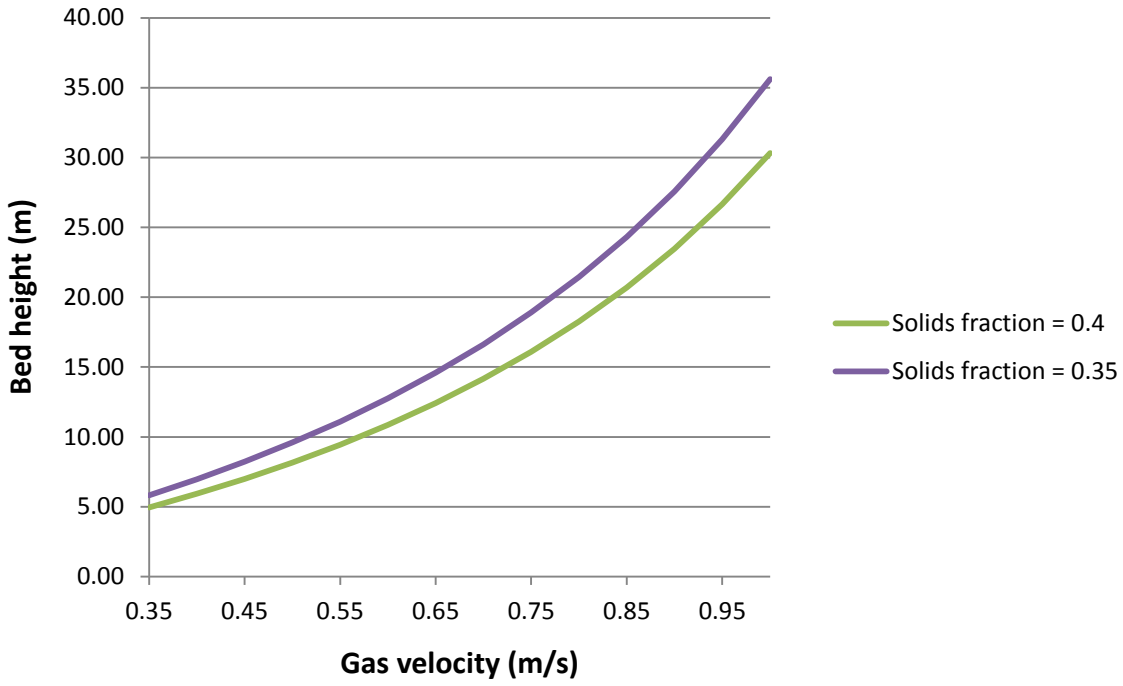

Figure 25: Required bed height to achieve 60 % synthesis gas conversion

For a reactor diameter of 8 m, the product from the reactor increases linearly with gas velocity for a constant per-pass conversion as shown in Figure 26.

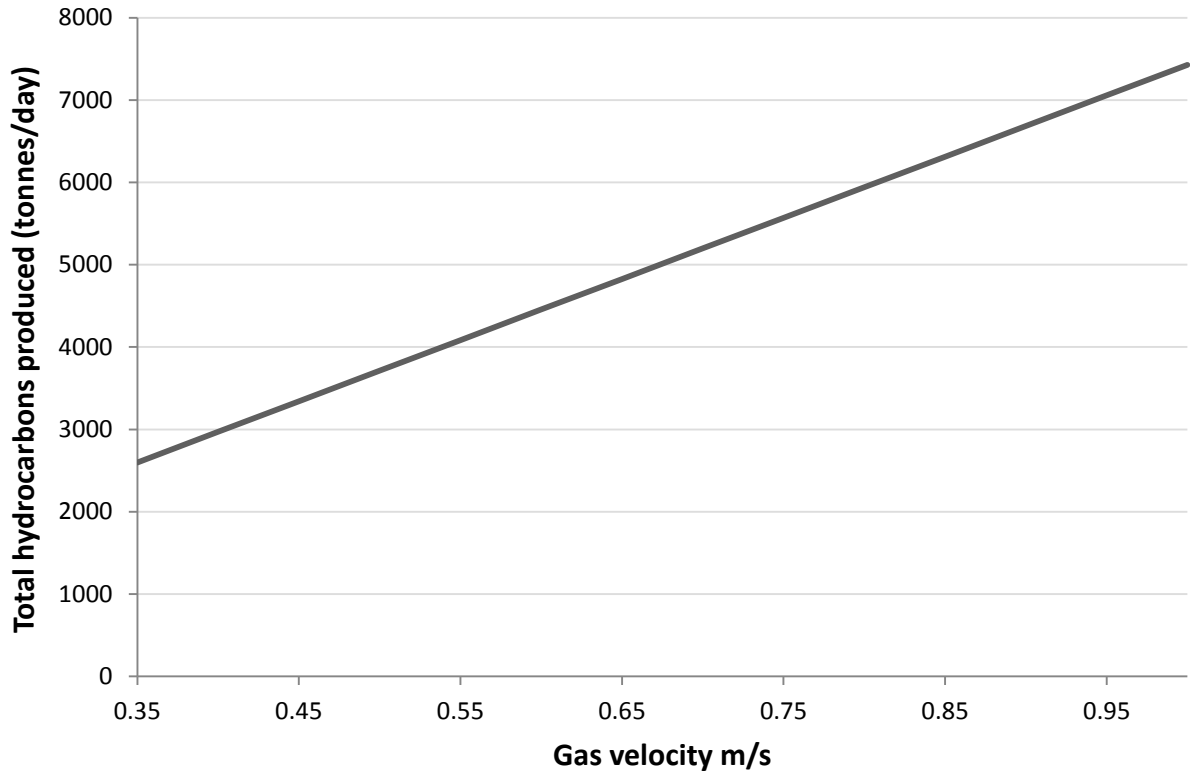

Figure 26: Total hydrocarbons produced as a function of inlet gas velocity

It should be noted that the catalyst productivity remains constant as the gas velocity varies due to the approach of maintaining a constant per-pass conversion.

The use of a slurry-phase reactor with a gas velocity of at least 0.35 m/s has been patented (Steynberg, 2010). This patent applies to reactors with an aspect ratio of less than 5 using a non-shifting catalyst at H_2 + CO conversion of at least 60 %. Subsequently, Breman (2014) disclosed the advantages of applying a slurry-phase reactor for hydrocarbon synthesis in general with an inlet superficial gas velocity above 0.50 m/s which is also supported by this work.

For the reactor productivity calculation, it is assumed that the reactor vessel would have two hemispherical heads. The area of the heads is added tom the area of the cylindrical section housing the slurry bed in order to calculate the hydrocarbon production from the reactor per unit of metal surface used to construct the reactor as shown in Figure 27.

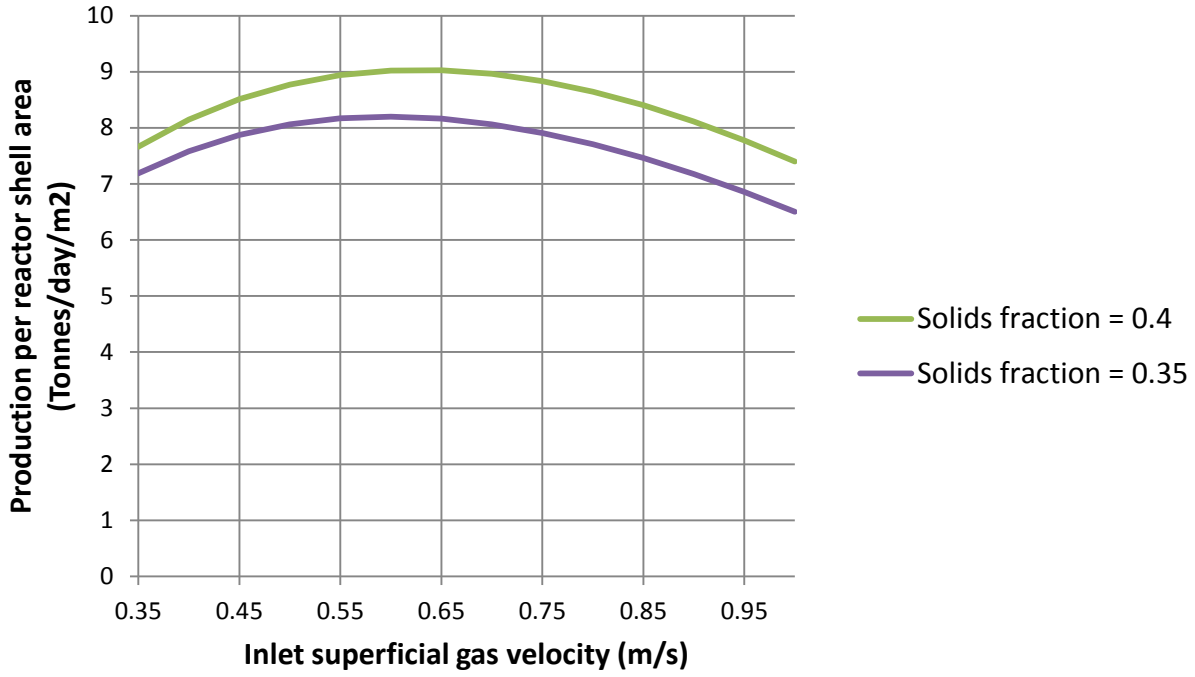

Figure 27: Reactor productivity versus gas velocity at 60 % H_2 + CO conversion

Using the average catalyst activity measured for the last 3 days up to 450 hours in experiment 2, the required bed height is 12.8 m at 0.6 m/s with a solids fraction of 0.35 to achieve 60 % H_2 + CO conversion. This is less than the reactor bed height of 24 m selected by Van der Laan *et al*. (1999) when evaluating the same solids fraction.

Raje and Davis (1997) generated data for a low potassium (0.311 wt.% K) catalyst operated at 270 ˚C using an H_2/CO ratio of 1.7 at 13 bar. Reaction runs lasted from 12 to 15 days with no observed catalyst deactivation. The water partial pressure never exceeded 1.2 bar which indicated that, relative to the current work, catalyst stability may improve with lower operating pressure and/or lower potassium content in the catalyst. The reaction rate constant,k, was determined to be 6.83 × 10^{-6} mol/s.g-cat.bar and absorption parameter, b, was 3.016 using the following rate equation:

$$r_{FTS} = k\frac{P_{CO}P_{H2}}{P_{CO}+ bP_{H2O}}$$

With this rate equation the required bed height at 0.6 m/s, 30 bar and with a solids fraction of 0.35 to achieve 60 % H_2 + CO conversion is 13.3 m. The methane and ethane selectivity was much higher for the catalyst tested by Raje and Davis (1997) so the catalyst tested for experiment 2 is still preferred.

The optimum reactor productivity increase is found at higher gas velocities with increasing solids fraction but the optimum is relatively flat in the range from about 0.55 to 0.75 m/s, tending towards a higher velocity at a higher catalyst concentration. Other associated equipment, outside the reactor, benefits from lower costs associated with economy of scale at the higher reactor capacity so it is likely that a velocity towards the upper end of this range, say 0.75 m/s, may be preferred even though the reactor productivity is slightly

lower. From Figure 25, it can be seen that the required bed height at 0.75 m/s with a catalyst volume fraction of 0.35 is 21.4 m and with a catalyst volume fraction of 0.4 it is 18.3 m. It is feasible to maintain the target conversion using on-line partial catalyst replacement, at this catalyst volume fraction, if the catalyst activity is allowed to decline further to 2.2×10^{-6} moles/s.g.bar. The required bed height is then 20.1 m which is still reasonable.

Back calculating the production from the highest reported reactor productivity by Van der Laan *et al*. (1999) (at a similar feed gas H_2/CO ratio) gives about 2750 tonnes/day at a gas velocity of 0.4 m/s. The new proposed reactor design, with a 20 degree higher operating temperature, using the measured catalyst activity for the last 3 days up to 450 hours in experiment 2 (which may differ from the activity used by Van der Laan *et al*.) and using a simplified fully mixed reactor model produces about 5350 tonnes/day of C_{2+} hydrocarbons at a gas velocity of 0.75 m/s.

The use of a more sophisticated reactor model by Van der Laan *et al*. (1999) introduces some plug flow characteristics which will have the effect that the desired target conversion will be predicted to be attained at a lower bed height for a selected catalyst fraction. This is a similar effect to using a higher activity catalyst. Nevertheless, the use of a more sophisticated reactor model does not improve predictions significantly for per-pass conversions at or below 60 %, as discussed previously.

Krishna and Sie (1999) reported an achievable reactor production using cobalt catalyst of 3000 tonnes/day in a 7 m diameter reactor which corresponds to about 4000 tonnes/day in an 8 m diameter reactor with a bed height of 30 m and operating at 40 bar and 240 ˚C. The reactor productivity for the proposed iron catalyst approach is therefore also expected to be favourable when compared to the cobalt catalyst option. When compared on the basis of total hydrocarbon products per unit of reactor shell surface, the proposed first stage reactor productivity for the iron catalyst is about 7.6 tonnes/day.m^2 compared to 3.7 tonnes/day.m^2 for the single stage reactor using cobalt catalyst.

The laboratory experiment at 260 ˚C (experiment 1), with an average synthesis gas (H_2 + CO) partial pressure of 30.3 bar, corresponds to reasonable inlet conditions for a slurry-phase reactor. Such a reactor could have outlet conditions similar to those in the CSTR laboratory experiment at 270 ˚C (experiment 2) with a synthesis gas partial pressure of 16 bar. A reasonable approximation of the catalyst productivity in such a reactor, expressed as total hydrocarbon products per tonne of catalyst, can be obtained from the average productivity at these two conditions. This can then be compared to the average catalyst productivity for the 450 hour laboratory test at 270 ˚C of 33.3 tonnes/day of hydrocarbons per tonne of catalyst (t/d.t).

The catalyst productivity at the conditions used for experiment 1, assuming that the catalyst activity is steady at the measured start-of-run catalyst activity, is 32 t/d.t. At the conditions used for experiment 2, with the catalyst activity for the last 3 days to 450 hours, the productivity is 30.8 t/d.t. This indicates that an average catalyst productivity of about 31.4 t/d.t is potentially achievable without resorting to any model calculations or extrapolations. This corresponds to about 1.3 gHC/g-cat/h or about 1.4 gHC/g-Fe/h.

6.6 Gas Holdup Dependence on the Catalyst Concentration in the Slurry

The reactor productivity is highly dependent on the amount of catalyst in the reactor due to the reaction kinetics on the catalyst surface being the rate controlling step. The amount of catalyst depends in turn on the fraction of slurry in the reactor and the concentration of catalyst in the slurry. The slurry fraction decreases as the gas holdup increases.

Good predictions of gas holdup in slurry bubble columns are obtained using the adapted two phase theory. The approach requires only a single parameter to be fitted to data at a single gas density, for a range of gas velocities in the churn-turbulent regime.

Above a small bubble saturation velocity, the dilute phase gas holdup is proportional to the superficial gas velocity to the power of 0.8. The constant fitted to match the dilute phase gas holdup is proportional to the relative gas density to the power 0.25.

The result is equation (17) i.e.:

$$\varepsilon = C_F(\rho_G/5.8)^{0.25}U^{0.8} + (0.36/(\exp(2.66\ \varphi/(1-\varphi))))(1-0.6(\rho_G/5.8)^{0.25}U^{0.8}) \quad (17)$$

As an example of how this equation may be applied, consider the following: taking the case of FT synthesis at 30 bar(g) with a gas density of 8.4 kg/m^3 then using equation (17) with C_F = 0.6, which matches the data from Koop (2003) and with a gas velocity of 0.8 m/s leads to a fractional gas holdup of about 0.61 with a solids fraction of 0.3, and about 0.59 with a solids fraction of 0.4. To avoid a potential hydrodynamic regime transition, the fractional gas holdup should be kept safely below 0.7.

It is desirable to load as much catalyst as possible since this allows a higher gas feed rate for the target reactant conversion and, hence, the reactor productivity is improved. Furthermore, the gas holdup attributed to small bubbles which remain in circulation in the reactor decreases as the catalyst concentration increases which also improves the utilization of the reactor volume leading to further increased reactor productivity.

It is desirable to avoid the exponential increase in slurry viscosity at very high slurry concentrations. At the upper limit of applicability of the OSU correlation, the slurry viscosity increases to 6.6 times the liquid viscosity (at a solids volume fraction of 0.415) and the small bubbles which remain in circulation then occupy less than 6 % of the fluidized slurry volume.

Practical constraints may be issues such as less effective heat transfer and less effective thermal mixing, with the suppressed slurry circulation at a high slurry viscosity, leading to excessive temperature gradients. Catalyst-liquid separation may also become more difficult. For the current reactor design comparisons, it is considered safer to keep within the upper limits used to develop the OSU correlation and to consider the use of a catalyst volume fraction of 0.3 at the start of run increasing to 0.4 at the end of run (or as a target continuous concentration using on-line catalyst addition and removal) as more catalyst is loaded to maintain conversion with a lower catalyst activity.

7. CONCLUSIONS & RECOMMENDATIONS FOR FURTHER WORK

A new approach to gas holdup prediction has been developed which closely matches the OSU prediction in the churn-turbulent regime above a small bubble saturation velocity. This theoretical approach, referred to as the adapted two-phase theory, can also closely match the experimental data from Koop (2003). At higher gas velocities, the new approach predicts higher gas holdup values than the OSU correlation. Although the physical properties of the paraffin liquid used at room temperature by Koop (2003) are similar to the liquid reactor wax at synthesis conditions, they are not identical. Therefore, it is anticipated that both the adapted two-phase theory correlation and the OSU correlation would require refitting of the model parameters to match the gas holdup for actual liquid wax product at synthesis conditions. However, only a single parameter has to be refitted to predict the effect of actual liquid properties when using the adapted two-phase theory while several parameters need to be refitted when using the OSU correlation.

The iron-catalysed system has the potential for higher reactor capacity than the cobalt-catalysed system due to the increased driving force for reactor heat removal. For improved reactor productivity, it is recommended that the pressure should be 30 bar or higher and the lined-out catalyst concentration in the slurry should be more than the 35 vol.% maximum considered by Van der Laan *et al*. (1999) . The target reactor inlet H_2/CO ratio should be close to the reactant consumption ratio (usage ratio) in order to achieve the best reactor productivity, i.e. a feed ratio between 1.0 and 1.3 for the catalyst of this study and preferably at or above 1.3 for GTL applications. As also proposed by Van der Laan *et al*. (1999), a two-stage reactor design approach is preferred but higher gas velocities are now recommended.

Applying the adapted two-phase theory and the measured catalyst performance at the conditions tested (temperature - 260 and 270 ˚C; pressure - 30 and 40 bar and feed H_2/CO ratio – 1.0 and 1.5), it has been found possible to significantly improve on previously proposed reactor productivity for the iron-catalysed slurry-phase reactor system for Fischer-Tropsch (FT) synthesis. An 8 m diameter first stage reactor for a two stage reactor configuration can produce 5350 tonnes/day of hydrocarbon product with an optimized reactor shell surface area of approximately 9 tonnes/day.m^2. This corresponds to a plant capacity of 16000 tonnes/day (about 125 000 bbl/d) using two first stage reactors and one second stage reactor to achieve an overall synthesis gas conversion of 90 %.

From the literature, there appear several recent advances in catalyst technology which will improve catalyst selectivity performance and catalyst stability relative to that of the catalyst tested for this study.

It is thus recommended that further experimental data be generated with optimized catalyst formulations, using gas inlet compositions compatible with the desired optimum gas loop design for a GTL facility, including the use of a feed H_2/CO ratio approaching the reactant usage ratio. It is further recommended to find the overall economic optimum, taking into account the value of the various hydrocarbon products for operating temperatures in the range from 250 to 270 ˚C, after also taking into account the feed gas composition and operating pressure which balance the slurry phase reactor productivity with considerations relating to the overall gas loop design.

It has been found that further work is required to address the high carbon dioxide selectivity which was measured at 270 ˚C, which is not directly compatible with GTL applications, before considering such applications using operating temperatures above 260 ˚C.

Two potential approaches have been identified to get the carbon dioxide selectivity into the preferred range. Firstly, catalyst promoters can be investigated to suppress the water gas shift activity of the catalyst. Secondly, a non-shifting catalyst could be used in one of the reactor stages. Operation at 260 ˚C fed at 1.3 H_2/CO ratio may provide suitable carbon dioxide selectivity but longer duration tests at higher conversions are required to verify the performance at this temperature.

REFERENCES

Aasberg-Peterson K., Christensen I., Dybkjaer I., Sehested M., Ostberg M., Coertzen R., Keyser M.J., Steynberg A.P.
Fischer-Tropsch Technology: Chapter 4 Synthesis gas production for FT synthesis
Studies in surface science and catalysis **152** (2004), 258 – 405

Abrevaya H.
Development of precipitated iron catalysts with improved stability
US Department of Energy, Final report Sept. 1987 – Sept. 1992 under contract AC-2287PC79812 (1993)

Adeyiga A.A,
Development of attrition resistant iron-based Fischer-Tropsch catalysts
US Department of Energy, Final Report for Grant No.: DE-FG26-99FT40619 (2003)

Allam R., Weaver A., White V., Byard D.B.
Process and apparatus for the production of hydrocarbon compounds from methane
US 8,455,555 (2013)

An X., Wu B.-S., Hou W., Wan H., Tao Z., Li T., Zhang Z., Xiang H., Li Y., Xu B. and Yi F.
The negative effect of residual sodium on iron-based catalyst for Fischer-Tropsch synthesis
Journal of Molecular Catalysis A: Chemical **263** (2007[a]) 266-272

An X., Wu B., Wan H.-J., Li T.-Z., Tao Z.-C., Xiang H.-W. and Li Y.-W.
Comparative study of iron-based Fischer-Tropsch synthesis catalyst promoted with potassium or sodium
Catalysis Communications **8 (2)** (2007[b]) 1957-1962

Bakkarud P.K.
Update on synthesis gas production for GTL
Catalysis Today **106** (2005) 30–33

Bach H.F. and Pilhofer T.
Variation of gas hold-up in bubble columns with physical properties of liquids and operating parameters of columns
Ger. Chem. Eng. **1** (1978) 270

Barnea E. and Mizrahi J.
A generalized approach to the fluid dynamics of particulate systems part I: General correlation for fluidization and sedimentation in solid multiparticle systems
The Chem. Eng J. **5** (1973) 171–189

Behkish A.
Hydrodynamics and mass transfer parameters in large-scale slurry bubble column reactors
PhD thesis, University of Pittsburgh (2004)

Behkish A., Lemoine R., Oukaci R., Morsi B.I.,
Novel correlations for gas holdup in large-scale slurry bubble column reactors operating under elevated pressures and temperatures
Chemical Engineering Journal **115** (2006) 157-171

Benham C.B., Bohn M.S. and Yakobson D.L.,
Producing liquid hydrocarbons from natural gas
US 6,534,552 (2003)

Van Berge P.J.,
Fischer-Tropsch studies in the slurry phase favouring wax production
PhD thesis, Potchefstroom Universiteit vir Christelike Hoër Onderwys (1994)

Bhatt B.L., Frame R., Hoek A., Kinnari K., Rao V.U.S. and Tungate F.L.,
Catalyst and process scale-up for Fischer-Tropsch synthesis
Top. Catal. **2** (1995) 235 - 257

Bhatt B.L. and Tijm P.J.A.
Slurry phase Fischer-Tropsch synthesis process development
In: Proceedings of 15th Annual Pittsburgh Coal Conference on Slurry Phase Fischer-Tropsch Synthesis Process Development (1998)

Booysen W.B.
Confidential personal communication
(2013)

Botes F.G.
Kinetic and selectivity modelling of the iron-based low-temperature Fischer-Tropsch synthesis
PhD Thesis, Eindhoven University of Engineering (2008)

Botes F.G. and Breman B.B.
Development and testing of a new macro kinetic expression for the iron-based low-temperature Fischer−Tropsch reaction
Industrial Engineering Chemical Research **45** (2006) 7415-7426

Botes F.G., Niemantsverdriet J.W. and van de Loosdrecht J.
A comparison of cobalt and iron based slurry phase Fischer-Tropsch synthesis
Catalysis Today (2013) article in press

Botton R., Cosserat D. and Charpentier J.C.
Influence of column diameter and high gas throughputs on the operation of a bubble column
Chem. Eng. J. **16** (1978) 107-115

Breman B.B.
Process for producing at least one product from at least one reactant in a slurry bed
US 20140107232 (2014)

Bukur D.B., Daly J.G., Patel S.A., Raphael M.L. and Tatterson G.B
Hydrodynamics of Fischer-Tropsch synthesis in slurry bubble column reactors
Final report prepared for the US DOE under contract DE-AC22-84PC70027 (1987)

Bukur D.B., Ma W.-P, Carreto-Vazquez V., Nowicki L. and Adeyiga A.A.
Attrition resistance and catalytic performance of spray-dried iron Fischer-Tropsch catalysts in a stirred-tank slurry reactor
Ind. Eng. Chem. Res. **43** (2004[a]) 1359-1365

Bukur D.B., Carreto-Vazquez V., Pham H.N. and Datye A.K.
Attrition properties of precipitated iron Fischer-Tropsch catalysts
Applied catalysis A: General **266 (1)** (2004[b]) 41-48

Bukur D.B., Carreto-Vazquez V.H. and Ma W.
Catalytic performance and attrition strength of spray dried iron catalysts for slurry phase Fischer-Tropsch synthesis
Applied catalysis A: General **388** (2010) 240-247

Chang J., Bai L., Teng B.-T., Zhang R.-L., Yang J., Xu Y.Y., Xiang H.-W. and Li Y.-W.
Kinetic modeling of Fischer-Tropsch synthesis over Fe-Cu-K-SiO_2 catalyst in slurry phase reactor
Chem. Eng. Sci. **62** (2007) 4983-4991

Claeys M.
Selektivität, Elementarschritte und kinetische modellierung bei der Fischer-Tropsch synthese
PhD Thesis, University of Karlsruhe (1997)

Claeys M. and van Steen E.
Fischer-Tropsch technology: Chapter 8 Basic studies
Studies in surface science and catalysis **152** (2004), 601

Darton R.C., LaNauze R.D., Davidson J.F. and Harrison D.
Bubble growth due to coalescence in fluidized beds
Trans I. Chem. E. **55** (1977)

Davis B.H.
Overview of reactors for liquid phase Fischer-Tropsch synthesis
Catalysis Today **71** (2002) 249-300

Deckwer W.-D.
Design and simulation of bubble column reactors
In: proceedings NATO-ASI "chemical reactor design and technology" June 1985, London, Ontario, Canada (1985)

Deckwer W-D.
Reactionstechnik in blasensaeulen
Otto Salle Velag GmbH & Co., Frankfurt am Main Verlag Sauerlaender AG, Aarau, Switzerland (1985);
Deckwer W-D.
Bubble Column Reactors
Translated by V. Cottrell, R.W. Field (ed.), John Wiley and Sons, New York (1992)

Deckwer W.-D., Kokuun R., Sanders E., Ledakowicz S
Kinetic studies of Fischer-Tropsch synthesis on suspended Fe/K catalyst. Rate inhibition by CO2 and H2O
Industrial Egineering Process Des.Dev. **25** (1986), 643-649

Deckwer W.-D., Louisi Y., Zaidi A. and Ralek M.
Hydrodynamic properties of the Fischer-Tropsch slurry process
Ind. Eng. Chem. Proc. Des. Dev. **19** (1980) 699

Deckwer W.-D., Serpemen Y., Ralek M. and Schmidt B.
Response to letter of Satterfield and Huff concerning mass transfer in Fischer-Tropsch slurry reactors
Chem. Eng. Sci. **36** (1981) 793

Van Deemter J.J.
Mixing and contacting in gas-solid fluidized beds
Chem. Eng. Sci. **13** (1961) 143-154

Donnelly T.J. and Satterfield C.N.
Product distributions of the Fischer-Tropsch synthesis on precipitated iron catalysts
Applied Catalysis **52** (1989) 93-114

Donnelly T.J., Yates I.C. and Satterfield C.N.
Analysis and prediction of product distributions of the Fischer-Tropsch synthesis
Energy & Fuels **2** (1988) 734

Dry M.E.
Predict carbonation rate on iron catalyst
Hydrocarbon Process **59(2)** (1980) 92

Dry M.E.
The Fischer-Tropsch process. Commercial aspects.
Catalysis Today **6** (1990) 183-206

Dry M.E.
Practical and theoretical aspects of the catalytic Fischer-Tropsch process
Applied Catalysis A: General **138** (1996) 319-344

Dry M.E.
Chemical concepts used for engineering purposes
Studies in Surface Science and Catalysis **152** (2004 [a]) Chapter 3, 196-257

Dry M.E.
Present and future applications of the Fischer-Tropsch process (editorial)
Applied Catalysis A: General **276** (2004 [b]) 1-3

Dry M.E.
FT catalysts
Studies in Surface Science and Catalysis **152** (2004[c]) Chapter 7, 533-600

Dry M.E. and Steynberg A.P.
Commercial FT process applications
Studies in Surface Science and Catalysis **152** (2004) Chapter 5, 406-481

van Dijk H.A.J.
The Fischer-Tropsch synthesis: A mechanistic study using transient isotopic tracing
PhD thesis (2001)

Egiebor N.O., Cooper W.C. and Wojciechowski B.W.
Carbon number distribution of Fischer-Tropsch CO-hydrogenation products from precipitated iron catalysts
The Canadian J. of Chem. Eng. **63, Issue 5** (1985) 826–834

Ellenberger J. and Krishna R.
A unified approach to the scale-up of gas-solid fluidized bed and gas-liquid bubble column reactors
Chem. Eng. Sci. **49, No. 24B** (1994) 5391-5411

Espinoza R.L., Steynberg A.P., Jager B. and Vosloo A.C.
Low Temperature Fischer-Tropsch from a Sasol perspective
Applied Catalysis A **186** (1999) 13-26

Fan L.S., Yang G.Q., Lee D.J., Tsuchiya K. and Luo X.
Some aspects of high-pressure phenomena of bubbles in liquids and liquid-solid suspensions
Chem. Eng. Sci. **54** (1999) 4681 – 4709

Farias F.E.M., Rabelo Neto R.C., Baldanxa M.A.S., Schmal M. and Fernandez F.A.N.
Effect of K promoter on the structure and catalytic behavior of supported iron-based catalysts in Fischer-Tropsch synthesis
Brazilian Journal of Chemical Engineering **28 (3)** (2011) 495-504

Fernandes F.A.N.
Modeling and product grade optimization of Fischer-Tropsch synthesis in a slurry reactor
Ind. Eng. Chem. Res. **45** (2006) 1047-1057

Fletcher J.V.
The effect of temperature on the Fischer-Tropsch selectivity and further mechanistic insights
MSc Thesis, UCT (2009)

Fox J.M. III
Fischer-Tropsch reactor selection
Catalysis Letters **7** (1990) 281-292

Frohning C.D., Kölbel H., Ralek.M., Rottig W., Schuur F. and Schulz H.
In Fischer-Tropsch-Synthese aus Kohle, Falbe J. (editor) chapter 8, Georg Thieme Verlag, Stuttgart (1977) 219-299

Geerlings J.J.C., Wilson J.H., Kramer G.J., Kuipers H.P., Hoek A. and Huisman H.M.
Fischer-Tropsch technology - from active site to commercial process
Applied Catalysis A: General **186** (1999) 27

Govender N.S., Janse van Vuuren M., Claeys M. and van Steen E.
Importance of the usage ratio in iron-based Fischer-Tropsch synthesis with recycle
Ind. Eng. Chem.Res. **45** (2006) 8629-8633

Graham A.L.
On the viscosity of suspensions of solid spheres
Applied Scientific Research **37, Issue 3-4** (1981) 275-286

Gray D. and Tomlinson G.
A technical and economic comparison of natural gas and coal feedstocks for Fischer-Tropsch synthesis
Studies in surface science and catalysis **107** (1997)145-149

Hall C.C., Gall, D. and Smith S.L.
Comparison of the fixed-bed, liquid-phase ("slurry"), and fluidized-bed techniques in the Fischer-Tropsch synthesis
Ordinary general meeting of The Institute of Petroleum, 26 March (1952)

Hammer H., Schrag H., Hektor K., Schönau K., Küsters W., Soemarno A., Sahabi U. and Napp W.
New subfunctions on hydrodynamics, heat and mass transfer for gas/liquid and gas/liquid/solid chemical and biochemical reactors
Front. Chem. Reac. Eng. (1984) 464-474

Hao Q., Wang H., Liu F., Bai L., Zhang Z., Xiang H. and Li Y.
Effect of calcination temperature on catalytic performance of iron-based catalyst for slurry Fischer-Tropsch synthesis reaction
Chinese J. Catal. **26(4)** (2005[a]) 340-348

Hao Q., Bai L., Li Y., Li X., Xiang H. and Li Y.
Effect of reaction parameters on catalytic performance of Fe/Cu/K/SiO_2 for slurry phase Fischer-Tropsch synthesis
Chinese J. Catal. **26 (9)** (2005[b]) 791-796

Hao Q.-L., Bai L., Hao X., Xiang H.-W., Li Y.-W., Yi F. and Xu, B.-F.
Effect of reduction temperature and duration on iron-based catalyst for slurry phase Fischer-Tropsch synthesis
J. Fuel Chem. Tech. **33 (5)** (2005[c]) 590-596

Hao Q.-L., Liu F.-X., Wang H., Chang J., Zhang H.-H., Bai L., Xiang H.-W., Li Y.W., Yi F. and Xu B.-F.
Effect of reduction temperature on a spray-dried iron-based catalyst for slurry Fischer-Tropsch synthesis
Journal of Molecular Catalysis A: **261** (2007) 104-111

Hao Q.-L., Bai L., Xiang H.-W. and Li Y.-W.
Phase transformations of a spray-dried iron catalyst for slurry Fischer–Tropsch synthesis during activation and reaction
Fuel Processing Technology **89** (2008[a]) 1358

Hao X., Djatmiko M.E., Xu Y., Wang Y., Chang J. and Li Y.
Simulation analysis of a gas-to-liquid process using Aspen Plus
Chem. Eng. Technol. **31, No. 2** (2008[b]) 188-196

Hesse P.J., Battino R., Scharlin P. and Wilhelm E.
Solubility of gases in liquids 20, solubility of He, Ne, Ar, Kr,N_2,O_2
Journal of Chemical Engineering Data **41** (1996)195–201

Hills J.H.
The operation of a bubble column at high throughputs 1. Gas holdup measurements
Chem. Eng. J. **12** (1976) 89- 99

Huff G.A. and Satterfield C.N.
Evidence for two chain growth probabilities on iron catalysts in the Fischer-Tropsch synthesis
Journal of Catalysis **85** (1984), 370-379

Hou W, Wu B, Yang Y,Hao Q, Tian L. Xiang H and Li Y
Effect of SiO_2 content on iron based catalysts for slurry Fischer–Tropsch synthesis
Fuel Processing Technology **89** (2008) 284-291

Iliuta I., Larachi F., Anfray J., Dromard N. and Schweich D.
Comparative simulations of cobalt- and iron-based Fischer-Tropsch synthesis slurry bubble column reactors
Ind. Eng. Chem Res. **47** (2008) 3861-3869)

Jager B. and Espinoza R.
Advances in low temperature Fischer-Tropsch synthesis
Catalysis Today **23** (1995) 17-28

Janse van Vuuren M.J.
Limits to prevent deactivation of SBR catalyst under CTL conditions
Memorandum to A.P. Steynberg, 4 November (2004)

Joshi J.B et al.
Review Article: Gas hold-up structure in bubble column reactors
PINSA **64 A no. 4** (1998) 441-567

Kantarci N. E.
Review: Bubble column reactors
Process Biochemistry **40** (2005) 2263-2283

Kölbel H. and Ralek M.
The Fischer-Tropsch synthesis in the liquid phase
Catal. Rev-.Sci. Eng. **21** (1980) 225

König L. and Gaube J.,
Chem. Ing. Tech. **55** (1983) 14

Koop K.
Fischer-Tropsch slurry bubble columns at elevated pressure. Part A: Gas holdup measurements
TwAIO report for research performed at CREL (Prof. M.H. Al-Dahhan) (2003)

Krishna R.
A scale-up strategy for a commercial scale bubble column slurry reactor for Fischer-Tropsch synthesis
Oil Gas Sci. Technol. **55** (2000) 359-393

Krishna R., De Swart J.W.A., Hennephof D.E., Ellenberger, J. and Hoefsloot H.C.J. Influence of increased gas density on the hydrodynamics of bubble column reactors, *A.I.Ch.E.J.* **40** (1994) 112-119

Krishna R. and Ellenberger J.
Gas holdup in bubble column reactors operating in the churn-turbulent flow regime
A.I.Ch.E.J. **42** (1996) 2637-2644

Krishna R., Ellenberger J. and Sie S.T.
Reactor development for conversion of natural gas to liquid fuels: A scale-up strategy relying on hydrodynamic analogies
Chem. Eng Sci. **52** (1996) 2041-2050

Krishna R., De Swart J.W.A., Ellenberger J., Martina G.B. and Maretto C.
Gas holdup in slurry bubble columns: Effect of column diameter and slurry concentrations
A.I.Ch.E.J. **43** (1997) 311-316

Krishna R., Urseanu M.I., van Baten J.M. and Ellenberger J.
Rise velocity of a swarm of large gas bubbles in liquids
Chem. Eng. Sci. **54** (1999[a]) 171-183

Krishna R., Urseanu M.I., van Baten J.M., Ellenberger J.
Influence of scale on the hydrodynamics of bubble columns operating in the churn-turbulent regime: experiments vs. Eulerian simulations
Chem. Eng. Sc. **54** (1999[b]) 4903-4911

Krishna R., Urseanu M.I. and Dreher A.J.
Gas hold-up in bubble columns: influence of alcohol addition versus operation at elevated pressures
Chem. Eng. and Proc. **39** (2000[a]) 371-378

Krishna R., van Baten J.M. and Urseanu M.I.
Three-phase Eulerian simulations of bubble column reactors operating in the churn-turbulent regime: a scale up strategy
Chem. Eng. Sci. **55** (2000[b]) 3275-3286

Krishna R. and Sie S.T.
Selection, design and scale-up aspects of Fischer-Tropsch reactors
Fuel Processing Technology **64** (2000) 73 - 105

Krieger and Dougherty
A mechanism for non-newtonian flow in suspensions of rigid spheres
Transactions of the Society of Rheology **III** (1959)137-152

Kunii D. and Levenspiel O.
Fluidization engineering 2nd edition
Butterworth-Heineman series in Chemical Engineering (1991)

Kuo J.C.W. *et al*.
Two-stage process for conversion of synthesis gas to high quality transportation fuels
Final Report to US DOE for contract no. DE-AC22-83PC60019 (1985)

Van der Laan G.P. and Beenackers A.A.C.M.
Hydrocarbon selectivity model for the gas-solid Fischer-Tropsch synthesis on precipitated iron catalysts
Industrial and engineering chemistry research **38** (1999), 1277-1290

Van der Laan G.P., Beenackers A.A.C.M and Krishna R.
Multicomponent reaction engineering model for Fe-catalyzed Fischer-Tropsch synthesis in commercial slurry bubble column reactors
Chem. Eng. Sci. **54** (1999) 5013-5019

Van der Laan G.P.
Kinetics, selectivity and scale up of the Fischer-Tropsch synthesis
PhD Thesis, University of Groningen (1999)

Letzel H.M., Schouten J.C., Krishna R. and van den Bleek C.M.
Characterization of regimes and regime transitions in bubble columns by chaos analysis and pressure signals.
*Chem. Eng. Sci. **52 (24)*** (1997) 4447-4459

Letzel M.
Hydrodynamics and mass transfer in bubble columns at elevated pressures
PhD thesis Technical University of Delft, the Netherlands (1998)

Levenspiel O.
Modeling in chemical engineering
Chem. Eng. Sci. **57** (2002) 4691-4696

Lide D.R.
Editor. Handbook of chemistry and physics, CRC Press *82 edition* (2002)

Lin T.J., Meng X. and Shi L.
Attrition studies of an iron Fischer-Tropsch catalyst used in a pilot–scale stirred tank slurry reactor
Ind. & Eng. Chem. Res. **51** (2012) 13123-13131

Liu Z., Shi S. and Li Y.
Coal liquefaction technologies – development in China and challenges in chemical reaction engineering
Chem. Eng. Sci. **65** (2010) 12-17

Luo M.
Development of China's CTL technology: 1970-2013
The Catalyst Review **Special Feature** (2013)

Luo X., Lee D.J., Lau R., Yang G. and Fan L.-S.
Maximum stable bubble size and gas holdup in high-pressure slurry bubble columns.
A.I.Ch.E.J. **45** (1999) 665-685

Ma W., Ding Y., Carreto Vázquez V.H. and Bukur D. B.
Study on catalytic performance and attrition strength of the Ruhrchemie catalyst for the Fischer–Tropsch synthesis in a stirred tank slurry reactor
Applied Catalysis A: General **268** (2004) 99–106

Malherbe J.A.
The effect of catalyst pre-treatment on the mechanical integrity and synthesis performance of an iron based Fischer-Tropsch catalyst
Masters Thesis – University of Cape Town (2006)

Maretto C. and Krishna R.
Modelling of a bubble column slurry reactor for Fischer-Tropsch synthesis
Catalysis Today **52** (1999) 279-289

May W.G.
Fluidized bed reactor studies
Chem. Engng. Prog. **55** (1959) 49-56

O'Brien R.J., Xu L., Spicer R.L., Davis B.H.
Activation study of precipitated iron Fischer-Tropsch catalysts
Energy & Fuels **10** (1996)

O'Brien R.J., Xu L., Spicer R.L., Bao S., Milburn D.R., Davis B.H.
Activity and selectivity of precipitated iron Fischer-Tropsch catalysts
Catalysis Today **36** (1997) 325-334

Patzlaff J., Liu Y., Graffmann C. and Gaube J.
Studies on product distributions of iron and cobalt catalyzed Fischer–Tropsch synthesis
Applied Catalysis A: General **186** (1999) 109

Poutsma M.L.
Assessment of advanced process concepts for liquefaction of low H_2/CO ratio synthesis gas based on the Kölbel slurry reactor and the Mobil gasoline Process
ORNL-5635, February (1980)

Qin S., Zhang C., Xu J., Yang Y., Xiang H. and Li Y.
Fe-Mo interactions and their influence on Fischer-Tropsch synthesis
Applied Catalysis A: General **392** (2011) 118-126

Qing M., Yang Y., Wu B., Xu J., Zhang C., Gao P. and Li Y.
Modification of Fe-SiO_2 interaction with zirconia for iron-based Fischer-Tropsch catalysts
Journal of Catalysis **279** (2011) 111-122

Qing M., Yang Y., Wu B., Wang H., Wang H., Xu J., Zhang C., Xiang H. and Li Y.
Effect of the zirconia addition manner on the modification of Fe-SiO_2 interaction
Catalysis Today **183** (2012) 79-87

Raje A.P. and Davis B.H.
Effect of vapor-liquid equilibrium on Fischer-Tropsch hydrocarbon selectivity for a deactivating catalyst in a slurry reactor
Energy & Fuels **10** (1996) 552-560

Raje A.P. and Davis B.H.
Fischer-Tropsch synthesis over iron-based catalysts in a slurry reactor. Reaction rates, selectivities and implications for improving hydrocarbon productivity.
Catalysis Today **36** (1997) 335-345

Rietema K.
Application of mechanical stress theory to fluidization
in A. Drinkenburg (ed.), Proc. Int. Symp. on Fluidization, Eindhoven, The Netherlands University Press, Amsterdam (1967) 154

Röper M.
Fischer-Tropsch synthesis
Catalysis in C1 Chemistry, Catalysis by Metal Complexes **4** (1983) 41-88

Rostrup-Nielsen J.R.
Syngas in perspective
Catalysis Today **71** (2002) 243-247

Sarup B., Wojciechowski B.W.
Studies of the Fischer-Tropsch synthesis on a cobalt catalyst: Evaluation of product distribution parameters from experimental data
Canadian J. of Chem. Eng. **66** (1988), 831-842

Satterfield C.N. and Huff G.A.
Effects of mass transfer on Fischer-Tropsch synthesis in slurry reactors
Chem. Eng. Sci. **35** (1980) 195-202

Schulz H.
Short history and present trends of Fischer-Tropsch synthesis
Applied Catalysis A: General **186** (1999) 3-12

Schulz H.
Comparing Fischer-Tropsch synthesis on iron- and cobalt catalysts: the dynamic of structure and function
Studies in Surface Science and Catalysis **163** (2007)

Schulz H. and Claeys M.
Kinetic modeling of Fischer-Tropsch product distributions
Applied Catalysis A: General **186 (1-2)** (1999) 91-107

Shaikh A. and Al-Dahhan M.H.
A review on flow regime transitions in bubble columns
Int. J. of Chem. React. Eng. **5 Review R1** (2007) 1-68

Shah Y., Kelkar B., Godbole S. and Deckwer W.-D.
Design parameters estimations for bubble column reactors
AIChE J. **28** (1982) 353

Shen J.,Schmetz E., Kawalkin G.J., Stiegel G.J., Noceti R.P., Winslow J.C., Kornosky R.M., Krastman D, Venkataraman V.K., Driscoll D.J., Cicero D.C., Haslebacher W.F., Hsieh B.C.B., Jain S.C. and Tennant J.B.
Commercial deployment of Fischer-Tropsch synthesis: the coproduction option
Topics in Catalysis **26 Nos. 1-4** (2003) 13-20

Shi B., Keogh R.A., Davis B.H.
Fischer-Tropsch synthesis: The formation of branched hydrocarbons in the Fe and Co catalyzed reaction
Journal of Molecular Catalysis A: Chemical **234** (2005[a]), 85-97

Shi B., Davis B.H.
Fischer-Tropsch synthesis: The paraffin to olefin ratio as a function of carbon number
Catalysis Today **106** (2005[b]), 129-131

Shroff M.D., Kalakkad D.S., Coulter K.E., Köhler S.D., Harrington M.S., Jackson N.B., Sault A.G. and Datye A.K.
Activation of precipitated iron Fischer-Tropsch synthesis catalysts
Journal of Catalysis **156** (1995) 185-207

van Steen E., Schulz H.
Polymerisation kinetics of the Fischer-Tropsch CO hydrogenation using iron and cobalt based catalysts
Applied Catalysis A: General **186** (1999), 309-320

Steynberg A.P., Vogel A.P., Price J.G., and Nel, H.G.
Technology targets for gas-to-liquids applications
Spring National Meeting of AIChE, Houston,22-26 April (2001)

Steynberg A.P.
Fischer-Tropsch technology: Introduction to Fischer-Tropsch technology
Studies in surface science and catalysis **152** (2004) Chapter 1, 1 – 63

Steynberg A.P.
Production of liquid and, optionally, gaseous hydrocarbons from gaseous reactants into an expanded slurry bed
US 7,772,291 (2010)

Steynberg A.P., Dry M.E., Davis B.H. and Breman B.B.
Fischer-Tropsch reactors
Studies in surface science and catalysis **152** (2004) Chapter 2, 64 – 196

Steynberg A.P. and Nel H.G.
Clean coal conversion options using Fischer-Tropsch technology
Fuel **83 (6)** (2004) 765-770

Steynberg A.P., Harris R., Smit J., Barry S. and Greeff I.
Recent Advances in Sasol's GTL Technology
World GTL Congress, Doha, Qatar (2013)

De Swart, J. Scale-up of a Fischer-Tropsch slurry reactor
PhD thesis, University of Amsterdam, (1996)

Teng B.-T., Chang J., Yang J., Wang G., Zhang C.-H., Xu Y.Y., Xiang H.-W. and Li Y.-W.
Water gas shift kinetics in Fischer-Tropsch synthesis over an industrial Fe-Mn catalyst
Fuel **84** (2005) 917-926

Thomas D.G.
Transport characteristics of suspensions: VIII. A note on viscosity of Newtonian suspensions of uniform spherical particles
J.of Colloid Science **20** (1965) 267–277

Toomey R.D. and Johnstone H.F.
Gaseous fluidization of solid particles
Chem. Engng. Prog. **48** (1952) 220-226

Vermeer D.J. and Krishna R.
Hydrodynamics and mass transfer in bubble columns operating in the churn-turbulent regime
Ind. Eng. Chem. Process Design & Dev. **20** (1981) 475-482

Vandu C.O., van den Berg B. and Krishna R.
Gas-liquid mass transfer in a slurry bubble column at high slurry concentration and high gas velocities
Chem. Eng. Technol. **28** (2005) 9

Vogel A., Breman B. and Steynberg A.
Intensification of commercial slurry phase reactors
Proceedings of NGCS8, studies in surface science and catalysis **167** (2007) 61-66

Vosloo A.C.
Die ontwikkeling van 'n teoretiese selektiwiteitsmodel vir die fischer-Tropsch sintese
PhD Thesis, University of Stellenbosh (1989)

Vosloo A.C., Gibson P. and Van Berge P.J.
21st Annual International Pittsburgh Coal Conference (2004), Osaka, Japan

Wan H.-J., Wu B.-S., Zhang C.-H., Teng B.-T., Tao Z.-C.,Yang Y., Zhu Y.-L., Xiang H.-W. and Li Y.-W.
Effect of Al_20_3/SiO_2 ratio on iron-based catalysts for Fischer-Tropsch synthesis
Fuel **85** (2006) 1371-1377

Wang Y.-N., Ma W.-P., Lu Y.-J., Yang J., Xu Y.-Y., Xiang H.W., Li Y.-W. Zhao Y.L. and Zhang B.J.
Kinetics modelling of Fischer-Tropsch synthesis over an industrial Fe-Cu-K catalyst
Fuel **82** (2003) 195-213

Wang Y., Fan W, Lui Y., Zeng Z., Hao X., Chang M., Zhang C., Xu Y., Xiang H. and Li Y.
Modeling of the Fischer-Tropsch synthesis in slurry bubble column reactors
Chem. Eng. and Proc. **47** (2008) 222-228

Werther J.
Hydrodynamics and mass transfer between bubble and emulsion phases in fluidized beds of sand and cracking catalyst
in Kunii D., Toei R. (eds.) Fluidization IV, Engineering Foundation, New York (1983) 93-102

Wilkinson P.M.
Physical aspects of the scale-up of high pressure bubble columns
PhD thesis, University of Groningen, The Netherlands (1991)

Wan H.-J., Wu B.-S., Zhang C.-H., Teng B.-T., Toa Z.-C., Yang Y., Zhu., Xiang H.-W. and Li Y-W.
Effect of Al2O3/SiO2 ratio on iron-based catalysts for Fischer-Tropsch synthesis
Fuel **85** (2006) 1371-1377

Wan H., Wu B., Zhang C., Xiang H. and Li Y.
Promotional effects of Cu and K on precipitated iron-based catalysts for Fischer-Tropsch synthesis
Journal of Molecular Catalysis A: Chemical **283** (2008) 33-42

Wang Y, Fan W, Liu Y., Zeng Z., Hao X., Chang M., Zhang C., Xu Y. Xiang H. and Li Y.
Modeling of the Fischer-Tropsch synthesis in slurry bubble column reactors
Chemical Engineering and Processing **47** (2008) 222-228

Wu B., Bai L., Xiang H., Li Y.-W., Zhang Z. and Zhong Bing
An active iron catalyst containing sulphur for Fischer-Tropsch synthesis
Fuel **83** (2004) 205-212

Xu J., Bartholomew C.H., Sudweeks J., and Eggett D.
Design, synthesis, and catalytic properties of silica-supported, Pt-promoted iron Fischer-Tropsch catalysts
Topics in Catalysis **26, Nos. 1-4** (2003) 55-71

Yang Y., Xiang H.-W., Tian L., Wang H., Zhang C.-H., Tao, Z.-C., Xu Y.-Y., Zhong B. and Li Y.-W.
Structure and Fischer-Tropsch performance of iron-manganese catalyst incorporated with SiO_2
Applied Catalysis A: General **284** (2005[a]) 105-122

Yang Y., Xiang H., Zhang R., Zhong B., Li Y.
A highly active and stable Fe-Mn catalyst for slurry Fischer-Tropsch synthesis
Catalysis Today **106** (2005[b]) 170-175

Yang Y., Sun Y., Tang Y., Liu Y., Wang H., Tian L., Wang H., Zhang, Z., Xiang H., Li Y.
Effect of magnesium promoter on iron-based catalyst for Fischer-Tropsch synthesis
Journal of Molecular Catalysis A: Chemical **245** (2006) 26-36

Yang G.Q., Du B. and Fan L.S.
Bubble formation and dynamic in gas-liquid-solid fluidization - A review
Chem. Eng. Sci. **62** (2007) 2-27

Yang Y., Wu B., Li Y. and Xiang H.
Fischer-Tropsch synthesis catalyst preparation and application thereof
US 2012/0022174 (2012)

Yu G.W., Xu Y.Y., Hao X., Li Y.W. and Liu G.-Q.
Process analysis for polygeneration of Fischer-Tropsch liquids and power with CO2 capture based on coal gasification
Fuel **89** (2010) 1070-1076

Zhang C.-H., Yang Y., Teng B.-T., Li T.Z., Zheng H.-Y., Xiang H.-W. and Li Y.-W.
Study of an iron-manganese Fischer-Tropsch synthesis catalyst promoted with copper
Journal of Catalysis **237** (2006) 405-415

Zhang J., Espinoza, R.L. and Mohedas S.
Slurry bubble reactor operated in well-mixed gas flow regime
US 6,914,082 (2005)

Zhang J. and Wright H.A.
Minimizing the volume or maximizing the production rate of slurry bubble reactors by using large gas flow rates and moderate single pass conversion
US 7,115,669 (2006)

Zhao R., Sudsakorn K., Goodwin Jr. J.G., Jothimurugesan K., Gangwal S.K. and Spivey J.J.
Attrition resistance of spray-dried iron F-T catalysts: effect of activation conditions
Catalysis Today **71** (2002) 319-326

Zhao G., Zhang C., Qin S., Xiang H. and Li Y.
Effect of interaction between potassium and structural promoters on Fischer-Tropsch performance in iron-based catalysts
Journal of Molecular Catalysis A: Chemical **286** (2008) 137-142

APPENDIX 1: Calculation of Expected and Measured Reaction Rate Constants

The rates for the two primary reactions, namely the Fischer-Tropsch (FT) synthesis reaction and the water gas shift reaction (WGS) are evaluated using the FT rate equation proposed by Botes and Breman (2006) and the WGS rate is examined assuming that it is first order in carbon monoxide.

The FT reaction rate, r_{FT} is thus first represented by the equations:

$$r_{FT} = k_{FT} \frac{p_{CO}(p_{H_2})^{0.5}}{(1+0.09p_{CO})^2}$$

where $k_{FT} = A_{FT}.e^{E/RT}$

The WGS reaction rate, r_{WGS} is thus first represented by:

$r_{WGS} = k_{WGS2}\, p_{CO}$

where $k_{WGS} = A_{WGS}.e^{E/RT}$

The focus is mainly on the start of run reaction rates in order to be comparable with other work.

To facilitate the comparison to the work of Van Berge (1994) the same units for the universal gas constant R are used, namely R = 62.36 mm Hg.dm^3/K.mol.

From experiment 1, the following information is available:

There were two periods at the start of run operating at a temperature of 240 ˚C (513 K). During the first period, the catalyst activity was much higher than expected at r_{FT} = 1.96 × 10^{-5} mole/g-cat.s which resulted in the catalyst being exposed to a water partial pressure of 10.3 bar. The activity then decreased for the following period to r_{FT} = 1.22 × 10^{-5} mole/g-cat.s when operating at a higher space velocity to control the water partial pressure.

For the experiment by Van Berge (1994) at 240 ˚C (513 K),
r_{FT} = 6.14 × 10^{-6} mole/g-cat.s with p_{CO} = 4.03 bar, p_{H_2} = 9.35 bar giving,
k_{FT} = 9.25 × 10^{-7} mole/g-cat.s.bar when dividing r_{FT} by $\frac{p_{CO}(p_{H_2})^{0.5}}{(1+0.09p_{CO})^2}$ and

For experiment 1 first period at 240 ˚C (513 K),
p_{CO} = 11.02 bar, p_{H_2} = 9.90 bar giving,
k_{FT} = 2.37 × 10^{-6} mole/g-cat.s.bar and
For experiment 1 second period at 240 ˚C (513 K),
p_{CO} = 16.15 bar, p_{H_2} = 15.07 bar giving,
k_{FT} = 1.21 × 10^{-6} mole/g-cat.s.bar

This indicates that the catalyst was still more active than the catalyst tested by Van Berge (1994) in spite of the exposure to the high water partial pressure.

For experiment 1 the following three periods operated at 245 ˚C (518 K) and the reaction rate increased steadily from r_{FT} = 1.33 × 10^{-5} mole/g-cat.s to r_{FT} = 1.52 × 10^{-5} mole/g-cat.s.

Over the next three periods in experiment 1, the temperature was increased to 255 ˚C (528 K) and the reaction rate continued to improve to 2.10 × 10^{-5} mole/g-cat.s. These conditions are useful for comparison to experiment 2 which operated for a short period at this temperature. For the final period in experiment 1 at 255 ˚C (528 K), p_{CO} = 15.96 bar, p_{H_2} = 14.70 bar giving,
k_{FT} = 2.12 × 10^{-6} mole/g-cat.s.bar

From experiment 2, the following information is available:

At 255 ˚C (528 K), r_{FT} = 1.56 × 10^{-5} mole/g-cat.s with p_{CO} = 4.68 bar, p_{H_2} = 7.41 bar giving,
k_{FT} = 2.47 × 10^{-6} mole/g-cat.s.bar

Van Berge (1994) determined the value of the activation energy E to be 89 kJ/mole which then results in,
$\ln(A_{FT})$ = ln(9.25 × 10^{-7})/(-89/(62.36 × 513)) giving
$\ln(A_{FT})$ = 4994

At 255 ˚C (528 K), the predicted value for k_{FT} is determined as follows:
$\ln k_{FT}$ = 4994 × (-89/ (62.36 × 528)) giving k_{FT} = 1.37 × 10^{-6} mole/g-cat.s.bar

$$\frac{p_{CO}(p_{H_2})^{0.5}}{(1+0.09p_{CO})^2} = \frac{4.68(7.41)^{0.5}}{(1+0.09(4.68))^2} = 6.31$$

So r_{FT} = 1.37 × 10^{-6} × 6.31 = 8.64 × 10^{-6} mole/g-cat.s which is lower than the measured value of 1.56 × 10^{-5} mole/g-cat.s.

For the first period at 270 ˚C (543 K), r_{FT} = 1.72 × 10^{-5} mole/g-cat.s

The reaction rate then improved to a peak value (averaged over 3 days) of,
r_{FT} = 3.06 × 10^{-5} mole/g-cat.s.

At 270 ˚C (543 K), the predicted value for k_{FT1} is determined as follows:
$\ln k_{FT}$ = 4994 × (-89/(62.36 × 543)) giving k_{FT} = 1.99 × 10^{-6} mole/g-cat.s.bar

$$\frac{p_{CO}(p_{H_2})^{0.5}}{(1+0.09p_{CO})^2} = \frac{7.15(12.98)^{0.5}}{(1+0.09(7.15))^2} = 4.72$$

So r_{FT} = 1.99 × 10^{-6} × 4.72 = 9.39 × 10^{-6} mole/g-cat.s which is much lower than the initial measured value of 1.72 × 10^{-5} mole/g-cat.s and very much lower than the peak value of 3.06 × 10^{-5} mole/g-cat.s which was achieved after the catalyst appeared to undergo further activation at this higher operating temperature.

In order to improve the prediction of the reaction rate 270 ˚C for experiment 2, the approach is taken to first adjust for the catalyst activity measured at 255 ˚C using k_{FT}. This means leads to an adjustment factor of 2.47/1.37 = 1.80 and this then increases the

predicted reaction rate to 1.69 × 10^{-5} mole/g-cat.s which is very close to the initial measured value of 1.72 × 10^{-5} mole/g-cat.s. This indicates that the activation energy determined by Van Berge (1994) is able to accurately predict the change in catalyst activity from 255 to 270 ˚C.

Having validated the Arrhenius extrapolation for the FT synthesis reaction from 255 ˚C to 270 ˚C the same approach is used for the water gas shift reaction. Van Berge (1994) determined the value of the activation energy E for the water gas shift reaction to be 116.4 kJ/mole.

For the experiment by Van Berge (1994) at 240 ˚C (513 K),
r_{WGS} = 1.60 × 10^{-6} mole/g-cat.s with p_{CO} = 4.03 bar giving,
k_{WGS} = 3.97 × 10^{-7} mole/g-cat.s.bar when dividing r_{FT} by p_{CO} with the assumption that the water gas shift reaction rate is first order with carbon monoxide.

$\ln(A_{WGS})$ = $\ln(3.97 \times 10^{-7})/(-116.4/ (62.36 \times 513))$ giving
$\ln(A_{WGS)}$ = 4169

At 255 ˚C (528 K), the predicted value for k_{WGS} is determined as follows:
$\ln k_{WGS}$ = 4169 × (-116.4/ (62.36 × 528)) giving k_{WGS} = 3.97 × 10^{-7} mole/g-cat.s.bar
So r_{WGS} = 3.97 × 10^{-7} × 4.68 = 1.86 × 10^{-6} mole/g-cat.s

At 255 ˚C, the measured rate for the water gas shift reaction in experiment 2,
r_{WGS} = 3.18 × 10^{-6} mole/g-cat.s which is significantly higher than the expected rate. The required adjustment ratio is 3.18/1.86 = 1.71 which is similar to the adjustment ratio for the FT reaction.

At 270 ˚C (543 K), the predicted value for k_{WGS} is determined as follows:
$\ln k_{WGS}$ = 4169 × (-116.4/ (62.36 × 543)) giving k_{WGS} = 6.27 × 10^{-7} mole/g-cat.s.bar and applying the adjustment ratio gives k_{WGS} = 1.07 × 10^{-6} mole/g-cat.s.bar which implies for p_{CO} = 7.15, r_{WGS} = 7.65 × 10^{-6} mole/g-cat.s.

At 270 ˚C, the initial measured rate for the water gas shift reaction in experiment 2 was 5.62 × 10^{-6} mole/g-cat.s which is lower than predicted but this increased over a period of nine days to a maximum value of 1.53 × 10^{-5} which is much higher than predicted. This resulted in the carbon dioxide selectivity increasing from an initial value of 28% to a maximum value of 34%. Further investigation of more sophisticated rate equations for the WGS reaction is not possible when the intrinsic activity is changing over such a wide range with run time at relatively constant operating conditions.

APPENDIX 2: Calculation of Reactor Productivity

The two primary costs for a slurry phase hydrocarbon synthesis reactor are the cost of the heat removal surfaces and the cost of the pressure vessel shell.

The cost of the heat removal surfaces is proportional to the temperature driving force and the heat removal duty. The heat removal surface and associated equipment cost will be more or less proportional to the amount of product produced at a given operating temperature. With the approach used of aiming for a target conversion at a given temperature, the heat exchange surface will be directly proportional to the gas velocity. There is no opportunity to decrease the cost per unit of product so the cost of the cooling equipment can be neglected in the optimization process.

The cost of the shell, at a given reactor diameter and given operating temperature and pressure, will be more or less proportional to the reactor shell surface area since the metal thickness should be constant at a given temperature, pressure and reactor diameter.

In order to optimize the reactor cost for a selected maximum practical reactor diameter, in this case 8 m, the following simplifying assumptions were made:

1) The slurry bed is contained in a cylinder and, on average, 20 % of the cylinder cross-sectional area is occupied by reactor internals.
2) No straight cylindrical section outside that required for the catalyst slurry bed is included.
3) There are two semi-hemispherical heads at either end of the reactor with a total surface area equal to a sphere of 8 m diameter i.e. $\pi D^2 = \pi 8^2 = 201$ m^2.

It is considered preferable to express reactor productivity in terms of the shell surface area rather than the slurry bed volume, used by some authors, since the shell surface area is more directly related to the reactor cost.

Using the data from the two laboratory experiments, a spreadsheet was set up to calculate the required commercial reactor surface area to match the laboratory reactor performance assuming that the commercial reactor is also well mixed. In reality, the commercial reactor will be more productive than the laboratory reactor due to the mixing characteristics being closer to plug flow. However, this should not change the shape of the curve of reactor productivity versus gas velocity at a constant target conversion but, in reality, a somewhat smaller bed height will be needed to reach the target conversion.

Table A is a copy of the spreadsheet page used for the reactor productivity calculations.

Table A

A	B	C	D	E	F	G	H
Reactor diameter (m)	Bed height (m)	Cross-sectional area (m^2)	Bed volume (m^3)	Fraction of bed volume free of internals	Solids fraction	Solids density (kg/m^3)	Feed Gas density (kg/m^3)
8	4.95	50.27	248.94	0.8	0.40	1957	8.42
8	5.93	50.27	298.13	0.8	0.40	1957	8.42
8	7.00	50.27	351.82	0.8	0.40	1957	8.42
8	8.17	50.27	410.58	0.8	0.40	1957	8.42
8	9.45	50.27	475.07	0.8	0.40	1957	8.42
8	10.86	50.27	546.07	0.8	0.40	1957	8.42
8	12.42	50.27	624.55	0.8	0.40	1957	8.42
8	14.16	50.27	711.64	0.8	0.40	1957	8.42
8	16.09	50.27	808.76	0.8	0.40	1957	8.42
8	18.25	50.27	917.66	0.8	0.40	1957	8.42
8	20.70	50.27	1040.49	0.8	0.40	1957	8.42
8	23.47	50.27	1180.02	0.8	0.40	1957	8.42
8	26.65	50.27	1339.77	0.8	0.40	1957	8.42
8	30.32	50.27	1524.35	0.8	0.40	1957	8.42

I	J	K	L	M	N	O	P
Gas holdup	Mass of catalyst in reactor (tonnes)	hydrogen partial pressure out (bar)	CO partial pressure out (bar)	Rate equation partial pressure ratio	FT rate constant	Mole fraction CO in feed	Fraction CO converted to hydrocarbons
0.33	104.2	13.18	4.12	11.71	2.75×10^{-6}	0.355	0.495
0.36	119.0	13.18	4.12	11.71	2.75×10^{-6}	0.355	0.495
0.39	133.9	13.18	4.12	11.71	2.75×10^{-6}	0.355	0.495
0.42	148.8	13.18	4.12	11.71	2.75×10^{-6}	0.355	0.495
0.45	163.7	13.18	4.12	11.71	2.75×10^{-6}	0.355	0.495
0.48	178.5	13.18	4.12	11.71	2.75×10^{-6}	0.355	0.495
0.51	193.4	13.18	4.12	11.71	2.75×10^{-6}	0.355	0.495
0.53	208.3	13.18	4.12	11.71	2.75×10^{-6}	0.355	0.495
0.56	223.2	13.18	4.12	11.71	2.75×10^{-6}	0.355	0.495
0.59	238.1	13.18	4.12	11.71	2.75×10^{-6}	0.355	0.495
0.61	252.9	13.18	4.12	11.71	2.75×10^{-6}	0.355	0.495
0.64	267.8	13.18	4.12	11.71	2.75×10^{-6}	0.355	0.495
0.66	282.7	13.18	4.12	11.71	2.75×10^{-6}	0.355	0.495
0.69	297.6	13.18	4.12	11.71	2.75×10^{-6}	0.355	0.495

Q	R	S	T	U	V	W	X
Gas velocity (m/s)	Temp. (K)	Pressure (bar)	CO molar flow (moles/s × 10^3)	Total hydro-carbons produced (tonnes/day)	C2+ hydro-carbons produced (tonnes/ day)	C2+ hydrocarbons produced per reactor surface area (reactor productivity tonnes/day. m^2)	Total hydro-carbons produced per tonne of catalyst (tonnes/day .tonne catalyst)
0.35	543	30.96	4.341	2599.4	2495.4	7.67	25.0
0.4	543	30.96	4.962	2970.8	2851.9	8.14	25.0
0.45	543	30.96	5.582	3342.1	3208.4	8.51	25.0
0.5	543	30.96	6.202	3713.5	3564.9	8.77	25.0
0.55	543	30.96	6.822	4084.8	3921.4	8.94	25.0
0.6	543	30.96	7.442	4456.2	4277.9	9.02	25.0
0.65	543	30.96	8.063	4827.5	4634.4	9.03	25.0
0.7	543	30.96	8.683	5198.9	4990.8	8.96	25.0
0.75	543	30.96	9.303	5570.2	5347.3	8.83	25.0
0.8	543	30.96	9.923	5941.5	5703.9	8.64	25.0
0.85	543	30.96	10.543	6312.9	6060.4	8.40	25.0
0.9	543	30.96	11.164	6684.2	6416.9	8.11	25.0
0.95	543	30.96	11.784	7055.6	6773.4	7.78	25.0
1	543	30.96	12.404	7426.9	7129.9	7.40	25.0

The spreadsheet is set up as follows:

1) The reactor cross-sectional area is inserted in column C and the fraction of the cross-sectional area free of internals (0.8) is inserted in column E.
2) The solids volume fraction, φ, is inserted in column F and the solids density is inserted in column G.
3) The feed gas density, $\rho_{G,}$ is inserted in column H.
4) The gas velocity, U, is inserted in column Q.
5) The gas holdup, ε, is calculated in column I using equation (17) with C_F = 0.6 to match the data using paraffin liquids (as shown in Table A), i.e.:
   $\varepsilon = C_F(\rho_G/5.8)^{0.25}U^{0.8} + (0.36/(\exp(2.66\ \varphi/(1-\varphi))))(1-0.6(\rho_G/5.8)^{0.25}U^{0.8})$
   The outlet gas flow is 60 % of the inlet gas flow so that the average gas velocity is 80 % of the open reactor shell inlet gas velocity. With the assumption that 20 % of the reactor cross-sectional area is occupied by internals, then the average gas velocity for the majority of the reactor length is the same as the open shell inlet gas velocity.
6) The mole fraction of CO reactant in the feed used in the laboratory experiment is inserted in column O.
7) The temperature is inserted in column R and the pressure is inserted in column S.
8) The molar feed flow of CO is calculated in column T as the product of the reactor cross-sectional area (C) and the gas velocity (Q) followed by converting the actual volume to the volume at standard temperature and pressure using the actual temperature and pressure (R and S) and then divided by 22414 to convert to moles per second.

9) The fractional CO conversion to hydrocarbon products from the laboratory experiment is inserted in column P.
10) The laboratory reactor outlet H_2 partial pressure is inserted in column K.
11) The laboratory reactor outlet CO partial pressure is inserted in column L.
12) The rate equation partial pressure ratio from the rate equation $r_{FT} = A\frac{P_{H_2}^{0.75}P_{CO}^{0.5}}{\left(1+k_{CO}P_{CO}^{0.5}\right)^2}$ is calculated in column M from the inserted hydrogen (K) and CO (L) partial pressures.
13) The FT rate constant, A, is calculated in column N by dividing the FT rate measured in the laboratory experiment (on average 2.75×10^{-5} moles CO/g-catalyst/s) by the partial pressure ratio (M).
14) The mass of catalyst in the reactor is calculated in column J by multiplying the CO molar flow (T) by the fractional CO conversion (P) and dividing by the product of the rate equation partial pressure ratio (M) and FT reaction rate constant (N).
15) The required commercial reactor bed height is calculated in column B by dividing the required mass of catalyst in the reactor from column J by the product of the reactor cross sectional area (C), the fraction of the bed volume free of internals (E), the solids fraction in the slurry, (1 - fractional gas holdup (I)) and the solids density.
16) The total hydrocarbons produced in a commercial reactor is calculated in column U by multiplying the CO molar flow (T) by the CO fractional conversion to obtain the carbon converted to hydrocarbons per second and then multiplying by the average hydrocarbon molecular weight per carbon atom of about 14 and converting from grams per second to tonnes per day.
17) The C2+ hydrocarbon productivity is calculated in column V by multiplying the total hydrocarbons by (1 - methane selectivity).
18) The reactor productivity is calculated in column W by dividing the C2+ hydrocarbon production from column V by ($\pi Dh + \pi D^2$) where h is the bed height; D is the reactor diameter; and there are two hemispherical heads with a total surface of a sphere of πD^2.
19) The catalyst productivity is calculated in column X by dividing the total hydrocarbons produced from column U by the required catalyst mass from column J.